

ATTITUDE DETERMINATION ERROR ANALYSIS SYSTEM (ADEAS)
MATHEMATICAL SPECIFICATIONS DOCUMENT

Prepared for
GODDARD SPACE FLIGHT CENTER

By
COMPUTER SCIENCES CORPORATION

Under
Contract NAS 5-31500
Task Assignment 59 212

Prepared by:

M. Nicholson 10/24/88
M. Nicholson Date

F. Markley (GSFC)
E. Seidewitz (GSFC)

Approved by:

R. Luczak 10-24-88
R. Luczak Date
Technical Supervisor

C. B. Spence 10-24-88
C. B. Spence Date
Technical Manager

(NASA-CR-189281) ATTITUDE DETERMINATION
ERROR ANALYSIS SYSTEM (ADEAS) MATHEMATICAL
SPECIFICATIONS DOCUMENT (Computer Sciences
Corp.) 183 p

N92-28210

Unclas
G3/64 0105100

ABSTRACT

This document presents the mathematical specifications of Release 4.0 of the Attitude Determination Error Analysis System (ADEAS), which provides a general-purpose linear error analysis capability for various spacecraft attitude geometries and determination processes. The analytical basis of the system is presented, and detailed equations are provided for both three-axis-stabilized and spin-stabilized attitude sensor models.

TABLE OF CONTENTS

<u>Section 1 - Introduction</u>	1-1
<u>Section 2 - Filter Specification</u>	2-1
2.1 System Model	2-1
2.2 Estimation and Covariance Analysis	2-6
2.3 Batch Filter	2-10
2.3.1 Estimation Errors	2-11
2.3.2 Covariance	2-15
2.3.3 Computation	2-25
2.4 Sequential Filter	2-29
2.4.1 Estimation Errors	2-29
2.4.2 Covariance	2-32
2.4.3 Computation	2-37
<u>Section 3 - Spin-Stabilized Spacecraft Models</u>	3-1
3.1 Attitude Generation	3-1
3.2 Dynamic Error Model	3-2
3.3 Sensor Models	3-4
3.3.1 IR Horizon Sensor Measurement Model and Partial Derivatives	3-6
3.3.2 V-Slit Star Sensor Measurement Model and Partial Derivatives	3-17
3.3.3 V-Slit Sun Sensor Measurement Model and Partial Derivatives	3-22
<u>Section 4 - Three-Axis Stabilized Spacecraft Models</u>	4-1
4.1 Attitude Generation	4-1
4.2 Dynamic Error Model	4-3
4.2.1 Attitude Error Parameterization	4-3
4.2.2 Attitude Error Propagation	4-11
4.2.3 Transition Matrix Computation	4-14
4.2.4 Random Excitation Covariance Matrix Computation	4-21
4.3 Sensor Models	4-27
4.3.1 Gyroscopes	4-31
4.3.2 IR Horizon Sensor Measurement Model and Partial Derivatives	4-35

TABLE OF CONTENTS (Cont'd)

Section 4 (Cont'd)

4.3.3	Three-Axis Magnetometer Measurement Model and Partial Derivatives	4-48
4.3.4	Fixed-Head Star Tracker Measurement Model and Partial Derivatives	4-52
4.3.5	Gimbaled Star Tracker Measurement Model and Partial Derivatives	4-57
4.3.6	Digital Sun Sensor Measurement Model and Partial Derivatives	4-63
4.3.7	Analog Sun Sensor Measurement Model and Partial Derivatives	4-71
4.3.8	Gimbaled Sun Sensor Measurement Model and Partial Derivatives	4-76

Section 5 - Reference Systems and Vectors 5-1

5.1	Coordinate Systems	5-1
5.1.1	Geocentric Inertial (GCI) Coordinate System.	5-1
5.1.2	Earth-Center Pointing Coordinate System.	5-2
5.1.3	Local Vertical Pointing Coordinate System.	5-3
5.1.4	Sun-Pointing Coordinate System.	5-4
5.2	Spaceraft Ephemeris Generation	5-5
5.2.1	Numerical Integration	5-5
5.2.2	Ephemeris File.	5-15
5.3	Geomagnetic Field Vector Computation	5-15
5.4	Sun and Moon Ephemeris Generation.	5-15
5.4.1	SLP File.	5-15
5.4.2	Analytic Sun Ephemeris Computation.	5-16
5.4.3	Analytic Moon Ephemeris Computation	5-18
5.5	Star Catalog Generation.	5-24
5.5.1	SKYMAP File	5-24
5.5.2	Uniform Star Distribution	5-24
5.6	Line-of-Sight Sensor Visibility.	5-26
5.6.1	Occultation	5-26
5.6.2	Interference.	5-27

References

LIST OF ILLUSTRATIONS

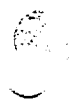
Figure

3-1	Right Ascension and Declination of the Nom- inal Spin Axis	3-2
3-2	IR Horizon Sensor Geometry, Sun Indexed.	3-7
3-3	V-Slit Star Scanner Spherical Geometry	3-18
3-4	V-Slit Star Scanner Plane Geometry	3-20
3-5	V-Slit Sensor Geometry	3-23
4-1	Small Rotation From True Spacecraft Axes to Estimated Spacecraft Axes.	4-4
4-2	Coordinate Geometry for Earth IR Horizon Sensor	4-36
4-3	Spherical Geometry for Earth IR Horizon Sensor	4-37
4-4	Fixed-Head Star Tracker Geometry	4-54
4-5	Gimbaled Star Tracker Geometry	4-58
4-6	Digital Sun Sensor Geometry.	4-64
4-7	Analog Sun Sensor Geometry	4-72
5-1	Definition of the GCI Coordinate System.	5-1

LIST OF TABLES

Table

4-1	Computation of Euler Angles From Attitude Matrix	4-6
4-2	Nonorthogonal Transformation Between Small Changes in Euler Angles ($\Delta\phi$, $\Delta\theta$, $\Delta\psi$) and Small Rotation About Body Axes ($\Delta\alpha_1$, $\Delta\alpha_2$, $\Delta\alpha_3$)	4-10
5-1	Series for λ_M	5-20
5-2	Series for θ_M	5-22
5-3	Series for κ_M	5-23



SECTION 1 - INTRODUCTION

The Attitude Determination Error Analysis System (ADEAS) provides a general-purpose linear error analysis capability for various spacecraft attitude determination processes. ADEAS does not process sensor data but simulates the attitude determination logic and computes the resulting attitude determination accuracy. The spacecraft attitude determination scenarios that can be analyzed by ADEAS are described below:

- From low-altitude Earth orbits to International Sun-Earth Explorer (ISEE)-3 type of Earth-Sun libration point orbits
- Spin-stabilized or three-axis-stabilized spacecraft attitudes
- Batch weighted-least-squares and sequential filter attitude determination methods
- Sensor complements, which are subsets of Sun sensors, Earth sensors, star sensors, gyros, and magnetometers.

These scenarios include most of the existing and anticipated Earth satellite attitude determination systems. A possible exception is that attitude rate information is assumed available for use in the propagation of satellite attitudes in the multiframe method. The rate information is usually provided by gyros.

The ADEAS system requirements are presented in Reference 1. The detailed mathematical specifications for ADEAS are presented in this document. Section 2 presents the mathematical formulations of linear error analyses for batch and sequential estimators. The formulations are general and not limited only to attitude determination systems. Sections 3

and 4 describe the attitude and sensor models included in the program. Section 5 specifies the reference systems and vectors used in ADEAS.

Although many of the algorithms have been extensively revised, this document is based in large part on Reference 2.

SECTION 2 - FILTER SPECIFICATION

This section presents the specifications for error analysis using batch and sequential filters. While ADEAS deals specifically with attitude determination, Section 2.1 presents a widely applicable system model, and Sections 2.2, 2.3, and 2.4 derive general error analysis equations for batch and Kalman filters. Sections 3 and 4 then deal with specializing the general specifications to the cases of spin-stabilized and three-axis-stabilized spacecraft.

2.1 SYSTEM MODEL

Let $\bar{\mathbf{x}}$ be an N-dimensional vector that characterizes the system under consideration. This state vector evolves in time according to the following dynamic model:

$$\dot{\bar{\mathbf{x}}}(t) = \bar{\mathbf{f}}(\bar{\mathbf{x}}(t), t) + \bar{\mathbf{u}}(t) \quad (2.1-1)$$

where the dynamic noise $\bar{\mathbf{u}}(t)$ is a Gaussian white noise process with mean and covariance given by

$$E[\bar{\mathbf{u}}(t)] = 0$$

$$E[\bar{\mathbf{u}}(t) \bar{\mathbf{u}}^T(t')] = \mathbf{Q}_u \delta(t - t')$$

($E[\dots]$ denotes taking the expectation value.) $\bar{\mathbf{x}}$ includes all parameters of interest necessary to compute $\dot{\bar{\mathbf{x}}}$ even though some parameters may have zero derivative. For spacecraft attitude determination, $\bar{\mathbf{x}}$ includes the spacecraft attitude parameters and additional dynamic parameters such as gyroscope biases and alignments.

The true value of the state vector is never exactly known but is instead estimated by the state estimate vector, \bar{x}^* . This estimate evolves in time according to

$$\dot{\bar{x}}^*(t) = \bar{f}(\bar{x}^*(t), t) \quad (2.1-2)$$

The state error vector given by

$$\Delta \bar{x}(t) \equiv \bar{x}(t) - \bar{x}^*(t)$$

is assumed to always remain small, so linear error analysis techniques may be used. To first order, then

$$\begin{aligned} \dot{\Delta \bar{x}}(t) &= \dot{\bar{x}}(t) - \dot{\bar{x}}^*(t) = \bar{f}(\bar{x}(t), t) - \bar{f}(\bar{x}^*(t), t) + \bar{u}(t) \\ &\approx \frac{\partial \bar{f}}{\partial \bar{x}}(t) \Delta \bar{x}(t) + \bar{u}(t) \end{aligned} \quad (2.1-3)$$

Integrating this formally gives

$$\Delta \bar{x}(t) = \phi(t, t_0) \Delta \bar{x}(t_0) + \bar{\psi}(t, t_0) \quad (2.1-4)$$

where the state transition matrix ϕ is given by

$$\begin{aligned} \dot{\phi}(t, t_0) &= \frac{\partial \bar{f}}{\partial \bar{x}}(t) \phi(t, t_0) \\ \phi(t_0, t_0) &= I \end{aligned} \quad (2.1-5)$$

and the random excitation vector $\bar{\psi}$ by

$$\bar{\psi}(t, t_0) \equiv \int_{t_0}^t \phi(t, t') \bar{u}(t') dt' \quad (2.1-6)$$

It follows from Equation (2.1-5) that ϕ obeys the group property

$$\phi(t_2, t_0) = \phi(t_2, t_1) \phi(t_1, t_0) \quad (2.1-7)$$

The random excitation vector satisfies the equation

$$\bar{\psi}(t, t_0) = \phi(t, t_1) \bar{\psi}(t_1, t_0) + \bar{\psi}(t, t_1) \quad (2.1-8)$$

A filter produces state estimates based on information obtained from measurements made at discrete times. Let y_i be a measurement value obtained at time t_i . In ADEAS, measurements performed simultaneously are treated as independent scalar measurements, so the times t_i need not be distinct. Measurements are related to the state vector by the following measurement model:

$$y_i = g_i(\bar{x}(t_i), \bar{p}) + v_i \quad (2.1-9)$$

where \bar{p} is a vector of measurement parameters and v_i is a Gaussian white noise process with mean and covariance given by

$$\begin{aligned} E[v_i] &= 0 \\ E[v_i^2] &= \sigma_i^2 \\ E[v_i v_j] &= 0 \quad \text{for } i \neq j \end{aligned} \quad (2.1-10)$$

Note that we will consider \bar{p} to include the parameters necessary for all possible measurements, not just those measurements made at any specific time t_i . For spacecraft attitude determination, \bar{p} would include all sensor alignments, biases, scale factors, etc.

The functions g_i are assumed to be known functions of imprecisely known arguments. Therefore, it is possible to compute expected measurement values by

$$y_i^* = g_i(\bar{x}^*(t_i), \bar{p}^*) \quad (2.1-11)$$

where \bar{p}^* is a vector of estimated measurement parameters. The measurement residual between the actual and computed measurements is then

$$\begin{aligned} \Delta y_i &= y_i - y_i^* = g_i(\bar{x}(t_i), \bar{p}) - g_i(\bar{x}^*(t_i), \bar{p}^*) + v_i \\ &\approx \frac{\partial g_i}{\partial \bar{x}} \Delta \bar{x}(t_i) + \frac{\partial g_i}{\partial \bar{p}} \Delta \bar{p} + v_i \end{aligned} \quad (2.1-12)$$

where $\Delta \bar{x}$ and $\Delta \bar{p} \equiv \bar{p} - \bar{p}^*$ are both assumed small.

The function $g_i(\bar{x}(t_i), \bar{p})$ can be written as

$$g_i(\bar{x}(t_i), \bar{p}) = (1 + k_i) h_i(\bar{x}(t_i), \bar{p}') + b_i + a_i \sin(\omega_i t_i + \psi_i) \quad (2.1-13)$$

where k_i = measurement scale factor error

b_i = sensor bias

a_i = amplitude of orbit-related or other unknown periodic error source

ω_i = frequency of periodic error source

ψ_i = phase angle of periodic error source

The parameters k_i , b_i , a_i , ω_i , and ψ_i are assumed to depend only on the measurement type and not on the measurement time. The frequencies ω_i and phases ψ_i are assumed to be exactly known.

The parameters k_i , b_i , and a_i are a subset of the vector of measurement parameters; the vector \bar{p}' contains the remaining measurement parameters. The partial derivatives of the measurement with respect to these parameters are especially simple:

$$\frac{\partial g_i}{\partial k_i} = h_i(\bar{x}(t_i), \bar{p}') \approx g_i \quad (2.1-14)$$

$$\frac{\partial g_i}{\partial b_i} = 1 \quad (2.1-15)$$

$$\frac{\partial g_i}{\partial a_i} = \sin (\omega_i t_i + \psi_i) \quad (2.1-16)$$

The partial derivatives with respect to \bar{x} and \bar{p}' are derived in Sections 3.3 and 4.3. In these sections, they are denoted by $\partial \bar{y}^*/\partial \bar{x}$ and $\partial \bar{y}^*/\partial \bar{p}$ rather than $\partial \bar{g}/\partial \bar{x}$ and $\partial \bar{g}/\partial \bar{p}$.

2.2 ESTIMATION AND COVARIANCE ANALYSIS

It is usually not necessary to estimate all of the state parameters. However, it is necessary to provide estimates for those measurement parameters that are not exactly known. Therefore, a filter should produce estimates for a set of solve-for parameters including a subset of the state parameters and a subset of the measurement parameters. The remaining parameters are then considered parameters whose values may contain errors that are not reduced during the estimation process.

The state error, measurement parameter error, and random excitation vectors and the state transition matrix are thus partitioned as follows:

$$\Delta \bar{x}(t) = \begin{bmatrix} \Delta \bar{s}_x(t) \\ \text{-----} \\ \Delta \bar{\beta}(t) \end{bmatrix} \quad (2.2-1a)$$

$$\Delta \bar{p} = \begin{bmatrix} \Delta \bar{s}_p \\ \text{---} \\ \Delta \bar{\gamma} \end{bmatrix} \quad (2.2-1b)$$

$$\bar{\Psi}(t, t_0) = \begin{bmatrix} \bar{\Psi}_s(t, t_0) \\ \hline \bar{\Psi}_\beta(t, t_0) \end{bmatrix} \quad (2.2-1c)$$

$$\Phi(t, t_0) = \begin{bmatrix} \Phi_s(t, t_0) & \Theta(t, t_0) \\ \hline 0 & \Phi_\beta(t, t_0) \end{bmatrix} \quad (2.2-1d)$$

where $\Delta \bar{s}(t) \equiv \begin{bmatrix} \Delta \bar{s}_x(t) \\ \hline \Delta \bar{s}_p \end{bmatrix} = \text{solve-for parameter vector}$

$\Delta \bar{\beta}(t) \equiv \text{dynamic consider parameter error vector}$

$\Delta \bar{\gamma} \equiv \text{measurement consider parameter error vector}$

The error equations (2.1-4) and (2.1-12) can then be rewritten as

$$\Delta \bar{s}(t) = \Phi(t, t_0) \Delta \bar{s}(t_0) + \Theta(t, t_0) \Delta \bar{\beta}(t_0) + \bar{\Psi}(t, t_0) \quad (2.2-2)$$

$$\Delta \bar{\beta}(t) = \Phi_\beta(t, t_0) \Delta \bar{\beta}(t_0) + \bar{\Psi}_\beta(t, t_0) \quad (2.2-3)$$

$$\Delta y_i = G_i \Delta \bar{s}(t_i) + \Gamma_i \Delta \bar{\gamma} + v_i \quad (2.2-4)$$

where

$$\Phi(t, t_0) \equiv \begin{bmatrix} \Phi_s(t, t_0) & 0 \\ \hline 0 & I \end{bmatrix} \quad (2.2-5)$$

$$\bar{\Psi}(t, t_0) \equiv \left[\begin{array}{c} \bar{\Psi}_s(t, t_0) \\ \hline 0 \end{array} \right] \quad (2.2-6)$$

$$\Theta(t, t_0) \equiv \left[\begin{array}{c} \Theta(t, t_0) \\ \hline 0 \end{array} \right] \quad (2.2-7)$$

$$G_i \equiv \frac{\partial g_i}{\partial \bar{s}} = \left[\begin{array}{c|c} \frac{\partial g_i}{\partial \bar{s}_x} & \frac{\partial g_i}{\partial \bar{s}_p} \end{array} \right] \quad (2.2-8)$$

$$r_i \equiv \frac{\partial g_i}{\partial \bar{\gamma}} \quad (2.2-9)$$

$$\frac{\partial g_i}{\partial \bar{x}} = \left[\begin{array}{c|c} \frac{\partial g_i}{\partial \bar{s}_x} & 0 \end{array} \right] \quad (2.2-10)$$

$$\frac{\partial g_i}{\partial \bar{p}} = \left[\begin{array}{c|c} \frac{\partial g_i}{\partial \bar{s}_p} & \frac{\partial g_i}{\partial \bar{\gamma}} \end{array} \right] \quad (2.2-11)$$

We have assumed that no measurements depend directly on any dynamic parameter that is not a solve-for parameter. Further, we have assumed that the time evolution of the dynamic consider parameters does not depend on any of the dynamic solve-for parameters.

The function of a full estimation system is to determine an estimate $\bar{s}^*(t)$ given measurements y_i . ADEAS, however, does not actually compute an estimate but determines how good an estimate would be if it were produced in a given situation.

ADEAS does this by computing the estimation covariance matrix defined by

$$P(t) \equiv E[\bar{\Delta s}(t) \bar{\Delta s}^T(t)] \quad (2.2-12)$$

ADEAS thus performs linear covariance analysis for batch and sequential filters. The covariance matrix $P(t)$ then provides a statistical measure of how good an estimate could be produced at time t of a given scenario.

The random excitation enters into this computation in the form of the random excitation covariance matrix, which is defined as

$$\begin{aligned} d(t, t_0) &\equiv E[\bar{\psi}(t, t_0) \bar{\psi}^T(t, t_0)] \\ &\equiv \begin{bmatrix} d_s(t, t_0) & d_{s\beta}(t, t_0) \\ \hline d_{s\beta}^T(t, t_0) & d_\beta(t, t_0) \end{bmatrix} \end{aligned} \quad (2.2-13)$$

where

$$\begin{aligned} d_s(t, t_0) &\equiv E[\bar{\psi}_s(t, t_0) \bar{\psi}_s^T(t, t_0)] \\ &= \int_{t_0}^t \begin{bmatrix} \phi_s(t, t') & \theta(t, t') \end{bmatrix} Q_u \begin{bmatrix} \phi_s^T(t, t') \\ \theta^T(t, t') \end{bmatrix} dt' \end{aligned} \quad (2.2-14)$$

$$\begin{aligned} d_\beta(t, t_0) &\equiv E[\bar{\psi}_\beta(t, t_0) \bar{\psi}_\beta^T(t, t_0)] \\ &= \int_{t_0}^t \begin{bmatrix} 0 & \phi_\beta(t, t') \end{bmatrix} Q_u \begin{bmatrix} 0 \\ \phi_\beta^T(t, t') \end{bmatrix} dt' \end{aligned} \quad (2.2-15)$$

$$d_{s\beta}(t, t_0) \equiv E \left[\bar{\psi}_s(t, t_0) \bar{\psi}_\beta^T(t, t_0) \right] \quad (2.2-16)$$

$$= \int_{t_0}^t \left[\phi_s(t, t') \mid \theta(t, t') \right] Q_u \left[\frac{0}{\phi_\beta^T(t, t')} \right] dt'$$

2.3 BATCH FILTER

A batch filter produces an estimate $\bar{s}^*(t_0)$ at an epoch time t_0 , based on a single batch of measurements \bar{y} that may have been made at various times. Thus,

$$\bar{y} \equiv \left[y_1, \dots, y_m \right]^T \quad (2.3-1)$$

where each y_i is a scalar measurement. Similarly,

$$\bar{y}^* \equiv \left[y_1^*, \dots, y_m^* \right]^T \quad (2.3-2)$$

and

$$\Delta \bar{y} \equiv \left[\Delta y_1, \dots, \Delta y_m \right]^T$$

The batch filter produces an estimate $\bar{s}^*(t_0)$ that gives \bar{y}^* , which minimizes the cost function

$$V = \Delta \bar{y}^T W \Delta \bar{y} + \Delta \bar{s}_A^{*T} W_A \Delta \bar{s}_A^* \quad (2.3-3)$$

where $W \equiv$ positive-definite symmetric measurement weight matrix

$$\begin{aligned}\Delta \bar{s}_A^* &\equiv \bar{s}_A^* - \bar{s}^*(t_0) = \bar{s}_A^* - \bar{s}(t_0) + \bar{s}(t_0) - \bar{s}^*(t_0) \\ &= \Delta \bar{s}(t_0) - \Delta \bar{s}_A\end{aligned}$$

$\bar{s}_A^* \equiv$ a priori estimate of $\bar{s}^*(t_0)$

$W_A \equiv$ non-negative-definite symmetric a priori weight matrix

2.3.1 ESTIMATION ERRORS

Since the batch filter determines $\bar{s}^*(t_0)$, it is necessary to relate $\Delta \bar{y}$ to $\Delta \bar{s}(t_0)$. Substituting Equation (2.2-2) into Equation (2.2-4) gives

$$\begin{aligned}\Delta y_i &\equiv G_i [\Phi(t_i, t_0) \Delta \bar{s}(t_0) + \Theta(t_i, t_0) \Delta \bar{\beta}(t_0) + \bar{\Psi}(t_i, t_0)] \\ &\quad + \Gamma_i \Delta \bar{\gamma}_i + v_i \quad (2.3-4) \\ &= F_i \Delta \bar{s}(t_0) + B_i \Delta \bar{\beta}(t_0) + \Gamma_i \Delta \bar{\gamma}_i + U_i + v_i\end{aligned}$$

where, using Equations (2.2-5) through (2.2-8)

$$F_i \equiv G_i \Phi(t_i, t_0) = \left[\frac{\partial g_i}{\partial \bar{s}_x} \phi_s(t_i, t_0) \mid \frac{\partial g_i}{\partial \bar{s}_p} \right] \quad (2.3-5)$$

$$B_i \equiv G_i \Theta(t_i, t_0) = \frac{\partial g_i}{\partial \bar{s}_x} \Theta(t_i, t_0) \quad (2.3-6)$$

$$U_i \equiv G_i \bar{\Psi}(t_i, t_0) = \frac{\partial g_i}{\partial \bar{s}_x} \bar{\Psi}_s(t_i, t_0) \quad (2.3-7)$$

Then,

$$\Delta \bar{y} = F \Delta \bar{s}(t_0) + \Delta \bar{e} \quad (2.3-8)$$

where $\Delta \bar{e} \equiv B \Delta \bar{\beta}(t_0) + \Gamma \Delta \bar{\gamma} + \bar{U} + \bar{N}$

$$F \equiv \begin{bmatrix} F_1 \\ \vdots \\ F_m \end{bmatrix} \quad B \equiv \begin{bmatrix} B_1 \\ \vdots \\ B_m \end{bmatrix} \quad \Gamma \equiv \begin{bmatrix} \Gamma_1 \\ \vdots \\ \Gamma_m \end{bmatrix} \quad (2.3-9)$$

$$\bar{U} \equiv [U_1, \dots, U_m]^T$$

$$\bar{N} \equiv [v_1, \dots, v_m]^T$$

Substituting Equation (2.3-8) into Equation (2.3-3) for the loss function then gives

$$\begin{aligned}
 V &= [F\bar{\Delta s}(t_0) + \Delta\bar{e}]^T W[F\bar{\Delta s}(t_0) + \Delta\bar{e}] \\
 &+ [\bar{\Delta s}(t_0) - \bar{\Delta s}_A]^T W_A[\bar{\Delta s}(t_0) - \bar{\Delta s}_A] \\
 &= \bar{\Delta s}^T(t_0) (W_A + F^T W F) \bar{\Delta s}(t_0) + \bar{\Delta s}^T(t_0) (F^T W \Delta\bar{e} - W_A \bar{\Delta s}_A) \\
 &+ (\Delta\bar{e}^T W F - \bar{\Delta s}_A^T W_A) \bar{\Delta s}(t_0) + \Delta\bar{e}^T W \Delta\bar{e} + \bar{\Delta s}_A^T W_A \bar{\Delta s}_A \\
 &= \left[\bar{\Delta s}(t_0) + W_N^{-1} (F^T W \Delta\bar{e} - W_A \bar{\Delta s}_A) \right]^T W_N \left[\bar{\Delta s}(t_0) \right. \\
 &\quad \left. + W_N^{-1} (F^T W \Delta\bar{e} - W_A \bar{\Delta s}_A) \right] \\
 &\quad - (F^T W \Delta\bar{e} - W_A \bar{\Delta s}_A)^T W_N^{-1} (F^T W \Delta\bar{e} - W_A \bar{\Delta s}_A) \\
 &\quad + \Delta\bar{e}^T W \Delta\bar{e} + \bar{\Delta s}_A^T W_A \bar{\Delta s}_A
 \end{aligned} \tag{2.3-10}$$

where

$$W_N = W_A + F^T W F = \text{normal matrix} \tag{2.3-11}$$

The final equality in Equation (2.3-10) is valid as long as W_N is nonsingular. The singularity (or ill-conditioning) of W_N indicates a lack of observability of the solve-for parameters from the measurements \bar{y} .

If W_N is nonsingular and positive-definite, then it is clear from the form of Equation (2.3-10) that V is minimized when

$$\begin{aligned}\Delta \bar{s}(t_0) &= -W_N^{-1} (F^T W \Delta \bar{e} - W_A \Delta \bar{s}_A) \\ &= -W_N^{-1} \{ F^T W [B \Delta \bar{\beta}(t_0) + \Gamma \Delta \bar{\gamma} + \bar{U} + \bar{N}] - W_A \Delta \bar{s}_A \} \\ &= \Delta \bar{s}_n(t_0) + \Delta \bar{s}_\gamma(t_0) + \Delta \bar{s}_\beta(t_0) + \Delta \bar{s}_u(t_0)\end{aligned}\quad (2.3-12)$$

where

$$\Delta \bar{s}_n(t_0) \equiv W_N^{-1} (W_A \Delta \bar{s}_A - F^T W \bar{N}) \quad (2.3-13)$$

$$\Delta \bar{s}_\gamma(t_0) \equiv -W_N^{-1} F^T W \Gamma \Delta \bar{\gamma} \quad (2.3-14)$$

$$\Delta \bar{s}_\beta(t_0) \equiv -W_N^{-1} F^T W B \Delta \bar{\beta}(t_0) \quad (2.3-15)$$

$$\Delta \bar{s}_u(t_0) \equiv -W_N^{-1} F^T W \bar{U} \quad (2.3-16)$$

The batch filter produces an estimate $\bar{s}^*(t_0)$ at the epoch time t_0 . This estimate may then be propagated to any other time t using Equation (2.1-2). In doing this the estimation

errors $\Delta \bar{s}$ propagate according to Equation (2.2-2). Substituting Equation (2.3-12) for $\Delta \bar{s}(t_0)$ into Equation (2.2-2) gives

$$\begin{aligned} \Delta \bar{s}(t) &= \Phi(t, t_0) \left[\Delta \bar{s}_n(t_0) + \Delta \bar{s}_\gamma(t_0) + \Delta \bar{s}_\beta(t_0) + \Delta \bar{s}_u(t_0) \right] \\ &\quad + \Theta(t, t_0) \Delta \bar{\beta}(t_0) + \bar{\Psi}(t, t_0) \\ &= \Delta \bar{s}_n(t) + \Delta \bar{s}_\gamma(t) + \Delta \bar{s}_\beta(t) + \Delta \bar{s}_u(t) \end{aligned} \quad (2.3-17)$$

where

$$\Delta \bar{s}_n(t) \equiv \Phi(t, t_0) \Delta \bar{s}_n(t_0) \quad (2.3-18)$$

$$\Delta \bar{s}_\gamma(t) \equiv \Phi(t, t_0) \Delta \bar{s}_\gamma(t_0) \quad (2.3-19)$$

$$\Delta \bar{s}_\beta(t) \equiv \Phi(t, t_0) \Delta \bar{s}_\beta(t_0) + \Theta(t, t_0) \Delta \bar{\beta}(t_0) \quad (2.3-20)$$

$$\Delta \bar{s}_u(t) \equiv \Phi(t, t_0) \Delta \bar{s}_u(t_0) + \bar{\Psi}(t, t_0) \quad (2.3-21)$$

2.3.2 COVARIANCE

Equation (2.3-17) gives the estimation errors induced by the systematic error sources $\Delta \bar{\gamma}$ and $\Delta \bar{\beta}$, the random error sources \bar{U} and \bar{N} and the a priori error $\Delta \bar{s}_A$. It is assumed that all

these error sources are uncorrelated. The covariance matrix $P(t)$ is

$$\begin{aligned} P(t) &\equiv E[\Delta \bar{s}(t) \Delta \bar{s}^T(t)] \\ &= P_n(t) + P_\gamma(t) + P_\beta(t) + P_u(t) \end{aligned} \quad (2.3-22)$$

where

$$P_n(t) \equiv E[\Delta \bar{s}_n(t) \Delta \bar{s}_n^T(t)] \quad (2.3-23)$$

$$P_\gamma(t) \equiv E[\Delta \bar{s}_\gamma(t) \Delta \bar{s}_\gamma^T(t)] \quad (2.3-24)$$

$$P_\beta(t) \equiv E[\Delta \bar{s}_\beta(t) \Delta \bar{s}_\beta^T(t)] \quad (2.3-25)$$

$$P_u(t) \equiv E[\Delta \bar{s}_u(t) \Delta \bar{s}_u^T(t)] \quad (2.3-26)$$

The following subsections discuss, in turn, each of these contributions to the overall covariance.

2.3.2.1 Data Noise Contribution

From Equations (2.3-18) and (2.3-23) we have

$$P_n(t) = \Phi(t, t_0) P_n(t_0) \Phi^T(t, t_0) \quad (2.3-27)$$

where from Equation (2.3-13)

$$P_n(t_0) = W_N^{-1} (W_A P_A W_A + F^T W R W F) W_N^{-1} \quad (2.3-28)$$

with

$$P_A \equiv E \begin{bmatrix} \Delta \bar{s}_A & \Delta \bar{s}_A^T \end{bmatrix} \quad (2.3-29)$$

$$R \equiv E[\overline{NN}^T] = \text{diag} \left(\sigma_1^2, \dots, \sigma_m^2 \right)$$

The a priori weight matrix is given by

$$W_A = P_A^{-1} \quad (2.3-30a)$$

where the a priori covariance is

$$P_A = \left[\begin{array}{c|c} P_{A\text{attitude}} & 0 \\ \hline 0 & P_{A\text{other}} \end{array} \right] \quad (2.3-30b)$$

with $P_{A\text{attitude}}$ being the a priori covariance of the attitude error parameters, as given in Section 3.2 or 4.2.1, and $P_{A\text{other}}$ being the a priori covariance of other solve-for parameters, assumed to be diagonal:

$$P_{A\text{other}} = \text{diag}(\sigma_{A1}^2, \dots, \sigma_{A n_{\text{other}}}^2) \quad (2.3-30c)$$

W is assumed to be a diagonal matrix of the form

$$W = \text{diag} \left(w_1, \dots, w_m \right) \quad (2.3-31)$$

Equations (2.3-28) through (2.3-31) give

$$P_n(t_0) = W_N^{-1} \left(W_A + \sum_{i=1}^m F_i^T F_i w_i^2 \sigma_i^2 \right) W_N^{-1} \quad (2.3-32)$$

where

$$W_N = W_A + \sum_{i=1}^m F_i^T F_i w_i \quad (2.3-33)$$

with the row vector F_i given by Equation (2.3-5). For minimum variance weighting, set $W = R^{-1}$ so that $P_n(t_0)$ assumes its minimum value $P_n(t_0) = W_N^{-1}$. Note that this only minimizes the data noise contribution to the total covariance.

2.3.2.2 Consider Parameter Contribution

It is assumed that all consider parameters are uncorrelated so that

$$\begin{aligned} E[\Delta\bar{\gamma}\Delta\bar{\gamma}^T] &= \text{diag} \left(\sigma_{\gamma_1}^2, \dots, \sigma_{\gamma_{n_\gamma}}^2 \right) \\ E \left[\Delta\bar{\beta}(t_0) \Delta\bar{\beta}^T(t_0) \right] &= \text{diag} \left(\sigma_{\beta_1}^2, \dots, \sigma_{\beta_{n_\beta}}^2 \right) \end{aligned} \quad (2.3-34)$$

Using this with Equations (2.3-14), (2.3-15), (2.3-19), (2.3-20), (2.3-24) and (2.3-25) gives

$$P_Y(t) = \Phi(t, t_0) \left\{ \sum_{i=1}^{n_Y} \sigma_{Y_i}^2 \left[\frac{\partial \bar{s}}{\partial \gamma_i}(t_0) \right] \left[\frac{\partial \bar{s}}{\partial \gamma_i}(t_0) \right]^T \right\} \Phi^T(t, t_0) \quad (2.3-35)$$

$$P_\beta(t) = \sum_{i=1}^{n_\beta} \sigma_{\beta_i}^2 \left[\Phi(t, t_0) \frac{\partial \bar{s}}{\partial \beta_i}(t_0) + \Theta_i(t, t_0) \right] \times \left[\Phi(t, t_0) \frac{\partial \bar{s}}{\partial \beta_i}(t_0) + \Theta_i(t, t_0) \right]^T \quad (2.3-36)$$

where, from Equations (2.3-14) and (2.3-15),

$$\frac{\partial \bar{s}}{\partial \gamma}(t_0) = -W_N^{-1} \sum_{i=1}^m F_i^T \Gamma_i w_i = \left[\frac{\partial \bar{s}}{\partial \gamma_1}(t_0) \mid \dots \mid \frac{\partial \bar{s}}{\partial \gamma_{n_Y}}(t_0) \right] \quad (2.3-37)$$

$$\frac{\partial \bar{s}}{\partial \beta}(t_0) = -W_N^{-1} \sum_{i=1}^m F_i^T B_i w_i = \left[\frac{\partial \bar{s}}{\partial \beta_1}(t_0) \mid \dots \mid \frac{\partial \bar{s}}{\partial \beta_{n_\beta}}(t_0) \right] \quad (2.3-28)$$

with

$$\Theta(t, t_0) = \left[\Theta_1(t, t_0) \mid \dots \mid \Theta_{n_\beta}(t, t_0) \right]$$

Γ_i , F_i , and B_i defined by Equations (2.2-9), (2.3-5), and (2.3-6), respectively; and w_i and W_N as in Section 2.3.2.1. The quantities Γ_i and B_i are row vectors of dimensionality n_γ and n_β , respectively.

2.3.2.3 Dynamic Noise Contribution

From Equations (2.3-16), (2.3-21), and (2.3-26) we have

$$\begin{aligned} P_u(t) = & D(t, t_0) + \Phi(t, t_0) P_u(t_0) \Phi^T(t, t_0) \\ & - \Phi(t, t_0) W_N^{-1} F^T W E \left[\bar{U} \bar{\Psi}^T(t, t_0) \right] \\ & - E \left[\bar{\Psi}(t, t_0) \bar{U}^T \right] W F W_N^{-1} \Phi^T(t, t_0) \end{aligned} \quad (2.3-39)$$

where

$$D(t, t_0) \equiv E \left[\bar{\Psi}(t, t_0) \bar{\Psi}^T(t, t_0) \right] = \left[\begin{array}{c|c} d_s(t, t_0) & 0 \\ \hline 0 & 0 \end{array} \right] \quad (2.3-40)$$

with d_s defined by Equation (2.2-14), and

$$P_u(t_0) = W_N^{-1} F^T W E [\bar{U} \bar{U}^T] W F W_N^{-1} \quad (2.3-41)$$

Using Equations (2.3-7), (2.3-9), and (2.3-31) gives

$$F^T W \bar{U} = \sum_{i=1}^m M_{G_i} \bar{\Psi}_s(t_i, t_0) \quad (2.3-42)$$

where

$$M_{G_i} \equiv F_i^T \frac{\partial g_i}{\partial \bar{s}_x} w_i \quad (2.3-43)$$

with F_i defined by Equation (2.3-5), and $\partial g_i / \partial \bar{s}_x$ defined by Equation (2.2-8).

The row vectors $\partial g_i / \partial \bar{s}_x$ have dimensionality equal to the number of dynamic solve-for parameters.

From Equation (2.3-42)

$$\begin{aligned} F^T W U U^T W F &= \left[\sum_{i=1}^m M_{G_i} \bar{\psi}_s(t_i, t_0) \right] \left[\sum_{j=1}^m M_{G_j} \bar{\psi}_s(t_j, t_0) \right]^T \\ &= \sum_{i=1}^m \left\{ M_{G_i} \bar{\psi}_s(t_i, t_0) \bar{\psi}_s^T(t_i, t_0) M_{G_i}^T \right. \\ &\quad + M_{G_i} \left[\sum_{j=1}^{i-1} \bar{\psi}_s(t_i, t_0) \bar{\psi}_s^T(t_j, t_0) M_{G_j}^T \right] \\ &\quad \left. + \left[\sum_{j=1}^{i-1} M_{G_j} \bar{\psi}_s(t_j, t_0) \bar{\psi}_s^T(t_i, t_0) \right] M_{G_i}^T \right\} \end{aligned} \quad (2.3-44)$$

Using this in Equation (2.3-41)

$$\begin{aligned}
 P_u(t_o) = & W_N^{-1} \sum_{i=1}^m \left\{ M_{G_i} d_s(t_i, t_o) M_{G_i}^T \right. \\
 & + M_{G_i} \left[\sum_{j=1}^{i-1} d'_s(t_i, t_j) M_{G_j}^T \right] \\
 & \left. + \left[\sum_{j=1}^{i-1} M_{G_j} d_s'^T(t_i, t_j) \right] M_{G_i}^T \right\} W_N^{-1}
 \end{aligned} \tag{2.3-45}$$

where d_s is defined by Equation (2.2-14) and for $t_i > t_j$

$$d'_s(t_i, t_j) \equiv E[\bar{\psi}_s(t_i, t_o) \bar{\psi}_s^T(t_j, t_o)] \tag{2.3-46}$$

Using Equation (2.2-1c), we see that this is the upper left-hand corner of the partitioned form of the larger matrix

$$\begin{aligned}
 d'(t_i, t_j) &= E[\bar{\psi}(t_i, t_o) \bar{\psi}^T(t_j, t_o)] \\
 &= \begin{bmatrix} d'_s(t_i, t_j) & d'_{s\beta}(t_i, t_j) \\ d'_{s\beta}^T(t_i, t_j) & d'_\beta(t_i, t_j) \end{bmatrix}
 \end{aligned} \tag{2.3-47}$$

This can be written, using Equation (2.1-8) and the fact that $E[\bar{\psi}(t_i, t_j) \bar{\psi}^T(t_j, t_o)] = 0$ for $t_i > t_j$, as

$$\begin{aligned}
 d'(t_i, t_j) &= \phi(t_i, t_j) d(t_j, t_o) \\
 &= \phi(t_i, t_o) \phi^{-1}(t_j, t_o) d(t_j, t_o)
 \end{aligned} \tag{2.3-48}$$

The group property of ϕ , Equation (2.1-7) has been used to obtain the last equality. Then combining Equations (2.2-1d), (2.2-13), (2.3-47), and (2.3-48) gives

$$d'_s(t_i, t_j) = [\phi_s(t_i, t_0) \mid \theta(t_i, t_0)] \phi^{-1}(t_j, t_0) \begin{bmatrix} d_s(t_j, t_0) \\ d_{s\beta}^T(t_j, t_0) \end{bmatrix} \quad (2.3-49)$$

Substituting Equation (2.3-49) into Equation (2.3-45) then gives

$$P_u(t_0) = W_N^{-1} \left\{ \sum_{i=1}^m \left[M_{G_i} d_s(t_i, t_0) M_{G_i}^T + M'_{G_i} Q_i + Q_i^T M_{G_i}^T \right] \right\} W_N^{-1} \quad (2.3-50)$$

where

$$Q_i \equiv \sum_{j=1}^{i-1} \phi^{-1}(t_j, t_0) \begin{bmatrix} d_s(t_j, t_0) \\ d_{s\beta}^T(t_j, t_0) \end{bmatrix} M_{G_j}^T \quad (2.3-51)$$

and

$$\begin{aligned} M'_{G_i} &\equiv M_{G_i} \left[\phi_s(t_i, t_0) \mid \theta(t_i, t_0) \right] \\ &= F_i^T \left[\frac{\partial g_i}{\partial s_x} \phi_s(t_i, t_0) \mid B_i \right] w_i \end{aligned} \quad (2.3-52)$$

where B_i is defined by Equation (2.3-6), and Equation (2.3-43) has been used in the last step.

From Equations (2.3-42), (2.3-46), (2.3-49), and (2.3-51) we also have:

$$\begin{aligned}
 F^T WE \left[\bar{U} \bar{\Psi}_S^T(t, t_0) \right] &= \sum_{i=1}^m M_{G_i} E \left[\bar{\Psi}_S(t_i, t_0) \bar{\Psi}_S^T(t, t_0) \right] \\
 &= \sum_{i=1}^{k-1} M_{G_i} E \left[\bar{\Psi}_S(t_i, t_0) \bar{\Psi}_S^T(t, t_0) \right] \\
 &\quad + \sum_{i=k}^m M_{G_i} E \left[\bar{\Psi}_S(t_i, t_0) \bar{\Psi}_S^T(t, t_0) \right] \quad (2.3-53) \\
 &= \sum_{i=1}^{k-1} M_{G_i} d_S'^T(t, t_i) + \sum_{i=k}^m M_{G_i} d_S'(t_i, t) \\
 &= Q_k^T \begin{bmatrix} \phi_S^T(t, t_0) \\ \theta^T(t, t_0) \end{bmatrix} + Q_k' \phi^{-1}(t, t_0) \begin{bmatrix} d_S(t, t_0) \\ d_{S\beta}^T(t, t_0) \end{bmatrix}
 \end{aligned}$$

where k is chosen so that $t_{k-1} < t \leq t_k$ and

$$Q_k' \equiv \sum_{i=k}^m M_{G_i}' \quad (2.3-54)$$

Then,

$$F^T WE \left[\bar{U} \bar{\Psi}^T(t, t_0) \right] = \left[F^T WE \left\{ \bar{U} \bar{\Psi}_S^T(t, t_0) \right\} \mid 0 \right] \quad (2.3-55)$$

and $P_u(t)$ can be computed by substituting Equations (2.3-40), (2.3-45), and (2.3-55) into Equation (2.3-39).

2.3.3 COMPUTATION

The analysis equations presented in the previous subsections have been carefully derived to allow efficient evaluation. This subsection outlines a procedure to efficiently perform these computations. This procedure is only intended to show the overall structure of the computations and does not necessarily cover all microefficiency details. The procedure has two stages: it first computes analysis results at the epoch time t_0 , and then uses these results to compute the various covariance matrices at a set of "output times" τ_1, \dots, τ_l . It is assumed that $t_0 \leq t_1 \leq t_2 \leq \dots \leq t_m$ and that $t_0 = \tau_1 < \tau_2 \dots < \tau_l$.

Stage 1: Compute Epoch Errors

The stage 1 procedure assumes that the following are available:

σ_i	See Equation (2.3-29)
W_A, w_i	See Equations (2.3-3) and (2.3-31)
$\partial g_i / \partial \bar{s}_x$	See Equation (2.2-8) and Sections 3.3 and 4.3
F_i	See Equation (2.3-5)
Γ_i	See Equation (2.2-9) and Sections 3.3 and 4.3
B_i	See Equation (2.3-6)
$D(t_i, t_0)$	See Equation (2.3-40) and Sections 3.2 and 4.2
$\Phi(t_i, t_0)$	See Equation (2.2-5) and Sections 3.2 and 4.2
$\phi_s(t_i, t_0)$	See Equation (2.2-1d) and Sections 3.2 and 4.2

$\Theta(t_i, t_o)$ See Equation (2.2-1d) and Sections 3.2 and 4.2

$\phi^{-1}(t_i, t_o)$ See Equations (2.1-5) and (2.1-7) and Sections 3.2 and 4.2

The procedure produces the covariance matrices P_n and P_u and the sensitivity matrices $\partial \bar{s} / \partial \bar{\gamma}$ and $\partial \bar{s} / \partial \bar{\beta}$, all at the epoch time t_o , and the intermediate matrices M'_{G_i} , P_N , Q_i , Q' , and Q_F . These results are accumulated during a single pass over all the measurements.

1. Initialize M_n , M_u , M_γ , M_β , Q' , Q_F , and Q_1 to zero.

2. For $i \leftarrow 1$ to m , do

a. $M_n \leftarrow M_n + F_i^T F_i w_i^2 \sigma_i^2$

b. $M_\gamma \leftarrow M_\gamma + F_i^T \Gamma_i w_i$

c. $M_G \leftarrow F_i^T \frac{\partial g_i}{\partial s_x} w_i$

d. $M_F \leftarrow F_i^T F_i w_i$

e. $M_B \leftarrow F_i^T B_i w_i$

f. Let $M_F = \begin{bmatrix} M_{F_S} & M_{F_P} \end{bmatrix}$ (with solve-for and consider columns) in $M'_{G_i} \leftarrow \begin{bmatrix} M_{F_S} & M_B \end{bmatrix}$

g. $M_u \leftarrow M_u + M_G d_s(t_i, t_o) M_G^T + M'_{G_i} Q_i + Q_i^T M'_{G_i}$

h. $M_\beta \leftarrow M_\beta + M_B$

i. $Q_{i+1} \leftarrow Q_i + \phi^{-1}(t_i, t_o) \begin{bmatrix} d_s(t_i, t_o) \\ d_{s\beta}^T(t_i, t_o) \end{bmatrix} M_G^T$

j. $Q_F \leftarrow Q_F + M_F$

k. $Q' \leftarrow Q' + M'_{G_i}$

3. $P_N \leftarrow (W_A + Q_F)^{-1}$
4. $P_n \leftarrow \begin{cases} P_N & , \text{ for minimum variance} \\ P_N (W_A + M_n) P_N & \text{ weighting} \\ & , \text{ otherwise} \end{cases}$
5. $P_u \leftarrow P_N M_u P_N$
6. $\frac{\partial \bar{s}}{\partial \gamma}(t_o) \leftarrow -P_N M_\gamma$
7. $\frac{\partial \bar{s}}{\partial \beta}(t_o) \leftarrow -P_N M_\beta$

Stage 2: Compute Error Analysis Results

In addition to the results of stage 1, the stage 2 procedure assumes that the following are available:

- $\sigma_{\gamma_i}, \sigma_{\beta_i}$ See Equation (2.3-34)
- $\Phi(\tau_i, t_o)$ See Equation (2.2-5) and Sections 3.2 and 4.2
- $D(\tau_i, t_o)$ See Equation (2.3-40) and Sections 3.2 and 4.2
- $\Theta(\tau_i, t_o)$ See Equation (2.2-7) and Sections 3.2 and 4.2

The procedure produces the covariance matrices $P_n(\tau_i)$, $P_\gamma(\tau_i)$, $P_\beta(\tau_i)$, $P_u(\tau_i)$, and $P(\tau_i)$ for each output time τ_i :

1. Set $k \leftarrow 1$
2. For $i \leftarrow 1$ to ℓ , do
 - a. $P_n(\tau_i) \leftarrow \Phi(\tau_i, t_o) P_n \Phi^T(\tau_i, t_o)$
 - b. Let $\frac{\partial \bar{s}}{\partial \gamma} = \Phi(\tau_i, t_o) \frac{\partial \bar{s}}{\partial \gamma}(t_o) = \left[\begin{array}{c|c|c} \frac{\partial \bar{s}}{\partial \gamma_1} & \cdots & \frac{\partial \bar{s}}{\partial \gamma_{n_\gamma}} \end{array} \right]$

in

$$P_Y(\tau_i) \leftarrow \sum_{j=1}^{n_Y} \sigma_{Y_j}^2 \frac{\partial \bar{s}}{\partial Y_j} \frac{\partial \bar{s}^T}{\partial Y_j}$$

c. Let $\frac{\partial \bar{s}}{\partial \beta} = \Phi(\tau_i, t_0) \frac{\partial \bar{s}}{\partial \beta}(t_0) + \Theta(\tau_i, t_0)$

$$= \left[\begin{array}{c|c} \frac{\partial \bar{s}}{\partial \beta_1} & \dots & \frac{\partial \bar{s}}{\partial \beta_{n_\beta}} \end{array} \right]$$

in

$$P_\beta(\tau_i) \leftarrow \sum_{j=1}^{n_\beta} \sigma_{\beta_j}^2 \frac{\partial \bar{s}}{\partial \beta_j} \frac{\partial \bar{s}^T}{\partial \beta_j}$$

d. While $t_k \leq \tau_i$, do

(1) $Q' \leftarrow Q' - M_{G_k}$

(2) $k \leftarrow k + 1$

e. Let $P' = \Phi(\tau_i, t_0) P_N \left\{ Q_k^T \left[\begin{array}{c|c} \phi_s^T(\tau_i, t_0) & 0 \\ \hline \theta^T(\tau_i, t_0) & 0 \end{array} \right] \right.$

$$\left. + Q'^T \phi^{-1}(\tau_i, t_0) \left[\begin{array}{c|c} d_s(\tau_i, t_0) & 0 \\ \hline d_{s\beta}^T(\tau_i, t_0) & 0 \end{array} \right] \right\}$$

in

$$P_u(\tau_i) = D(\tau_i, t_0)$$

$$+ \Phi(\tau_i, t_0) P_u \Phi^T(\tau_i, t_0) - P' - P'^T$$

$$f. \quad P(\tau_i) \leftarrow P_n(\tau_i) + P_\gamma(\tau_i) + P_\beta(\tau_i) + P_u(\tau_i)$$

2.4 SEQUENTIAL FILTER

A sequential filter produces an estimate $\bar{s}^*(t)$ based on measurements taken at discrete times $t_i \leq t$. Between distinct measurement times, the state estimate $\bar{x}^*(t)$ is propagated using Equation (2.1-2). For each measurement y_i , the solve-for parameters are updated based on the pre-update state $\bar{x}^*(i-)$ and the measurement. Typically, this update has the following form:

$$\bar{s}^*(i+) = \bar{s}^*(i-) + K_i \Delta y_i \quad (2.4-1)$$

where $\bar{s}^*(i+)$ and $\bar{s}^*(i-)$ denote the estimate of solve-for parameters immediately after and immediately before incorporating the information contained in the measurement. This notation must be distinguished from $\bar{s}^*(t_i)$, which denotes the solve-for parameter estimate incorporating the information contained in all the measurements at t_i , which may include measurements other than y_i . The gain matrix K_i determines how much the propagated state is corrected, based on the measurement residual Δy_i ; this is a column vector with dimension equal to the number of solve-for parameters.

2.4.1 ESTIMATION ERRORS

The estimation error immediately after an update is

$$\begin{aligned} \Delta \bar{s}(i+) &= \bar{s}(t_i) - \bar{s}^*(i+) = \bar{s}(t_i) - \bar{s}^*(i-) - K_i \Delta y_i \\ &= \Delta \bar{s}(i-) - K_i \Delta y_i, \end{aligned} \quad (2.4-2)$$

since the true state is continuous at t_i . Substituting Equation (2.2-4) for Δy_i gives

$$\Delta \bar{s}(i+) = (I - K_i G_i) \Delta \bar{s}(i-) - K_i (\Gamma_i \Delta \bar{\gamma} + v_i) \quad (2.4-3)$$

We divide $\Delta \bar{s}(t)$ into separate contributions due to measurement noise, measurement consider parameters, dynamic consider parameters and dynamic noise:

$$\Delta \bar{s}(t) = \Delta \bar{s}_n(t) + \Delta \bar{s}_\gamma(t) + \Delta \bar{s}_\beta(t) + \Delta \bar{s}_u(t) \quad (2.4-4)$$

These obey the update equations

$$\Delta \bar{s}_n(i+) = (I - K_i G_i) \Delta \bar{s}_n(i-) - K_i v_i \quad (2.4-5)$$

$$\Delta \bar{s}_\gamma(i+) = (I - K_i G_i) \Delta \bar{s}_\gamma(i-) - K_i \Gamma_i \Delta \bar{\gamma} \quad (2.4-6)$$

$$\Delta \bar{s}_\beta(i+) = (I - K_i G_i) \Delta \bar{s}_\beta(i-) \quad (2.4-7)$$

$$\Delta \bar{s}_u(i+) = (I - K_i G_i) \Delta \bar{s}_u(i-) \quad (2.4-8)$$

consistently with Equations (2.4-3) and (2.4-4). If $t_i = t_{i+1}$, then $\Delta \bar{s}(i+) = \Delta \bar{s}(i+1-)$, and similar relations hold for $\Delta \bar{s}_n$, $\Delta \bar{s}_\gamma$, $\Delta \bar{s}_\beta$, and $\Delta \bar{s}_u$.

If $t_i \neq t_{i+1}$, which means that y_i is the last measurement processed at t_i , $\Delta \bar{s}(t_i)$ is equal to $\Delta \bar{s}(i+)$, since it incorporates the information contained in all the measurements for times less than or equal to t_i . Then from

Equation (2.2-2), propagating the estimate $\bar{s}^*(t_i)$ will result in an error for $t_i \leq t < t_{i+1}$ given by

$$\Delta \bar{s}(t) = \Phi(t, t_i) \Delta \bar{s}(t_i) + \Theta(t, t_i) \Delta \bar{\beta}(t_i) + \bar{\Psi}(t, t_i) \quad (2.4-9)$$

The limit of $\Delta \bar{s}(t)$ as t approaches t_{i+1} is the estimate error $\Delta \bar{s}(t_{i+1}-)$. Inserting Equations (2.2-3) and (2.4-4) into Equation (2.4-9) gives the following propagation equations for the noise and consider components of the estimation error

$$\Delta \bar{s}_n(t) = \Phi(t, t_i) \Delta \bar{s}_n(t_i) \quad (2.4-10)$$

$$\Delta \bar{s}_\gamma(t) = \Phi(t, t_i) \Delta \bar{s}_\gamma(t_i) \quad (2.4-11)$$

$$\Delta \bar{s}_\beta(t) = \Phi(t, t_i) \Delta \bar{s}_\beta(t_i) + \Theta(t, t_i) \phi_\beta(t_i, t_o) \Delta \bar{\beta}(t_o) \quad (2.4-12)$$

$$\Delta \bar{s}_u(t) = \Phi(t, t_i) \Delta \bar{s}_u(t_i) + \Theta(t, t_i) \bar{\psi}_\beta(t_i, t_o) \quad (2.4-13)$$

$$+ \bar{\Psi}(t, t_i)$$

The complete specification of $\Delta \bar{s}_n$, $\Delta \bar{s}_\gamma$, $\Delta \bar{s}_\beta$, and $\Delta \bar{s}_u$ requires the initial conditions

$$\Delta \bar{s}_n(t_o) = \Delta \bar{s}(t_o) \quad (2.4-14)$$

$$\Delta \bar{s}_\gamma(t_o) = \Delta \bar{s}_\beta(t_o) = \Delta \bar{s}_u(t_o) = 0 \quad (2.4-15)$$

2.4.2 COVARIANCE

Equation (2.4-4) gives the estimation errors induced by the systematic error sources $\Delta\bar{\gamma}$ and $\Delta\bar{\beta}$ and the random error sources \bar{u} and v_i . It is assumed that all these error sources are uncorrelated. The covariance matrix $P(t)$ is then

$$\begin{aligned} P(t) &\equiv E[\Delta\bar{s}(t) \Delta\bar{s}^T(t)] \\ &= P_n(t) + P_\gamma(t) + P_\beta(t) + P_u(t) \end{aligned} \quad (2.4-16)$$

where

$$P_n(t) \equiv E[\Delta\bar{s}_n(t) \Delta\bar{s}_n^T(t)] + D^*(t, t_0) \quad (2.4-17)$$

$$P_\gamma(t) \equiv E[\Delta\bar{s}_\gamma(t) \Delta\bar{s}_\gamma^T(t)] \quad (2.4-18)$$

$$P_\beta(t) \equiv E[\Delta\bar{s}_\beta(t) \Delta\bar{s}_\beta^T(t)] \quad (2.4-19)$$

$$P_u(t) \equiv E[\Delta\bar{s}_u(t) \Delta\bar{s}_u^T(t)] - D^*(t, t_0) \quad (2.4-20)$$

The matrix $D^*(t, t_0)$ represents an estimate of the dynamic noise used to compute the gain matrix. It obeys the update equation at measurement y_i :

$$D^*(i+, t_0) = (I - K_i G_i) D^*(i-, t_0) (I - K_i G_i)^T \quad (2.4-21)$$

If $t_i \neq t_{i+1}$, $D^*(t, t_0)$ obeys the propagation equation for $t_i \leq t < t_{i+1}$

$$D^*(t, t_0) = \Phi(t, t_i) D^*(t_i, t_0) \Phi^T(t, t_i) + D^*(t, t_i) \quad (2.4-22a)$$

with

$$D^*(t, t_i) = \left[\begin{array}{c|c} d_s^*(t, t_i) & 0 \\ \hline 0 & 0 \end{array} \right] \quad (2.4-22b)$$

and

$$d_s^*(t, t_i) = \int_{t_i}^t [\phi_s(t, t') \mid \theta(t, t')] Q_u^* \left[\begin{array}{c} \phi_s^T(t, t') \\ \hline \theta^T(t, t') \end{array} \right] dt' \quad (2.4-22c)$$

Q_u^* is a diagonal matrix of estimates of the covariances of the dynamic noise. The matrix $D^*(t, t_0)$ has the initial value $D^*(t_0, t_0) = 0$.

The following subsections discuss each of these contributions to the overall covariance. In each case, the propagation step is unnecessary if $t_i = t_{i+1}$.

2.4.2.1 Noise-Induced Contribution

From Equations (2.4-10), (2.4-17), and (2.4-22) we have

$$P_n(t) = \Phi(t, t_i) P_n(t_i) \Phi^T(t, t_i) + D^*(t, t_i) \quad (2.4-23)$$

for $t_i \leq t < t_{i+1}$. From Equations (2.4-5), (2.4-17), and (2.4-21), the covariance update is

$$P_n(i+) = (I - K_i G_i) P_n(i-)(I - K_i G_i)^T + K_i R_i K_i^T. \quad (2.4-24)$$

with

$$R_i \equiv E \left[v_i^2 \right] = \sigma_i^2 \quad (2.4-25)$$

The initial value $P_n(t_0)$ is the a priori covariance P_A , given by Equation (2.3-30b).

For Kalman filtering, K_i is chosen to be the Kalman gain defined by

$$K_i = P_n(i-) G_i^T \left[G_i P_n(i-) G_i^T + R_i \right]^{-1} \quad (2.4-26)$$

Note that a Kalman filter minimizes only the noise-induced contribution to the overall covariance.

2.4.2.2 Consider Parameter Contribution

It is assumed that all consider parameters are (initially) uncorrelated so that

$$E[\Delta \bar{\gamma} \Delta \bar{\gamma}^T] = \text{diag} \left(\sigma_{\gamma_1}^2, \dots, \sigma_{\gamma_{n_\gamma}}^2 \right) \quad (2.4-27)$$

$$E[\Delta \bar{\beta}(t_0) \Delta \bar{\beta}^T(t_0)] = \text{diag} \left(\sigma_{\beta_1}^2, \dots, \sigma_{\beta_{n_\beta}}^2 \right) \quad (2.4-28)$$

Using this with Equations (2.4-18) and (2.4-19) and defining $\partial \bar{s} / \partial \bar{\gamma}$ and $\partial \bar{s} / \partial \bar{\beta}$ so that

$$\Delta \bar{s}_{\gamma}(t) = \frac{\partial \bar{s}}{\partial \bar{\gamma}}(t) \Delta \bar{\gamma} \quad (2.4-29)$$

$$\Delta \bar{s}_{\beta}(t) = \frac{\partial \bar{s}}{\partial \bar{\beta}}(t) \Delta \bar{\beta}(t_0) \quad (2.4-30)$$

then gives

$$P_{\gamma}(t) = \sum_{i=1}^{n_{\gamma}} \sigma_{\gamma_i}^2 \left[\frac{\partial \bar{s}}{\partial \gamma_i}(t) \right] \left[\frac{\partial \bar{s}}{\partial \gamma_i}(t) \right]^T \quad (2.4-31)$$

$$P_{\beta}(t) = \sum_{i=1}^{n_{\beta}} \sigma_{\beta_i}^2 \left[\frac{\partial \bar{s}}{\partial \beta_i}(t) \right] \left[\frac{\partial \bar{s}}{\partial \beta_i}(t) \right]^T \quad (2.4-32)$$

where, from Equations (2.4-11) and (2.4-12),

$$\frac{\partial \bar{s}}{\partial \bar{\gamma}}(t) = \Phi(t, t_i) \frac{\partial \bar{s}}{\partial \bar{\gamma}}(t_i) = \left[\frac{\partial \bar{s}}{\partial \gamma_1} \mid \cdots \mid \frac{\partial \bar{s}}{\partial \gamma_{n_{\gamma}}} \right] \quad (2.4-33)$$

$$\frac{\partial \bar{s}}{\partial \bar{\beta}}(t) = \Phi(t, t_i) \frac{\partial \bar{s}}{\partial \bar{\beta}}(t_i) + \Theta(t, t_i) \phi_{\beta}(t_i, t_0) \quad (2.4-34)$$

$$= \left[\frac{\partial \bar{s}}{\partial \beta_1} \mid \cdots \mid \frac{\partial \bar{s}}{\partial \beta_{n_{\beta}}} \right]$$

Using Equations (2.4-29) and (2.4-30) in Equations (2.4-6) and (2.4-7) gives the following update equations:

$$\frac{\partial \bar{s}}{\partial \gamma} (i+) = (I - K_i G_i) \frac{\partial \bar{s}}{\partial \gamma} (i-) - K_i \Gamma_i \quad (2.4-35)$$

$$\frac{\partial \bar{s}}{\partial \beta} (i+) = (I - K_i G_i) \frac{\partial \bar{s}}{\partial \beta} (i-) \quad (2.4-36)$$

Both these matrices are zero at the initial time t_0 .

2.4.2.3 Residual Dynamic Noise Contribution

From Equations (2.4-13), (2.4-20), and (2.4-22) we have

$$\begin{aligned} P_u(t) = & \Phi(t, t_i) P_u(t_i) \Phi^T(t, t_i) + \Phi(t, t_i) P_{u\beta}(t_i) \Theta^T(t, t_i) \\ & + \Theta(t, t_i) P_{u\beta}^T(t_i) \Phi^T(t, t_i) + \Theta(t, t_i) d_\beta(t_i, t_0) \Theta^T(t, t_i) \\ & + D(t, t_i) - D^*(t, t_i) \end{aligned} \quad (2.4-37)$$

where

$$P_{u\beta}(t) \equiv E \left[\Delta \bar{s}_u(t) \bar{\psi}_\beta^T(t, t_0) \right] \quad (2.4-38)$$

and d_β is defined by Equation (2.2-15).

It follows from Equations (2.1-8), (2.2-1c), and (2.2-1d) that

$$\bar{\psi}_\beta(t, t_0) = \Phi_\beta(t, t_i) \bar{\psi}_\beta(t_i, t_0) + \bar{\psi}_\beta(t, t_i) \quad (2.4-39)$$

Using this and Equation (2.4-13) in Equation (2.4-38) gives

$$\begin{aligned} P_{u\beta}(t) = & \Phi(t, t_i) P_{u\beta}(t_i) \Phi_{\beta}^T(t, t_i) \\ & + \Theta(t, t_i) d_{\beta}(t_i, t_o) \Phi_{\beta}^T(t, t_i) \\ & + D_{s\beta}(t, t_i) \end{aligned} \quad (2.4-40)$$

where

$$D_{s\beta}(t, t_i) \equiv E \left[\bar{\Psi}(t, t_i) \bar{\Psi}_{\beta}^T(t, t_i) \right] = \begin{bmatrix} d_{s\beta}(t, t_i) \\ \hline 0 \end{bmatrix} \quad (2.4-41)$$

with $d_{s\beta}$ given by Equation (2.2-16).

Using Equation (2.4-39) in Equation (2.2-15) gives

$$d_{\beta}(t, t_o) = \Phi_{\beta}(t, t_i) d_{\beta}(t_i, t_o) \Phi_{\beta}^T(t, t_i) + d_{\beta}(t, t_i) \quad (2.4-42)$$

From Equations (2.4-8), (2.4-20), and (2.4-21), the covariance updates for P_u and $P_{u\beta}$ are

$$P_u(i+) = (I - K_i G_i) P_u(i-) (I - K_i G_i)^T$$

$$P_{u\beta}(i+) = (I - K_i G_i) P_{u\beta}(i-)$$

Both P_u and $P_{u\beta}$ are zero at the initial time t_o .

2.4.3 COMPUTATION

The analysis equations presented in the previous subsections have been carefully derived to allow efficient evaluation. This subsection outlines a procedure to efficiently perform

these computations. This procedure is only intended to show the overall structure of the computation and is not concerned with all microefficiency details. The procedure propagates an initial covariance P_A to the output times τ_1, \dots, τ_l , performing measurement updates at times t_1, \dots, t_m . It is assumed that $t_0 \leq t_1 \leq t_2 \leq \dots \leq t_m$ and that $t_0 = \tau_1 < \tau_2 < \dots < \tau_l$.

The procedure assumes that the following are available:

P_A	See Equation (2.3-30) and Sections 3.2 and 4.2
σ_i	See Equation (2.4-25)
G_i	See Equation (2.2-8) and Sections 3.3 and 4.3
Γ_i	See Equation (2.2-9) and Sections 3.3 and 4.3
$\Phi(t, t')$	See Equation (2.2-5) and Sections 3.2 and 4.2
$\Theta(t, t')$	See Equation (2.2-7) and Sections 3.2 and 4.2
$\phi(t, t')$	See Equation (2.1-5) and Sections 3.2 and 4.2
$\phi_\beta(t, t')$	See Equation (2.2-1d) and Sections 3.2 and 4.2
$D(t, t')$	See Equation (2.3-40) and Sections 3.2 and 4.2
$d(t, t')$	See Equation (2.2-13) and Sections 3.2 and 4.2
$d_\beta(t, t')$	See Equation (2.2-15) and Sections 3.2 and 4.2

$D_{s\beta}(t, t')$ See Equation (2.4-41) and Sections 3.2 and 4.2

$D^*(t, t')$ See Equation (2.4-21)

$\sigma_{\gamma_i}, \sigma_{\beta_i}(t_0)$ See Equations (2.4-27) and (2.4-28)

The procedure produces the covariance matrices $P_n(\tau_i)$, $P_\gamma(\tau_i)$, $P_\beta(\tau_i)$, $P_u(\tau_i)$, and $P(\tau_i)$ and the analysis matrices $\phi(\tau_i, \tau_{i-1})$ and $d(\tau_i, \tau_{i-1})$ for each output time τ_i :

1. Set $P_n \leftarrow P_A$
Initialize $\partial \bar{s} / \partial \bar{\gamma}$, $\partial \bar{s} / \partial \bar{\beta}$, P_u , $P_{u\beta}$, d , and d_β to zero
Initialize ϕ to the $N \times N$ identity matrix
Set $i \leftarrow 1$, $k \leftarrow 1$, $t' \leftarrow t_0$

2. While $i \leq l$ do:

Let $t = \min(\tau_i, t_k)$ in

- a. If $t \neq t'$ then:

$$(1) \quad P_n \leftarrow \Phi(t, t') P_n \Phi^T(t, t') + D^*(t, t')$$

$$(2) \quad \frac{\partial \bar{s}}{\partial \bar{\gamma}} \leftarrow \Phi(t, t') \frac{\partial \bar{s}}{\partial \bar{\gamma}}$$

$$(3) \quad \frac{\partial \bar{s}}{\partial \bar{\beta}} \leftarrow \Phi(t, t') \frac{\partial \bar{s}}{\partial \bar{\beta}} + \Theta(t, t') \phi_\beta(t, t')$$

$$(4) \quad P_u \leftarrow \Phi(t, t') P_u \Phi^T(t, t') \\
+ \Phi(t, t') P_{u\beta} \Theta^T(t, t') \\
+ \Theta(t, t') P_{u\beta}^T \Phi^T(t, t') \\
+ \Theta(t, t') d_\beta \Theta^T(t, t') \\
+ D(t, t') - D^*(t, t')$$

$$(5) \quad P_{u\beta} \leftarrow \Phi(t, t') P_{u\beta} \Phi_{\beta}^T(t, t') \\ + \Theta(t, t') d_{\beta} \Phi_{\beta}^T(t, t') + D_{s\beta}(t, t')$$

$$(6) \quad d_{\beta} \leftarrow \Phi_{\beta}(t, t') d_{\beta} \Phi_{\beta}^T(t, t') + d_{\beta}(t, t')$$

$$(7) \quad \phi \leftarrow \Phi(t, t') \phi$$

$$(8) \quad d \leftarrow \Phi(t, t') d \Phi^T(t, t') + d(t, t')$$

b. If $t = t_k$ then:

Let

$$K = P_n G_k^T (G_k P_n G_k^T + \sigma_k^2)^{-1}$$

$$M = I - KG_k$$

in

$$(1) \quad P_n \leftarrow MP_n M^T + K \sigma_k^2 K^T$$

$$(2) \quad \frac{\partial \bar{S}}{\partial \gamma} \leftarrow M \frac{\partial \bar{S}}{\partial \gamma} - K \Gamma_k$$

$$(3) \quad \frac{\partial \bar{S}}{\partial \beta} \leftarrow M \frac{\partial \bar{S}}{\partial \beta}$$

$$(4) \quad P_u \leftarrow MP_u M^T$$

$$(5) \quad P_{u\beta} \leftarrow MP_{u\beta}$$

$$(6) \quad k \leftarrow k + 1$$

c. If $t = \tau_i$ then:

$$\text{Let } \frac{\partial \bar{s}}{\partial \gamma} = \left[\frac{\partial \bar{s}}{\partial \gamma_1} \mid \dots \mid \frac{\partial \bar{s}}{\partial \gamma_{n_\gamma}} \right]$$

$$\frac{\partial \bar{s}}{\partial \beta} = \left[\frac{\partial \bar{s}}{\partial \beta_1} \mid \dots \mid \frac{\partial \bar{s}}{\partial \beta_{n_\beta}} \right]$$

in

$$(1) \quad P_n(\tau_i) \leftarrow P_n$$

$$(2) \quad P_\gamma(\tau_i) \leftarrow \sum_{j=1}^{n_\gamma} \sigma_{\gamma_j}^2 \left(\frac{\partial \bar{s}}{\partial \gamma_j} \right) \left(\frac{\partial \bar{s}}{\partial \gamma_j} \right)^T$$

$$(3) \quad P_\beta(\tau_i) \leftarrow \sum_{j=1}^{n_\beta} \sigma_{\beta_j}^2(t_o) \left(\frac{\partial \bar{s}}{\partial \beta_j} \right) \left(\frac{\partial \bar{s}}{\partial \beta_j} \right)^T$$

$$(4) \quad P_u(\tau_i) \leftarrow P_u$$

$$(5) \quad P(\tau_i) \leftarrow P_n(\tau_i) + P_\gamma(\tau_i) + P_\beta(\tau_i) + P_u(\tau_i)$$

$$(6) \quad \phi(\tau_i, \tau_{i-1}) \leftarrow \phi$$

$$(7) \quad d(\tau_i, \tau_{i-1}) \leftarrow d$$

(8) Reset d to zero and ϕ to the $N \times N$ identity matrix

$$(9) \quad i \leftarrow i + 1$$

d. $t' \leftarrow t$

SECTION 3 - SPIN-STABILIZED SPACECRAFT MODELS

As Section 2 discussed estimation filtering in a general sense, this section provides specific attitude and sensor models for spinning spacecraft. These models provide the basis for the construction of the state transition, measurement partial derivative, and random excitation matrices used in Section 2.

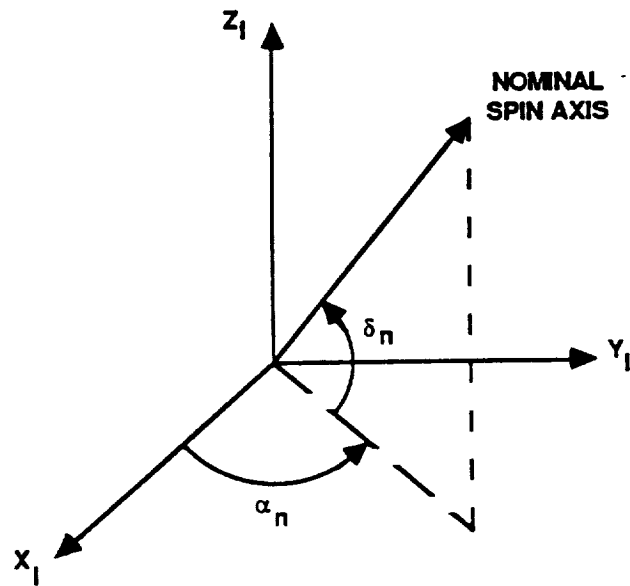
3.1 ATTITUDE GENERATION

For spin-stabilized spacecraft, the attitude is determined by the direction of the spin axis. The nominal spin axis is assumed to be fixed in inertial space and is specified by its right ascension α_n and its declination δ_n as shown in Figure 3-1. The actual spin axis may drift from this inertially fixed nominal position. ADEAS provides a model for sinusoidal variations of the actual spin axis about the nominal axis:

$$\alpha^*(t) = \alpha_n + a_\alpha \sin [\zeta (t - t_0) + b_\alpha] \quad (3.1-1)$$

$$\delta^*(t) = \delta_n + a_\delta \sin [\zeta (t - t_0) + b_\delta] \quad (3.1-2)$$

where the amplitudes a_α and a_δ are constant dynamic parameters, while the frequency ζ and the phases b_α and b_δ are assumed to be exactly known. The spin-axis attitude defined by α^* and δ^* is used in all sensor model computations.



0450 S12/4/1

Figure 3-1. Right Ascension and Declination of the Nominal Spin Axis

3.2 DYNAMIC ERROR MODEL

If we define a state vector \bar{x} by

$$\bar{x} = \begin{bmatrix} \alpha \\ \delta \\ a_\alpha \\ a_\delta \end{bmatrix} \quad (3.2-1)$$

then differentiating Equations (3.1-1) and (3.1-2) gives the dynamic model for spin-stabilized spacecraft in the form of Equation (2.1-1):

$$\dot{\bar{x}}(t) = \begin{bmatrix} a_\alpha \zeta \cos [\zeta(t - t_0) + b_\alpha] \\ a_\delta \zeta \cos [\zeta(t - t_0) + b_\delta] \\ 0 \\ 0 \end{bmatrix} + \begin{bmatrix} u_\alpha(t) \\ u_\delta(t) \\ 0 \\ 0 \end{bmatrix} \quad (3.2-2)$$

where u_α and u_δ are dynamic noise processes that induce additional attitude variations.

From Equation (3.2-2), the state transition matrix, as defined by Equation (2.1-5), is then

$$\phi(t, t') = \begin{bmatrix} 1 & 0 & \phi_\alpha & 0 \\ 0 & 1 & 0 & \phi_\delta \\ 0 & 0 & 1 & 0 \\ 0 & 0 & 0 & 1 \end{bmatrix} \quad (3.2-3a)$$

with

$$\phi_\alpha \equiv \sin [\zeta(t - t_0) + b_\alpha] - \sin [\zeta(t' - t_0) + b_\alpha] \quad (3.2-3b)$$

and

$$\phi_\delta \equiv \sin [\zeta(t - t_0) + b_\delta] - \sin [\zeta(t' - t_0) + b_\delta] \quad (3.2-3c)$$

The inverse of the state transition matrix is

$$\phi^{-1}(t, t') = \begin{bmatrix} 1 & 0 & -\phi_\alpha & 0 \\ 0 & 1 & 0 & -\phi_\delta \\ 0 & 0 & 1 & 0 \\ 0 & 0 & 0 & 1 \end{bmatrix} \quad (3.2-4)$$

The a priori covariance of the attitude error parameters is

$$P_{\text{Attitude}} = \text{diag} \left(\sigma_\alpha^2, \sigma_\delta^2 \right) \quad (3.2-5)$$

Defining $\bar{\psi}$ as in Equation (2.1-6) the random excitation matrix is

$$d(t, t') \equiv E \left[\bar{\psi}(t, t') \bar{\psi}^T(t, t') \right] = \begin{bmatrix} Q_{\alpha} & 0 & 0 & 0 \\ 0 & Q_{\delta} & 0 & 0 \\ 0 & 0 & 0 & 0 \\ 0 & 0 & 0 & 0 \end{bmatrix} \Delta t \quad (3.2-6)$$

where

$$\begin{aligned} E \left[\bar{u}_{\alpha}(t) \bar{u}_{\alpha}^T(t') \right] &= Q_{\alpha} \delta(t - t') \\ E \left[\bar{u}_{\delta}(t) \bar{u}_{\delta}^T(t') \right] &= Q_{\delta} \delta(t - t') \end{aligned} \quad (3.2-7)$$

The partitioning of d in Equation (3.2-6) is not the same as the partitioning in Equation (2.2-13); the two partitionings are related by row and column interchanges depending on the selection of dynamic solve-for and consider parameters.

3.3 SENSOR MODELS

The spin-axis sensors modeled by ADEAS are

- IR horizon sensor
- V-slit star scanner
- V-slit Sun sensor

For a spin-stabilized spacecraft, the primary attitude information is given by the spin-axis direction \hat{U} , which is

expressible in terms of its right ascension α and declination δ in GCI coordinates as

$$\hat{U}^I = \begin{bmatrix} \cos \delta & \cos \alpha \\ \cos \delta & \sin \alpha \\ \sin \delta \end{bmatrix} \quad (3.3-1)$$

The sensed data can be expressed in terms of a reference vector \hat{R} , which is the unit vector in the direction of a sensed object.

Since the spin-angle itself is not of interest, the direction of the projection of the reference vector \hat{R} in the spin-plane conveys no attitude information. Meaningful measurements of any reference vector \hat{R} give the following form of the measurement function $h(\bar{x}, \bar{p}')$ of Equation (2.1-13):

$$h(\bar{x}, \bar{p}') = h(C_r, \bar{p}') \quad (3.3-2)$$

where h is a sensor-specific function

and C_r is the projection of the unit reference vector \hat{R} onto the spacecraft spin axis, or cosine of the angle between \hat{R}^I and \hat{U}^I ;

$$C_r = R_x^I \cos \delta \cos \alpha + R_y^I \cos \delta \sin \alpha + R_z^I \sin \delta \quad (3.3-3)$$

where the superscript I denotes GCI coordinates.

For all spin-stabilized spacecraft sensors, the functional dependence of the measurement on the spacecraft attitude, parameterized by the right ascension and declination of the spin axis, is through the projection C_r . Since the attitude errors are always a subset of the solved-for vector, the

partial derivatives of the measurements with respect to the attitude are computed as

$$\frac{\partial y^*}{\partial \alpha} = \frac{\partial h}{\partial C_r} \frac{\partial C_r}{\partial \alpha} = \frac{\partial h}{\partial C_r} \left[-R_x^I \cos \delta \sin \alpha + R_y^I \cos \delta \cos \alpha \right] \quad (3.3-4a)$$

$$\begin{aligned} \frac{\partial y^*}{\partial \delta} &= \frac{\partial h}{\partial C_r} \frac{\partial C_r}{\partial \delta} \\ &= \frac{\partial h}{\partial C_r} \left[-R_x^I \sin \delta \cos \alpha - R_y^I \sin \delta \sin \alpha + R_z^I \cos \delta \right] \end{aligned} \quad (3.3-4b)$$

The formulation of h and its partial derivatives with respect to the projection C_r is thus a key to the sensor-related error analysis computations. The expressions for $h(C_r, \bar{p}')$ are given below for each sensor as well as a complete list of all partial derivatives for each sensor.

3.3.1 IR HORIZON SENSOR MEASUREMENT MODEL AND PARTIAL DERIVATIVES

The measurement model for the IR horizon sensor is shown in Figure 3-2. This model describes both the conical scan IR sensor, which has a fixed scan cone angle γ , and the panoramic attitude sensor (PAS), which has a varying scan cone angle. Since the scan cone angle of a PAS is constant for each complete revolution of the spacecraft, the analysis can be carried out for a fixed scan cone angle. The analyst defines the parameters describing how the scan cone angle changes per revolution. If a zero incremental change is specified, the PAS will be identical to the conical scan IR horizon sensor. If the increment is not zero, the scan cone angle will increase each revolution until it reaches a user-defined upper limit and then decrease by the same incremental amount until it reaches the user-defined lower limit. This

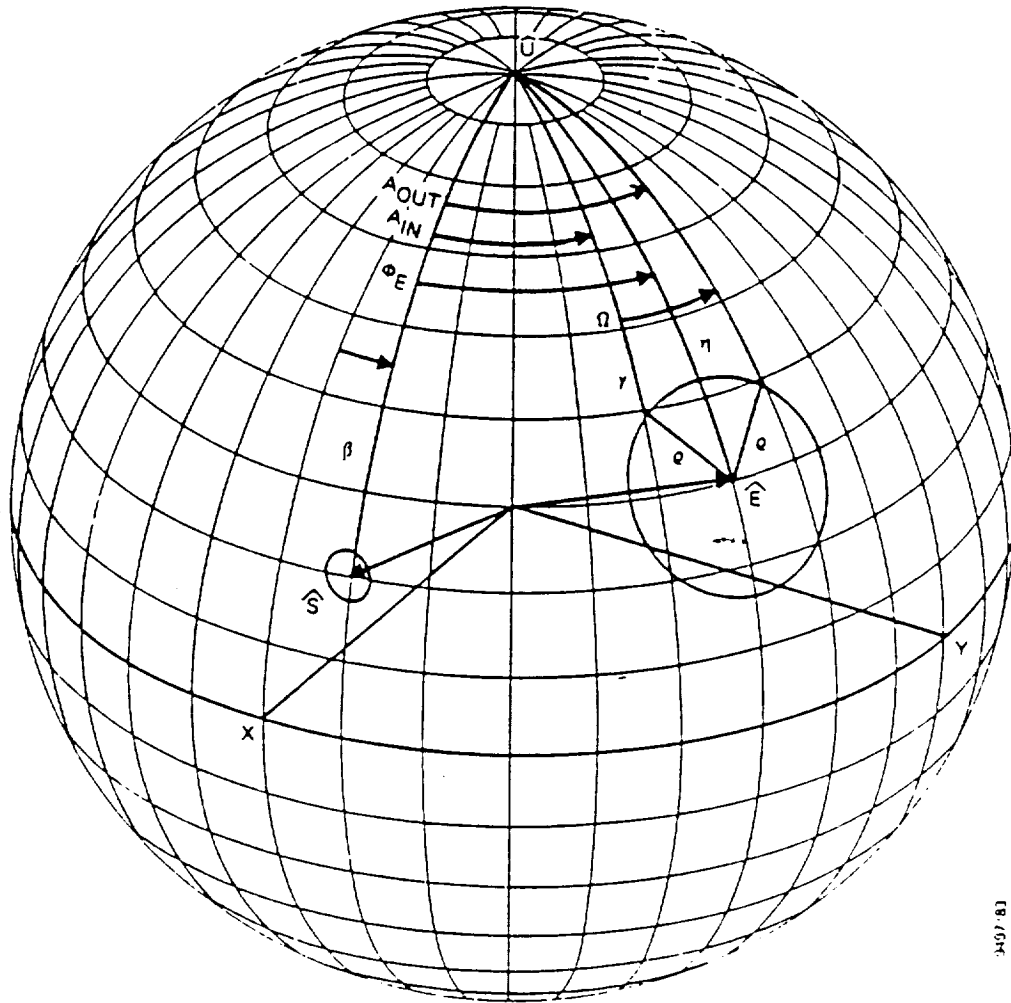


Figure 3-2. IR Horizon Sensor Geometry, Sun Indexed

is the only ADEAS sensor model that uses the projections onto the spacecraft spin axis of two external reference vectors, i.e., the Sun vector and the Earth vector. The measurements of the horizon sensor are the Sun to Earth-in azimuth, Sun to Earth-out azimuth, Earth width, and Earth azimuth with respect to the Sun. The measurements are calculated as

$$y^* = \text{Earth width} = h(C_S, C_E) \\ \equiv \Omega = 2 \cos^{-1} \left\{ \frac{\cos \rho - \cos \eta \cos \gamma}{\sin \eta \sin \gamma} \right\} \quad (3.3-5)$$

$$y^* = \text{Earth azimuth} = h(C_S, C_E) \\ \equiv \Phi_E = \cos^{-1} \left\{ \frac{\cos \psi - \cos \eta \cos \beta}{\sin \eta \sin \beta} \right\} \quad (3.3-6)$$

$$y^* = \text{Earth-in} = h(C_S, C_E) = A_{IN} = \Phi_E - \frac{1}{2} \Omega \quad (3.3-7)$$

$$y^* = \text{Earth-out} = h(C_S, C_E) = A_{OUT} = \Phi_E + \frac{1}{2} \Omega \quad (3.3-8)$$

where C_S = projection of the unit Sun vector \hat{S}^I onto the spacecraft spin axis = $\cos \beta = \hat{S}^I \cdot \hat{U}^I$
 C_E = projection of the unit Earth vector \hat{E}^I onto the spacecraft spin axis = $\cos \eta = \hat{E}^I \cdot \hat{U}^I$
 β = Sun angle, angle between the spin axis and the Sun vector
 η = Earth angle, angle between the spin axis and the Earth vector
 $\cos \psi$ = projection of the Sun vector on the Earth vector
 $= \hat{E}^I \cdot \hat{S}^I$
 ρ = Earth angular radius
 $= \sin^{-1} [(r + h_t)/R]$
 r = Earth radius (km)
 h_t = IR tangent height (km)

R = magnitude of the spacecraft position vector
(km)

γ = sensor scan cone angle (deg)

Equation (3.3-6) does not uniquely determine Φ_E ; the sign of the angle is not determined. To resolve this ambiguity the sign of a vector product is used. Assume that the \cos^{-1} function returns an angle in the range $0 \leq \Phi_E \leq 180$.

If $(\hat{U}^I \times \hat{S}^I) \cdot \hat{E}^I \geq 0$ then Equation (3.3-6) gives the correct range.

If $(\hat{U}^I \times \hat{S}^I) \cdot \hat{E}^I < 0$ then use the following equation,

$$\Phi_E = 360^\circ - \cos^{-1} \left\{ \frac{\cos \psi - \cos \eta \cos \beta}{\sin \eta \sin \beta} \right\} \quad (3.3-9)$$

The measurement parameters, which the user may select as either solved for or considered, for the IR horizon sensor are

1. The scan cone angle (deg)
2. The Earth angular radius (deg)
3. The distance from the Earth to the spacecraft (km)
4. The IR tangent height (km)
5. The Earth-in bias (deg)
6. The Earth-in scale factor
7. The amplitude of the Earth-in periodic measurement error (deg)
8. The Earth-out bias (deg)
9. The Earth-out scale factor
10. The amplitude of the Earth-out periodic measurement error (deg)

11. The Earth width bias (deg)
12. The Earth width scale factor
13. The amplitude of the Earth width periodic measurement error (deg)
14. The Earth azimuth bias (deg)
15. The Earth azimuth scale factor
16. The amplitude of the Earth azimuth periodic measurement error (deg)

In addition to specifying a name and uncertainty for each of the measurement parameters designated as either solved for or considered, the analyst must also provide the following:

1. The initial sensor scan cone angle (deg)
2. The incremental scan cone angle (deg)
3. The minimum scan cone angle (deg)
4. The maximum scan cone angle (deg)
5. The IR tangent height (km)
6. The frequency and phase angle of the Earth-in periodic measurement error
7. The frequency and phase angle of the Earth-out periodic measurement error
8. The frequency and phase angle of the Earth width periodic measurement error
9. The frequency and phase angle of the Earth azimuth periodic measurement error

When scheduling the IR horizon sensor the user may use one or two of the sensor outputs for the error analysis computations. Since all outputs have units of degrees, the user-supplied value of the sensor white noise standard deviation

for each measurement has units of degrees. The errors in the Earth-in and Earth-out measurements are assumed to have equal standard deviations σ_A and to be uncorrelated with one another. Then, it follows from Equations (3.3-7) and (3.3-8) that the errors in the Earth-width and Earth azimuth measurements are uncorrelated, and that their standard deviations are

$$\begin{aligned}\sigma_{\Phi_E} &= \sigma_A / \sqrt{2} \\ \sigma_{\Omega} &= \sqrt{2} \sigma_A\end{aligned}\tag{3.3-10}$$

The correlations between the pairs (Ω, A_{IN}) , (Ω, A_{OUT}) , (Φ_E, A_{IN}) , and (Φ_E, A_{OUT}) are ignored if any such pair is selected.

Partial of the Earth azimuth wrt the projection of the Sun vector \hat{S} :

$$\frac{\partial \Phi_E}{\partial C_S} = \frac{\cos \eta - \sin \eta \cot \beta \cos \Phi_E}{\sin \eta \sin \beta \sin \Phi_E}\tag{3.3-11}$$

Partial of the Earth azimuth wrt the projection of the Earth vector \hat{E} :

$$\frac{\partial \Phi_E}{\partial C_E} = \frac{\cos \beta - \cot \eta \sin \beta \cos \Phi_E}{\sin \eta \sin \beta \sin \Phi_E}\tag{3.3-12}$$

Partial of the Earth azimuth wrt the sensor scan cone angle:

$$\frac{\partial \Phi_E}{\partial \gamma} = 0\tag{3.3-13}$$

Partial of the Earth azimuth wrt the Earth angular radius:

$$\frac{\partial \Phi_E}{\partial \rho} = 0 \quad (3.3-14)$$

Partial of the Earth azimuth wrt the IR tangent height:

$$\frac{\partial \Phi_E}{\partial h_t} = 0 \quad (3.3-15)$$

Partial of the Earth azimuth wrt the distance from the spacecraft to Earth:

$$\frac{\partial \Phi_E}{\partial R} = 0 \quad (3.3-16)$$

Partial of the Earth azimuth wrt the bias b:

$$\frac{\partial \Phi_E}{\partial b} = 1 \quad (3.3-17)$$

Partial of the Earth azimuth wrt the scale factor k:

$$\frac{\partial \Phi_E}{\partial k} \approx h(C_S, C_E) = \cos^{-1} \left\{ \frac{\cos \psi - \cos \eta \cos \beta}{\sin \eta \sin \beta} \right\} \quad (3.3-18)$$

Partial of the Earth azimuth wrt the amplitude of the periodic error:

$$\frac{\partial \Phi_E}{\partial a} = \sin (\omega t + \psi) \quad (3.3-19)$$

Partial of the Earth width wrt the projection of the Sun vector \hat{S} :

$$\frac{\partial \Omega}{\partial C_S} = 0 \quad (3.3-20)$$

Partial of the Earth width wrt the projection of the Earth vector \hat{E} :

$$\frac{\partial \Omega}{\partial C_E} = 2 \left[\frac{\cos \gamma - \sin \gamma \cos \frac{\Omega}{2} \cot \eta}{\sin \gamma \sin \eta \sin \frac{\Omega}{2}} \right] \quad (3.3-21)$$

Partial of the Earth width wrt the sensor scan cone angle:

$$\frac{\partial \Omega}{\partial \gamma} = 2 \left[\frac{\cos \gamma \sin \eta \cos \frac{\Omega}{2} - \sin \gamma \cos \eta}{\sin \gamma \sin \eta \sin \frac{\Omega}{2}} \right] \quad (3.3-22)$$

Partial of the Earth width wrt the Earth angular radius:

$$\frac{\partial \Omega}{\partial \rho} = 2 \left[\frac{\sin \rho}{\sin \gamma \sin \eta \sin \frac{\Omega}{2}} \right] \quad (3.3-23)$$

Partial of the Earth width wrt the IR tangent height:

$$\frac{\partial \Omega}{\partial h_t} = \frac{\partial \Omega}{\partial \rho} \left[\frac{1}{R \cos \rho} \right] \quad (3.3-24)$$

Partial of the Earth width wrt the distance from the spacecraft to Earth:

$$\frac{\partial \Omega}{\partial R} = - \frac{\partial \Omega}{\partial \rho} \frac{\tan \rho}{R} \quad (3.3-25)$$

Partial of the Earth width wrt the bias b:

$$\frac{\partial \Omega}{\partial b} = 1 \quad (3.3-26)$$

Partial of the Earth width wrt the scale factor k:

$$\frac{\partial \Omega}{\partial k} \approx h(C_S, C_E) = 2 \cos^{-1} \left\{ \frac{\cos \rho - \cos \eta \cos \gamma}{\sin \eta \sin \gamma} \right\} \quad (3.3-27)$$

Partial of the Earth width wrt the amplitude of the periodic error:

$$\frac{\partial \Omega}{\partial a} = \sin (\omega t + \psi) \quad (3.3-28)$$

Partial of the Earth-in angle wrt the projection of the Sun vector \hat{S} :

$$\frac{\partial A_{IN}}{\partial C_S} = \frac{\partial \Phi_E}{\partial C_S} \quad (3.3-29)$$

Partial of the Earth-in angle wrt the projection of the Earth vector \hat{E} :

$$\frac{\partial A_{IN}}{\partial C_E} = \frac{\partial \Phi_E}{\partial C_E} - \frac{1}{2} \frac{\partial \Omega}{\partial C_E} \quad (3.3-30)$$

Partial of the Earth-in angle wrt the sensor scan cone angle:

$$\frac{\partial A_{IN}}{\partial \gamma} = - \frac{1}{2} \frac{\partial \Omega}{\partial \gamma} \quad (3.3-31)$$

Partial of the Earth-in angle wrt the Earth angular radius:

$$\frac{\partial A_{IN}}{\partial \rho} = - \frac{1}{2} \frac{\partial \Omega}{\partial \rho} \quad (3.3-32)$$

Partial of the Earth-in angle wrt the IR tangent height:

$$\frac{\partial A_{IN}}{\partial h_t} = - \frac{1}{2} \frac{\partial \Omega}{\partial h_t} \quad (3.3-33)$$

Partial of the Earth-in angle wrt the distance from the spacecraft to Earth:

$$\frac{\partial A_{IN}}{\partial R} = - \frac{1}{2} \frac{\partial \Omega}{\partial R} \quad (3.3-34)$$

Partial of the Earth-in angle wrt the bias b:

$$\frac{\partial A_{IN}}{\partial b} = 1 \quad (3.3-35)$$

Partial of the Earth-in angle wrt the scale factor k:

$$\frac{\partial A_{IN}}{\partial k} \approx h(C_S, C_E) = \Phi_E - \frac{1}{2} \Omega \quad (3.3-36)$$

Partial of the Earth-in angle wrt the amplitude of periodic error:

$$\frac{\partial A_{IN}}{\partial a} = \sin (\omega t + \psi) \quad (3.3-37)$$

Partial of the Earth-out angle wrt the projection of the Sun vector \hat{S} :

$$\frac{\partial A_{OUT}}{\partial C_S} = \frac{\partial \Phi_E}{\partial C_S} \quad (3.3-38)$$

Partial of the Earth-out angle wrt the projection of the Earth vector \hat{E} :

$$\frac{\partial A_{OUT}}{\partial C_E} = \frac{\partial \Phi_E}{\partial C_E} + \frac{1}{2} \frac{\partial \Omega}{\partial C_E} \quad (3.3-39)$$

Partial of the Earth-out angle wrt the sensor scan cone angle:

$$\frac{\partial A_{OUT}}{\partial \gamma} = \frac{1}{2} \frac{\partial \Omega}{\partial \gamma} \quad (3.3-40)$$

Partial of the Earth-out angle wrt the Earth angular radius:

$$\frac{\partial A_{OUT}}{\partial \rho} = \frac{1}{2} \frac{\partial \Omega}{\partial \rho} \quad (3.3-41)$$

Partial of the Earth-out angle wrt the IR tangent height:

$$\frac{\partial A_{OUT}}{\partial h_t} = \frac{1}{2} \frac{\partial \Omega}{\partial h_t} \quad (3.3-42)$$

Partial of the Earth-out angle wrt the distance from the spacecraft to Earth:

$$\frac{\partial A_{OUT}}{\partial R} = \frac{1}{2} \frac{\partial \Omega}{\partial R} \quad (3.3-43)$$

Partial of the Earth-out angle wrt the bias b:

$$\frac{\partial A_{OUT}}{\partial b} = 1 \quad (3.3-44)$$

Partial of the Earth-out angle wrt the scale factor k:

$$\frac{\partial A_{OUT}}{\partial k} \approx h(C_S, C_E) = \Phi_E + \frac{1}{2} \Omega \quad (3.3-45)$$

Partial of the Earth-out angle wrt the amplitude of periodic error:

$$\frac{\partial A_{OUT}}{\partial a} = \sin (\omega t + \psi) \quad (3.3-46)$$

3.3.2 V-SLIT STAR SENSOR MEASUREMENT MODEL AND PARTIAL DERIVATIVES

The V-slit star sensor contains two slits, one parallel to the spin axis, the other at an oblique angle, as in Figure 3-3. The raw measurement is the time Δt between the crossing of each slit by the star image focused by an optical system. ADEAS uses as its preprocessed measurement y^* the rotation angle of the spacecraft between the star crossings, given as $\omega \Delta t$ where ω is the angular rotation rate of the spacecraft. This measurement is a function of the cosine of the star angle σ between the star vector \hat{S}^I and the spin vector as

$$y^* \equiv M = \text{rotation angle} = h(C_S) \quad (3.3-47)$$

$$= \sin^{-1} [\tan (\gamma - \sigma) \tan \Sigma] + A$$

where C_S = projection of the unit Sun vector \hat{S}^I onto the spacecraft spin axis = $\cos \sigma = \hat{S}^I \cdot \hat{U}^I$

σ = star angle

γ = mounting angle of the optical axis of the star scanner

Σ = tilt of oblique slit

A = separation of center of slits, the angle between the two lines perpendicular to the spin axis from that axis to the intersections of the slits with the plane scanned by the optical axis

Though this expression is exact only when the mounting angle is 90 degrees and there is no rotation of the star scanner about its optical axis, it is a good approximation when the lengths of the slits are small, typically 10 degrees.

To determine the sensitivity of the measurement with respect to a rotation of the slits about the optical axis, a different measurement model is used.

$$\begin{aligned} y^* = \text{rotation angle} = h(C_S) = & \sin^{-1} [\tan (\gamma - \sigma) \tan (\Sigma + \Theta)] \\ & - \sin^{-1} [\tan (\gamma - \sigma) \tan \Theta] \\ & + \frac{B}{\cos \Theta} + \frac{A - B}{(1 - \tan \Theta \tan \Sigma) \cos \Theta} \end{aligned} \quad (3.3-48)$$

where Θ = rotation of the slits about the optical axis

B = angular distance between the optical axis and the vertical slit

The last two terms of this model are based on plane geometry (Figure 3-4).

The geometrical limitation on the visibility of the V-slit star sensor requires that the star angle be between the minimum and maximum values of

$$\sigma_{\min} = \gamma - \frac{1}{2} \lambda \quad (3.3-49)$$

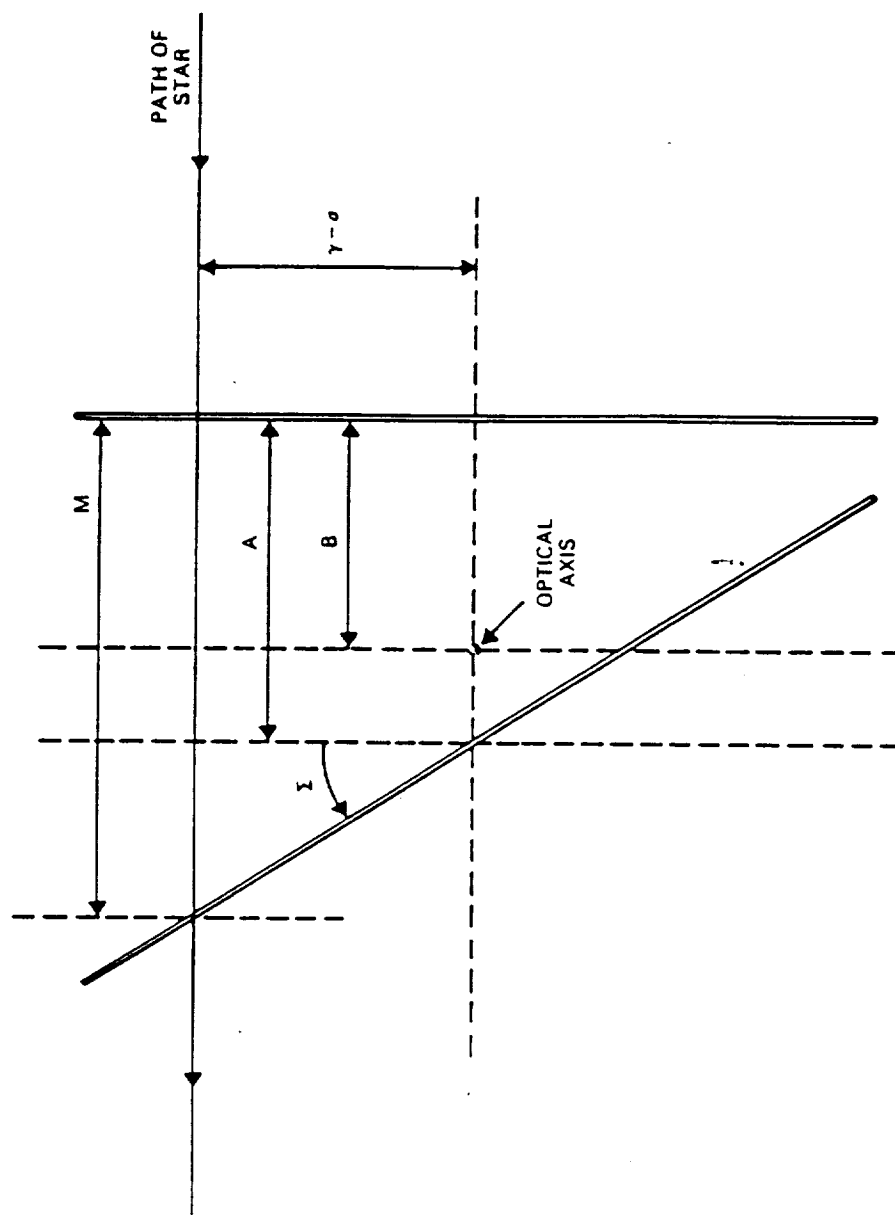


Figure 3-4. V-Slit Star Scanner Plane Geometry

$$\sigma_{\max} = \gamma + \frac{1}{2} \lambda \quad (3.3-50)$$

where λ is the length of the vertical slit.

The measurement parameters, which the user may select as either solved for or considered, for the V-slit star sensor are

1. The measurement bias (deg)
2. The measurement scale factor
3. The amplitude of the measurement periodic error (deg)
4. The separation of the center of the slits (deg)
5. The tilt of the oblique slit (deg)
6. The rotation of the slits about the optical axis (deg)

Even though the rotation of the slits about the optical axis is always nominally 0 degrees, it may have a specified uncertainty and hence be designated as an error parameter.

In addition to specifying a name and uncertainty for each of the measurement parameters designated as either solved for or considered, the analyst must also provide the following:

1. The frequency and phase angle of the periodic measurement error
2. The separation of the center of the slits (deg)
3. The tilt of the oblique slit (deg)
4. The angular distance between the optical axis and the vertical slit (deg)
5. The length of the vertical slit (deg)

When scheduling the V-slit star scanner, the analyst does not have a choice of measurements to use, since there is only one. Since the rotation angle has units of degrees, the sensor white noise standard deviation has units of degrees.

Partial of the rotation angle M wrt the projection of the star vector \hat{S} :

$$\frac{\partial M}{\partial C_s} = \frac{1}{\sin \sigma} \frac{\partial M}{\partial \gamma} \quad (3.3-51)$$

Partial of the rotation angle M wrt the separation of the center of the slits:

$$\frac{\partial M}{\partial A} = 1 \quad (3.3-52)$$

Partial of the rotation angle M wrt the tilt of the slit:

$$\frac{\partial M}{\partial \Sigma} = \frac{\tan (\gamma - \sigma)}{\cos^2 \Sigma \cos (M - A)} \quad (3.3-53)$$

Partial of the rotation angle M wrt the mounting angle of the optical axis:

$$\frac{\partial M}{\partial \gamma} = \frac{\tan \Sigma}{\cos^2 (\gamma - \sigma) \cos (M-A)} \quad (3.3-54)$$

Partial of the rotation angle M wrt rotation of the slits about the optical axis, from Equation (3.3-43):

$$\frac{\partial M}{\partial \theta} = (A - B) \tan \Sigma + \tan (\gamma - \sigma) \tan^2 \Sigma \quad (3.3-55)$$

in the limit $\Theta \rightarrow 0$ and $\gamma - \sigma \ll 1$.

Partial of the rotation angle M wrt the bias b:

$$\frac{\partial M}{\partial b} = 1 \quad (3.3-56)$$

Partial of the rotation angle M wrt the scale factor k:

$$\frac{\partial M}{\partial k} \approx h(C_S) = A + \sin^{-1} [\tan (\gamma - \sigma) \tan \Sigma] \quad (3.3-57)$$

Partial of the rotation angle M wrt the amplitude of the periodic error:

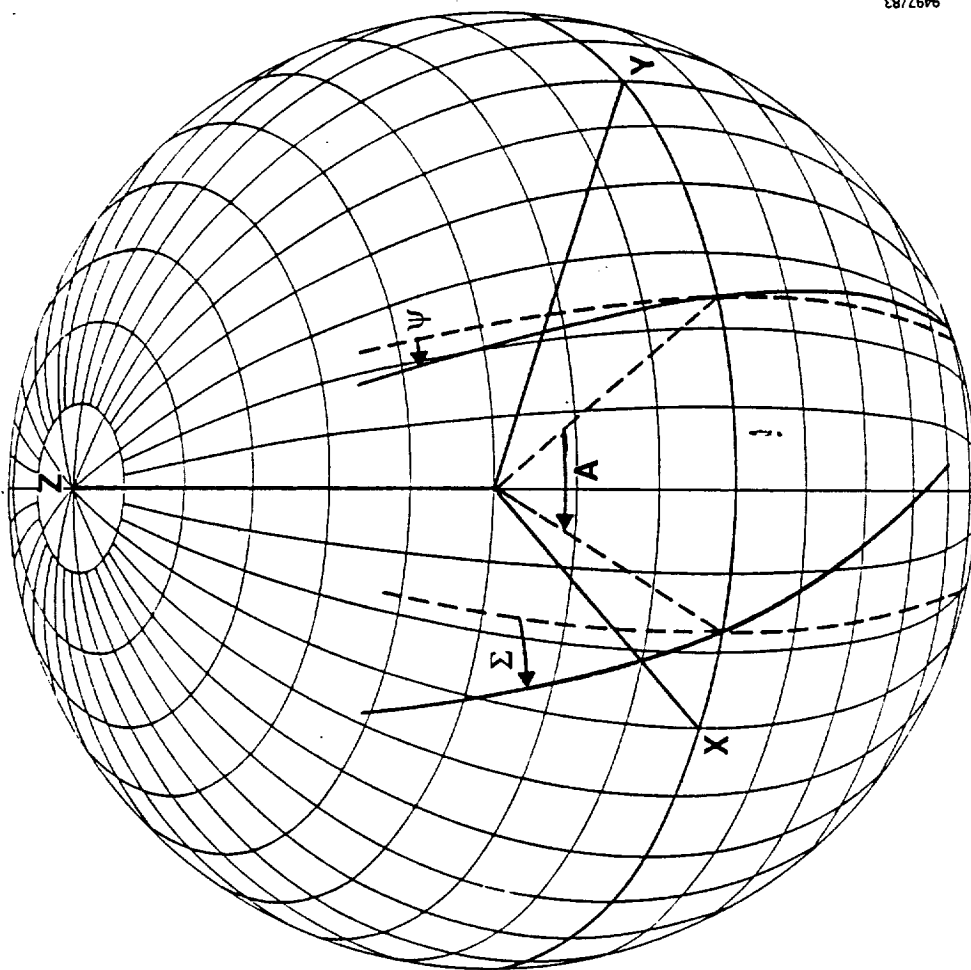
$$\frac{\partial M}{\partial a} = \sin (\omega t + \psi) \quad (3.3-58)$$

3.3.3 V-SLIT SUN SENSOR MEASUREMENT MODEL AND PARTIAL DERIVATIVES

The V-slit Sun sensor contains two slits of equal length, one parallel to the spin axis, the other at an oblique angle, as in Figure 3-5, from which is determined the time Δt between Sun crossings. ADEAS uses as its preprocessed measurement y^* the rotation angle of the spacecraft between Sun crossings given as $\omega \Delta t$ where ω is the angular rotation rate of the spacecraft. This measurement is a function of the cosine of the Sun angle β between the Sun vector \hat{S}^I and the spin vector.

The rotation angle is given by

$$M = \sin^{-1} (\cot \beta \tan \Sigma) - \sin^{-1} (\cot \beta \tan \Psi) + A \quad (3.3-59)$$



9497/83

Figure 3-5. V-Slit Sensor Geometry

in the general case illustrated in Figure 3-5. ADEAS only models the special case of $\Psi = 0$, in which case the measurement equation is

$$y^* \equiv M = \text{rotation angle} = h(C_S) = \sin^{-1} (\cot \beta \tan \Sigma) + A \quad (3.3-60)$$

where C_S = projection of the unit Sun vector \hat{S}^I onto the spacecraft spin axis = $\cos \beta$

Σ = tilt of the oblique slit

A = angle between the lines formed by the intersection of each slit with the x-y plane, the coordinate frame being the spacecraft's principal axes, with the spin vector parallel to the z-axis

This is the same as the V-slit star sensor model, Equation (3.3-47), with $\gamma = \pi/2$ and $\sigma = \beta$.

If the two slits have the same lengths, as is assumed in ADEAS, the slit with the greatest tilt (Σ) will define the maximum and minimum β that can be measured. Thus, the geometrical limitation on the visibility of the V-slit Sun sensor requires that the Sun angle β be between the minimum and maximum values of

$$\beta_{\min} = 90 \text{ deg} - \sin^{-1} (\sin (\lambda/2) \cos \Sigma) \text{ deg} \quad (3.3-61)$$

$$\beta_{\max} = 90 \text{ deg} + \sin^{-1} (\sin (\lambda/2) \cos \Sigma) \text{ deg} \quad (3.3-62)$$

where λ is the length of the slits.

The measurement parameters, which the user may select as either solved for or considered, for the V-slit Sun sensor are

1. The measurement bias (deg)
2. The measurement scale factor

3. The amplitude of the measurement periodic error (deg)
4. The angle A between the lines formed by the intersection of each slit with the x-y plane (deg)
5. The tilt of the oblique slit (deg)
6. The tilt of the vertical slit (deg)

Note that even though the tilt of the vertical slit is always nominally 0 degrees, it may have a specified uncertainty and hence be designated as an error parameter.

In addition to specifying a name and uncertainty for each of the measurement parameters designated as either solved for or considered, the analyst must also provide the following:

1. The frequency and phase angle of the periodic measurement error
2. The angle A between the lines formed by the intersection of each slit with the x-y plane (deg)
3. The tilt of the oblique slit (deg)
4. The length of the slits (deg)

When scheduling the V-slit Sun sensor, the analyst does not have a choice of measurements to use, since there is only one. Since the rotation angle has units of degrees, the sensor white noise standard deviation has units of degrees.

Partial of the rotation angle M wrt the projection of the unit Sun vector \hat{S} :

$$\frac{\partial M}{\partial C_s} = \frac{\tan \Sigma}{\sin^3 \beta \cos (M - A)} \quad (3.3-63)$$

Partial of the rotation angle M wrt the angle between lines of slit intersection with the xy plane:

$$\frac{\partial M}{\partial A} = 1 \quad (3.3-64)$$

Partial of the rotation angle M wrt the tilt of the tilted slit:

$$\frac{\partial M}{\partial \Sigma} = \frac{\cot \beta}{\cos^2 \Sigma \cos (M - A)} \quad (3.3-65)$$

Partial of the rotation angle M wrt the tilt of the vertical slit:

$$\frac{\partial M}{\partial \Psi} = -\cot \beta \quad (3.3-66)$$

Partial of the rotation angle M wrt the bias b:

$$\frac{\partial M}{\partial b} = 1 \quad (3.3-67)$$

Partial of the rotation angle M wrt the scale factor k:

$$\frac{\partial M}{\partial k} \approx h(C_S) = A + \sin^{-1} (\cot \beta \tan \Sigma) \quad (3.3-68)$$

Partial of the rotation angle M wrt the amplitude of the periodic error:

$$\frac{\partial M}{\partial a} = \sin (\omega t + \psi) \quad (3.3-69)$$



SECTION 4 - THREE-AXIS STABILIZED SPACECRAFT MODELS

As Section 2 discussed estimation filtering in a general sense, this section provides specific attitude and sensor models for three-axis stabilized spacecraft. These models provide the basis for the construction of the state transition, measurement partial derivative, and random excitation matrices used in Section 2.

4.1 ATTITUDE GENERATION

For three-axis stabilized spacecraft, the attitude is defined by the 3×3 orthogonal transformation matrix $A_{B/R}$ from some reference coordinate system (see Section 5.1) to the spacecraft body coordinate system. The nominal spacecraft attitude $A'_{B/R}$ evolves over time based on the body components of the nominal spacecraft angular velocity $\bar{\omega}'_{B/R}$ relative to the reference coordinate system (see Section 16.1 of Reference 3):

$$\dot{A}'_{B/R}(t) = -\tilde{\omega}'_{B/R}(t) A'_{B/R}(t) \quad (4.1-1)$$

where $\tilde{\omega}'_{B/R}$ is the 3×3 antisymmetric matrix defined from $\bar{\omega}'_{B/R}$ by:

$$\tilde{\omega}'_{B/R} \equiv \begin{bmatrix} 0 & -\omega'_{B/Rz} & \omega'_{B/Ry} \\ \omega'_{B/Rz} & 0 & -\omega'_{B/Rx} \\ -\omega'_{B/Ry} & \omega'_{B/Rx} & 0 \end{bmatrix} \quad (4.1-2)$$

In addition, ADEAS models sinusoidal stabilization errors about the nominal attitude:

$$A_{B/R}(t) = \phi_e(t) A'_{B/R}(t) \quad (4.1-3)$$

where

$$\phi_e(t) \equiv I + \frac{[\tilde{e}(t)]^2}{|\bar{e}(t)|^2} [1 - \cos |\bar{e}(t)|] - \frac{\tilde{e}(t)}{|\bar{e}(t)|} \sin |\bar{e}(t)| \quad (4.1-4)$$

and \tilde{e} is an antisymmetric matrix defined from a vector \bar{e} similar to Equation (4.1-2). The variation vector \bar{e} is given by

$$e_i = a_i \sin [\zeta_i (t - t_0) + \gamma_i] \quad i = 1, 2, 3 \quad (4.1-5)$$

where the amplitudes a_i , the frequencies ζ_i , and the phases γ_i are all constant. The attitude matrix

$$A_{B/I} = A_{B/R} A_{R/I} \quad (4.1-6)$$

is used for all sensor model computations, where the inertial-to-reference matrices $A_{R/I}$ for different reference frames are found in Section 5.1.

For ADEAS, the nominal attitude $A'_{B/R}(t)$ is specified by an initial attitude and a set of attitude rates. The initial attitude $A'_{B/R}(t_0)$ may be specified by Euler angles or a quaternion (see Reference 3, Section 12.1 and Appendix E).

The angular velocity $\bar{\omega}'_{B/R}$ is specified between discrete times t_i in one of two ways. The first is as a set of constant Euler angle rates, $\dot{\phi}$, $\dot{\theta}$, $\dot{\psi}$. The Euler angles for $t_{i-1} \leq t < t_i$ are given by

$$\begin{aligned} \phi(t) &= \phi(t_{i-1}) + \dot{\phi}_i(t - t_{i-1}) \\ \theta(t) &= \theta(t_{i-1}) + \dot{\theta}_i(t - t_{i-1}) \\ \psi(t) &= \psi(t_{i-1}) + \dot{\psi}_i(t - t_{i-1}) \end{aligned} \quad (4.1-7)$$

If the initial attitude is specified by Euler angles and $\bar{\omega}'_{B/R}$ by Euler angle rates, the same Euler axis sequence is used for both. If the initial attitude is specified by a quaternion and $\bar{\omega}'_{B/R}$ by Euler angle rates, the initial Euler angles $\phi(t_0)$, $\theta(t_0)$, and $\psi(t_0)$ are computed from the initial attitude matrix $A'_{B/R}(t_0)$ using the equations in Table 4-1. The correct quadrants for ϕ and ψ are determined by the fact that the signs of the numerator and denominator of the argument of \tan^{-1} are the signs of the sine and cosine, respectively, of the angle. If both the numerator and denominator of the expression for $\tan \phi$ are zero, ϕ is set to zero.

The second means of specifying $\bar{\omega}'_{B/R}$ between the discrete times t_i is as a constant vector of components in the body frame. When $\bar{\omega}'_{B/R}$ is constant, the solution to Equation (4.1-1) is

$$A'_{B/R}(t) = \phi_A(t, t_{i-1}) A'_{B/R}(t_{i-1}) \quad (4.1-8)$$

where $\bar{\omega}'_{B/R}$ is constant for $t_{i-1} \leq t < t_i$ and

$$\begin{aligned} \phi_A(t, t_{i-1}) \equiv I + \frac{[\tilde{\omega}'_{B/R}]^2}{|\bar{\omega}'_{B/R}|^2} [1 - \cos |\bar{\omega}'_{B/R}| (t - t_{i-1})] \\ - \frac{\tilde{\omega}'_{B/R}}{|\bar{\omega}'_{B/R}|} \sin |\bar{\omega}'_{B/R}| (t - t_{i-1}) \end{aligned} \quad (4.1-9)$$

4.2 DYNAMIC ERROR MODEL

Let $A_{B/R}$ be the true spacecraft attitude and $A^*_{B/R}$ be an estimate of the attitude. For all internal processing, ADEAS represents the error in $A^*_{B/R}$ by the first order error vector $\Delta\bar{\theta}$. The components of this vector represent the small rotations needed about each of the spacecraft body axes to

Table 4-1. Computation of Euler Angles From Attitude Matrix (1 of 3)

i-j-k	EULER ANGLES
1-2-3	$\phi = \tan^{-1} \left[-A_{32}/A_{33} \right]$ $\Theta = \sin^{-1} (A_{31})$ $\psi = \tan^{-1} \left[\frac{A_{13} \sin \phi + A_{12} \cos \phi}{A_{23} \sin \phi + A_{22} \cos \phi} \right]$
1-3-2	$\phi = \tan^{-1} \left[A_{23}/A_{22} \right]$ $\Theta = \sin^{-1} (-A_{21})$ $\psi = \tan^{-1} \left[\frac{A_{12} \sin \phi - A_{13} \cos \phi}{-A_{32} \sin \phi + A_{33} \cos \phi} \right]$
2-3-1	$\phi = \tan^{-1} \left[-A_{13}/A_{11} \right]$ $\Theta = \sin^{-1} (A_{12})$ $\psi = \tan^{-1} \left[\frac{A_{21} \sin \phi + A_{23} \cos \phi}{A_{31} \sin \phi + A_{33} \cos \phi} \right]$
2-1-3	$\phi = \tan^{-1} \left[A_{31}/A_{33} \right]$ $\Theta = \sin^{-1} (-A_{32})$ $\psi = \tan^{-1} \left[\frac{A_{23} \sin \phi - A_{21} \cos \phi}{-A_{13} \sin \phi + A_{11} \cos \phi} \right]$

Table 4-1. Computation of Euler Angles From Attitude Matrix (2 of 3)

i-j-k	EULER ANGLES
3-1-2	$\phi = \tan^{-1} \left[-A_{21}/A_{22} \right]$ $\theta = \sin^{-1} (A_{23})$ $\psi = \tan^{-1} \left[\frac{A_{32} \sin \phi + A_{31} \cos \phi}{A_{12} \sin \phi + A_{11} \cos \phi} \right]$
3-2-1	$\phi = \tan^{-1} \left[A_{12}/A_{11} \right]$ $\theta = \sin^{-1} (-A_{13})$ $\psi = \tan^{-1} \left[\frac{A_{31} \sin \phi - A_{32} \cos \phi}{-A_{21} \sin \phi + A_{22} \cos \phi} \right]$
1-2-1	$\phi = \tan^{-1} \left[A_{12}/-A_{13} \right]$ $\theta = \cos^{-1} (A_{11})$ $\psi = \tan^{-1} \left[\frac{-A_{33} \sin \phi - A_{32} \cos \phi}{A_{23} \sin \phi + A_{22} \cos \phi} \right]$
1-3-1	$\phi = \tan^{-1} \left[A_{13}/A_{12} \right]$ $\theta = \cos^{-1} (A_{11})$ $\psi = \tan^{-1} \left[\frac{-A_{22} \sin \phi + A_{23} \cos \phi}{-A_{32} \sin \phi + A_{33} \cos \phi} \right]$

Table 4-1. Computation of Euler Angles From Attitude Matrix (3 of 3)

i-j-k	EULER ANGLES
2-1-2	$\phi = \tan^{-1} [A_{21}/A_{23}]$ $\theta = \cos^{-1} (A_{22})$ $\psi = \tan^{-1} \left[\frac{-A_{33} \sin \phi + A_{31} \cos \phi}{-A_{13} \sin \phi + A_{11} \cos \phi} \right]$
2-3-2	$\phi = \tan^{-1} [A_{23}/-A_{21}]$ $\theta = \cos^{-1} (A_{22})$ $\psi = \tan^{-1} \left[\frac{-A_{11} \sin \phi - A_{13} \cos \phi}{A_{31} \sin \phi + A_{33} \cos \phi} \right]$
3-1-3	$\phi = \tan^{-1} [A_{31}/-A_{32}]$ $\theta = \cos^{-1} (A_{33})$ $\psi = \tan^{-1} \left[\frac{-A_{22} \sin \phi - A_{21} \cos \phi}{A_{12} \sin \phi + A_{11} \cos \phi} \right]$
3-2-3	$\phi = \tan^{-1} [A_{32}/A_{31}]$ $\theta = \cos^{-1} (A_{33})$ $\psi = \tan^{-1} \left[\frac{-A_{11} \sin \phi + A_{12} \cos \phi}{-A_{21} \sin \phi + A_{22} \cos \phi} \right]$

align them with the estimated body axes (see Figure 4-1). The true and estimated attitudes are then related by

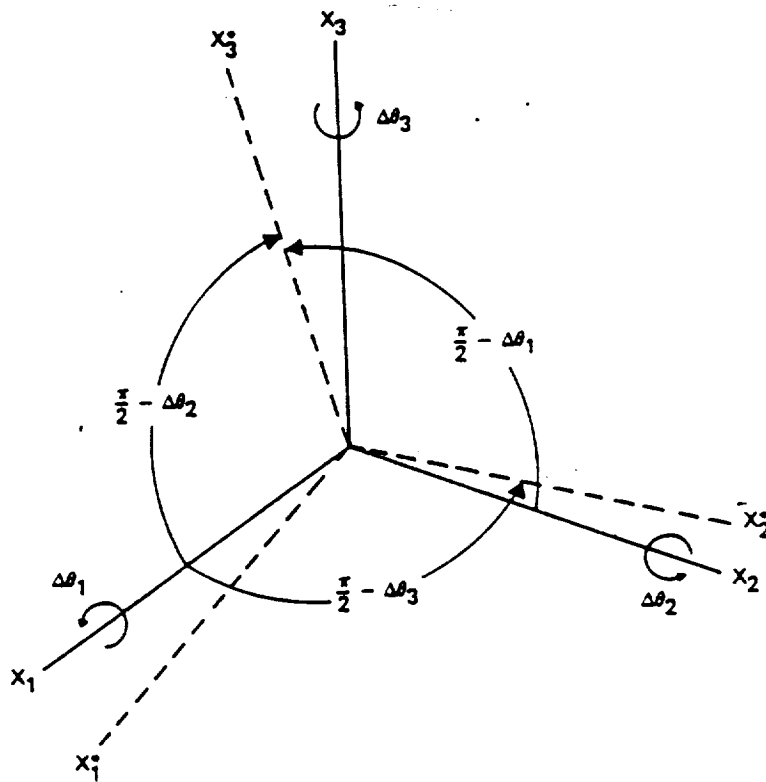
$$A_{B/R}^* \approx (I + \Delta\tilde{\Theta}) A_{B/R} \quad (4.2-1)$$

where the antisymmetric matrix $\Delta\tilde{\Theta}$ is defined similarly to Equation (4.1-2).

4.2.1 ATTITUDE ERROR PARAMETERIZATION

While the error vector $\Delta\tilde{\Theta}$ is useful for internal computations, ADEAS provides two additional attitude error parameterizations for convenience of input and output: Euler angle errors and quaternion errors.

Euler angle errors represent the difference in the Euler angles between the Euler sequence rotating the reference coordinate system to the true spacecraft body system and the Euler sequence rotating the reference system to the estimated body system. The explicit forms for the attitude matrix in terms of the 12 possible Euler sequences are given in Table E-1 of Reference 3. The relationship between the attitude error vector and the Euler angle errors is analogous to the relationship between the angular velocity vector and the Euler angle rates. This analogy holds because the attitude errors and the actual angular motion in an infinitesimal time Δt are both infinitesimal. Therefore, the transformations between the components of the attitude error vector $\Delta\tilde{\Theta}$ and the Euler angle errors $\Delta\phi$, $\Delta\theta$, $\Delta\psi$ can be obtained from the well known relations relating Euler angle rates and the angular velocity components. The following table of transformations (Table 4-2) for 12 different Euler sequences is adapted from Reference 3.



9-67/83

Figure 4-1. Small Rotation From True Spacecraft Axes to Estimated Spacecraft Axes

Table 4-2. Nonorthogonal Transformation Between Small Changes in Euler Angles ($\Delta\phi$, $\Delta\theta$, $\Delta\psi$) and Small Rotation About Body Axes ($\Delta\theta_1$, $\Delta\theta_2$, $\Delta\theta_3$)

EULER ANGLE SEQUENCE			INDEX VALUES			TRANSFORMATION FROM $\Delta\theta_1, \Delta\theta_2, \Delta\theta_3$ TO $\Delta\phi, \Delta\theta, \Delta\psi$	INVERSE TRANSFORMATION
\uparrow	θ	ψ	i	j	k		
1	2	3	1	2	3	$\begin{bmatrix} \cos \psi \sec \theta & -\sin \psi \sec \theta & 0 \\ \sin \psi & \cos \psi & 0 \\ -\cos \psi \tan \theta & \sin \psi \tan \theta & 1 \end{bmatrix}$	$\begin{bmatrix} \cos \theta \cos \psi & \sin \psi & 0 \\ -\cos \theta \sin \psi & \cos \psi & 0 \\ \sin \theta & 0 & 1 \end{bmatrix}$
1	3	2	1	3	2	$\begin{bmatrix} \cos \psi \sec \theta & \sin \psi \sec \theta & 0 \\ -\sin \psi & \cos \psi & 0 \\ \cos \psi \tan \theta & \sin \psi \tan \theta & 1 \end{bmatrix}$	$\begin{bmatrix} \cos \theta \cos \psi & -\sin \psi & 0 \\ \cos \theta \sin \psi & \cos \psi & 0 \\ -\sin \theta & 0 & 1 \end{bmatrix}$
1	2	1	1	2	3	$\begin{bmatrix} 0 & \sin \psi \csc \theta & \cos \psi \sec \theta \\ 0 & \cos \psi & -\sin \psi \\ 1 & -\sin \psi \cot \theta & -\cos \theta \cot \theta \end{bmatrix}$	$\begin{bmatrix} \cos \theta & 0 & 1 \\ \sin \theta \sin \psi & \cos \psi & 0 \\ \sin \theta \cos \psi & -\sin \psi & 0 \end{bmatrix}$
1	3	1	1	3	2	$\begin{bmatrix} 0 & \sin \psi \csc \theta & -\cos \psi \csc \theta \\ 0 & \cos \psi & \sin \psi \\ 1 & -\sin \psi \cot \theta & \cos \psi \cot \theta \end{bmatrix}$	$\begin{bmatrix} \cos \theta & 0 & 1 \\ \sin \psi \sin \theta & \cos \psi & 0 \\ -\sin \theta \cos \psi & \sin \psi & 0 \end{bmatrix}$

9969-1116-1/87

The three columns of the inverse transformation matrix represent the axes of Euler rotations expressed in the orthogonal body axes. It should be noted that the adjacent columns are orthogonal. Similarly, the adjacent rows of the transformation matrix are orthogonal. The Euler angles ϕ , θ , and ψ are derived from the attitude matrix $A_{B/R}$ by the transformations in Table 4-1.

The quaternion errors represent the difference in the quaternion describing the rotation from the reference coordinate system to the true spacecraft body system and the quaternion describing the rotation from the reference system to the estimated body system (Section 12.1 of Reference 3). As in the case of Euler angle errors, the relationship to the attitude error vector is analogous to the relationship between the angular velocity and the quaternion rates. Multiplying the dynamic equations of motion for quaternions by Δt gives (see Section 16.1 of Reference 3)

$$\begin{bmatrix} \Delta q_1 \\ \Delta q_2 \\ \Delta q_3 \\ \Delta q_4 \end{bmatrix} = \frac{1}{2} \begin{bmatrix} q_4 & -q_3 & q_2 \\ q_3 & q_4 & -q_1 \\ -q_2 & q_1 & q_4 \\ -q_1 & -q_2 & -q_3 \end{bmatrix} \begin{bmatrix} \Delta \theta_1 \\ \Delta \theta_2 \\ \Delta \theta_3 \end{bmatrix} \quad (4.2-2)$$

where the quaternion $\bar{q} = (q_1, q_2, q_3, q_4)$ is derived from the attitude matrix $A_{B/R}$ computed as in Section 4.1.

As stated previously, the error vector $\Delta \bar{\theta}$ is used for internal computations. Thus, the a priori covariance of the attitude error parameters is always given by

$$P_{Aattitude} = E \left[\Delta \bar{\theta}(t_0) \Delta \bar{\theta}^T(t_0) \right] \quad (4.2-3a)$$

The assumption is made in ADEAS, however, that the initial uncertainties in the parameters used for input and output are uncorrelated. Thus, the form of the a priori covariance of the attitude error parameters depends on which parameterization is used for input and output.

If the attitude error vector is used for input and output, then

$$P_{\text{Attitude}} = \text{diag} \left(\sigma_{\theta_1}^2, \sigma_{\theta_2}^2, \sigma_{\theta_3}^2 \right) \quad (4.2-3b)$$

If Euler angle errors are used for input and output, then

$$P_{\text{Attitude}} = B \left[\text{diag} \left(\sigma_{\phi}^2, \sigma_{\theta}^2, \sigma_{\psi}^2 \right) \right] B^T \quad (4.2-3c)$$

where B is the appropriate matrix from the last column of Table 4-2.

The situation is more complicated if quaternion errors are used for input and output since the quaternion errors are not independent but must obey the normalization condition

$$\bar{q}^T \Delta \bar{q} = 0 \quad (4.2-3d)$$

Thus, we assume that the quaternion errors are given by

$$\Delta \bar{q} = (I - \bar{q} \bar{q}^T) \delta \bar{q} \quad (4.2-3e)$$

where the components of $\delta \bar{q}$ are assumed to be independent so that

$$E[\delta \bar{q} \delta \bar{q}^T] = \text{diag} \left(\sigma_{q_1}^2, \sigma_{q_2}^2, \sigma_{q_3}^2, \sigma_{q_4}^2 \right) \quad (4.2-3f)$$

With the $\Delta\bar{q}$ given by Equation (4.2-3e), Equation (4.2-3d) is satisfied automatically. It would be inconsistent with Equation (4.2-3d) to assume that $E[\Delta\bar{q}\Delta\bar{q}^T]$ had the form of the right side of Equation (4.2-3f). Now we find from Equations (4.2-2), (4.2-3a), (4.2-3e), and (4.2-3f) that

$$P_{\text{Attitude}} = 4B_q^T \text{diag} \left[\left(\sigma_{q_1}^2, \sigma_{q_2}^2, \sigma_{q_3}^2, \sigma_{q_4}^2 \right) \right] B_q \quad (4.2-3g)$$

if quaternion errors are used for input and output, where B_q is the 4×3 matrix appearing in Equation (4.2-2).

4.2.2 ATTITUDE ERROR PROPAGATION

The true attitude $A_{B/I}$ relative to inertial space, given by Equation (4.1-6), evolves according to

$$\dot{A}_{B/I}(t) = -\tilde{\omega}_{B/I}(t) A_{B/I}(t) \quad (4.2-4)$$

where

$$\tilde{\omega}_{B/I} = \tilde{\omega}_{B/R} + \tilde{\omega}_{R/I} \quad (4.2-5)$$

is the angular velocity of the spacecraft relative to inertial space, with $\tilde{\omega}_{R/I}$ being the angular velocity of the reference coordinate system. All angular velocity components in Equation (4.2-5) are in body coordinates. Similarly, the estimated attitude

$$A_{B/I}^* = A_{B/R}^* A_{R/I} \quad (4.2-6)$$

evolves according to

$$\dot{\bar{A}}_{B/I}^*(t) = -\tilde{\omega}_{B/I}^*(t) A_{B/I}^*(t) \quad (4.2-7)$$

where $\bar{\omega}_{B/I}^*$ is the column vector of angular velocity components in the body coordinate system derived using the gyroscope measurement model (see Section 4.3.1).

From Equation (4.2-1) and using Equations (4.1-6), (4.2-1), and (4.2-4) through (4.2-7) we have

$$\begin{aligned} \frac{d}{dt} \Delta \tilde{\Theta} &= \frac{d}{dt} \left(A_{B/R}^* A_{B/R}^T \right) = \frac{d}{dt} \left(A_{B/I}^* A_{B/I}^T \right) \\ &= \dot{A}_{B/I}^* A_{B/I}^T + A_{B/I}^* \dot{A}_{B/I}^T \\ &= -\tilde{\omega}_{B/I}^* A_{B/I}^* A_{B/I}^T + A_{B/I}^* A_{B/I}^T \tilde{\omega}_{B/I} \\ &= -\tilde{\omega}_{B/I}^* \Delta \tilde{\Theta} + \Delta \tilde{\Theta} \tilde{\omega}_{B/I} - \tilde{\omega}_{B/I}^* + \tilde{\omega}_{B/I} \end{aligned} \quad (4.2-8)$$

Let

$$\Delta \tilde{\omega}_{B/I} = \tilde{\omega}_{B/I}^* - \tilde{\omega}_{B/I} \quad (4.2-9)$$

and assume that $\Delta \tilde{\omega}_{B/I}$ is small. Then, to first order

$$\frac{d}{dt} \Delta \tilde{\Theta} = -\tilde{\omega}_{B/I} \Delta \tilde{\Theta} + \Delta \tilde{\Theta} \tilde{\omega}_{B/I} - \Delta \tilde{\omega}_{B/I} \quad (4.2-10a)$$

Or, in vector form

$$\dot{\Delta \tilde{\Theta}}(t) = -\tilde{\omega}_{B/I}(t) \Delta \tilde{\Theta}(t) - \Delta \tilde{\omega}_{B/I}(t) \quad (4.2-10b)$$

According to the gyroscope model of Section 4.3.1

$$\Delta \bar{\omega}_{B/I}(t) = \Delta \bar{b}(t) + \Omega(t) \Delta \bar{k} - \tilde{\omega}_{B/I}(t) \Delta \bar{\epsilon} - \bar{u}_{\theta}(t) \quad (4.2-11)$$

where $\Delta \bar{b}$ is the gyro bias error (a first-order Markov process), $\Delta \bar{k}$ is the gyro scale factor error, $\Delta \bar{\epsilon}$ is the gyro alignment error vector, \bar{u}_{θ} is a white noise process and

$$\Omega(t) \equiv \text{diag} [\bar{\omega}_{B/I}(t)] \quad (4.2-12)$$

The attitude error $\Delta \bar{\theta}$ is nominally zero and thus can be included with $\Delta \bar{b}$, $\Delta \bar{k}$, and $\Delta \bar{\epsilon}$ in a composite state error vector

$$\Delta \bar{x} \equiv \begin{bmatrix} \Delta \bar{\theta} \\ \Delta \bar{b} \\ \Delta \bar{k} \\ \Delta \bar{\epsilon} \end{bmatrix} \quad (4.2-13)$$

Combining Equations (4.2-10), (4.2-11), and (4.3-22) then gives the following state error equation:

$$\dot{\Delta \bar{x}}(t) = \begin{bmatrix} -\tilde{\omega}_{B/I}(t) & -I & -\Omega(t) & \tilde{\omega}_{B/I}(t) \\ 0 & -I/\tau & 0 & 0 \\ 0 & 0 & 0 & 0 \\ 0 & 0 & 0 & 0 \end{bmatrix} \Delta \bar{x}(t) + \begin{bmatrix} \bar{u}_{\theta}(t) \\ \bar{u}_b(t) \\ 0 \\ 0 \end{bmatrix} \quad (4.2-14)$$

where $\bar{u}_b(t)$ is a white noise process.

4.2.3 TRANSITION MATRIX COMPUTATION

Integrating Equation (4.2-14) then gives for the state transition matrix, as defined by Equation (2.1-5)

$$\phi(t, t') = \begin{bmatrix} \phi_{\theta\theta}(t, t') & \phi_{\theta b}(t, t') & \phi_{\theta k}(t, t') & I - \phi_{\theta\theta}(t, t') \\ 0 & \phi_{bb}(t, t') & 0 & 0 \\ 0 & 0 & I & 0 \\ 0 & 0 & 0 & I \end{bmatrix} \quad (4.2-15)$$

where

$$\dot{\phi}_{\theta\theta}(t, t') = -\tilde{\omega}_{B/I}(t) \phi_{\theta\theta}(t, t') \quad (4.2-16)$$

$$\dot{\phi}_{\theta b}(t, t') = -\tilde{\omega}_{B/I}(t) \phi_{\theta b}(t, t') - I e^{-(t-t')/\tau} \quad (4.2-17)$$

$$\dot{\phi}_{\theta k}(t, t') = -\tilde{\omega}_{B/I}(t) \phi_{\theta k}(t, t') - \Omega(t) \quad (4.2-18)$$

$$\phi_{bb}(t, t') = I e^{-(t-t')/\tau} \quad (4.2-19)$$

This partitioning of the transition matrix is different from the partitioning of Equation (2.2-1d); the two partitionings are related by row and column interchanges, depending on the selection of dynamic solve-for and consider parameters.

Now Equation (4.2-16) has an identical form as Equation (4.2-4) for the attitude $A_{B/I}$. Thus, $\phi_{\theta\theta}$ must also act as a transition matrix for $A_{B/I}$.

$$A_{B/I}(t) = \phi_{\theta\theta}(t, t') A_{B/I}(t') \quad (4.2-20)$$

or

$$\phi_{\theta\theta}(t, t') = A_{B/I}(t) A_{B/I}^T(t') \quad (4.2-21)$$

Given a solution for $\phi_{\theta\theta}$, Equations (4.2-17) and (4.2-18) can be integrated to give

$$\phi_{\theta b}(t, t') = - \int_{t'}^t \phi_{\theta\theta}(t, t'') e^{-(t''-t')/\tau} dt'' \quad (4.2-22)$$

$$\phi_{\theta k}(t, t') = - \int_{t'}^t \phi_{\theta\theta}(t, t'') \Omega(t'') dt'' \quad (4.2-23)$$

Substituting Equation (4.2-21) into these gives

$$\begin{aligned} \phi_{\theta b}(t, t') &= -A_{B/I}(t) \int_{t'}^t A_{B/I}^T(t'') e^{-(t''-t')/\tau} dt'' \\ &\quad (4.2-24) \end{aligned}$$

$$= -A_{B/I}(t) A_{b}^T(t, t')$$

$$\begin{aligned} \phi_{\theta k}(t, t') &= -A_{B/I}(t) \int_{t'}^t A_{B/I}^T(t'') \Omega(t'') dt'' \\ &\quad (4.2-25) \end{aligned}$$

$$= -A_{B/I}(t) A_{k}^T(t, t')$$

where

$$A_D(t, t') \equiv \int_{t'}^t A_{B/I}(t'') e^{-(t''-t')/\tau} dt'' \quad (4.2-26)$$

$$A_K(t, t') \equiv \int_{t'}^t \Omega(t'') A_{B/I}(t'') dt'' \quad (4.2-27)$$

Over a small interval Δt such that $|\bar{\omega}_{B/I}| \Delta t \ll 1$, the transition matrix $\phi_{\theta\theta}$ can be approximated, to first order in $|\bar{\omega}_{B/I}| \Delta t$, by

$$\phi_{\theta\theta}(t, t - \Delta t) \approx I - \tilde{\omega}_{B/I}(t) \Delta t \quad (4.2-28)$$

Assuming also that $\Delta t/\tau \ll 1$, then, to first order:

$$e^{-\Delta t/\tau} \approx 1 - \Delta t/\tau \quad (4.2-29)$$

Using Equations (4.2-28) and (4.2-29) in Equation (4.2-22) gives

$$\begin{aligned} \phi_{\theta b}(t, t - \Delta t) &\approx - \int_{t-\Delta t}^t [I - \tilde{\omega}_{B/I}(t)(t - t'')] \left(1 - \frac{t'' - t + \Delta t}{\tau}\right) dt'' \\ &\approx - \int_{t-\Delta t}^t \left[\left(1 - \frac{t'' - t + \Delta t}{\tau}\right) I - \tilde{\omega}_{B/I}(t)(t - t'') \right] dt'' \\ &= -I\Delta t + \frac{1}{2} \left[\frac{1}{\tau} I + \tilde{\omega}_{B/I}(t) \right] \Delta t^2 \end{aligned} \quad (4.2-30)$$

Note that this result is still first order in $|\bar{\omega}_{B/I}| \Delta t$ and $\Delta t/\tau$ even though it is second order in Δt . Using Equations (4.2-28) and (4.2-29) again gives

$$\phi_{\theta b}(t, t - \Delta t) \approx -\frac{1}{2} \Delta t \left[I e^{-\Delta t/\tau} + \phi_{\theta\theta}(t, t - \Delta t) \right] \quad (4.2-31)$$

Or, by Equation (4.2-21)

$$\begin{aligned} \phi_{\Theta b}(t, t - \Delta t) \approx & -\frac{1}{2} \Delta t A_{B/I}(t) \left[A_{B/I}^T(t) e^{-\Delta t/\tau} \right. \\ & \left. + A_{B/I}^T(t - \Delta t) \right] \end{aligned} \quad (4.2-32)$$

Then, from Equation (4.2-24)

$$A_b(t, t - \Delta t) \approx \frac{1}{2} \Delta t \left[A_{B/I}(t) e^{-\Delta t/\tau} + A_{B/I}(t - \Delta t) \right] \quad (4.2-33)$$

Substituting Equation (4.2-28) into Equation (4.2-23), and taking Ω to be approximately constant over the interval Δt , gives

$$\begin{aligned} \phi_{\Theta k}(t, t - \Delta t) \approx & - \int_{t-\Delta t}^t [I - \tilde{\omega}_{B/I}(t)(t - t'')] \Omega_{ave}(t) dt'' \\ & \approx - \left[I \Delta t - \frac{1}{2} \tilde{\omega}_{B/I}(t) \Delta t^2 \right] \Omega_{ave}(t) \end{aligned} \quad (4.2-34)$$

where we have written $\Omega_{ave}(t)$ to emphasize that this is really the average Ω over the time interval from $t - \Delta t$ to t .

Using Equations (4.2-28) and (4.2-21) then gives

$$\begin{aligned} \phi_{\Theta k}(t, t - \Delta t) \approx & -\frac{1}{2} [I + \phi_{\Theta \Theta}(t, t - \Delta t)] \Omega_{ave}(t) \Delta t \\ = & -\frac{1}{2} A_{B/I}(t) \left[A_{B/I}^T(t) \right. \\ & \left. + A_{B/I}^T(t - \Delta t) \right] \Omega_{ave}(t) \Delta t \end{aligned} \quad (4.2-35)$$

Then, from Equation (4.2-25)

$$A_k(t, t - \Delta t) \approx \frac{1}{2} \Omega_{ave}(t) \Delta t [A_{B/I}(t) + A_{B/I}(t - \Delta t)] \quad (4.2-36)$$

In many cases, it is necessary to propagate the covariance over an interval $t - t'$ that is large enough so that either or both of Equations (4.2-28) and (4.2-29) would be violated for $\Delta t = t - t'$. In this case, the full interval is broken up into n equal steps of length:

$$\Delta t = (t - t')/n \quad (4.2-37)$$

$$\text{where } n = 1 + \text{TRUNC}\{\max[|\bar{\rho}(t, t')|, (t - t')/\tau]/\delta\} \quad (4.2-38)$$

δ is a user-specified tolerance, TRUNC is the truncation function, i.e., TRUNC(x) is the largest integer less than or equal to x , and $\bar{\rho}(t, t')$ is the net rotation of the spacecraft with respect to inertial space between times t' and t . If gyro biases are neither solved-for nor considered, $1/\tau$ is set to zero, so that it does not affect the number of steps. Equations (4.2-37) and (4.2-38) then guarantee that

$$\max(|\bar{\omega}_{ave}| \Delta t, \Delta t/\tau) \leq \delta \quad (4.2-39)$$

where the average angular velocity $\bar{\omega}_{ave}$ is related to the total rotation by

$$\bar{\rho}(t, t') = \bar{\omega}_{ave}(t - t') \quad (4.2-40)$$

The vector $\bar{\rho}(t, t')$ is computed by using Equation (4.2-40) and the analogs of Equations (4.1-7) and (4.1-8) for rotations with respect to inertial space, which give

$$\begin{aligned} A_{B/I}(t) A_{B/I}^T(t') &= I + \frac{[\tilde{\rho}(t, t')]^2}{|\bar{\rho}(t, t')|^2} [1 - \cos |\bar{\rho}(t, t')|] \\ &\quad - \frac{\tilde{\rho}(t, t')}{|\bar{\rho}(t, t')|} \sin |\bar{\rho}(t, t')| \end{aligned} \quad (4.2-41)$$

The trace of this equation gives

$$|\bar{\rho}(t, t')| = \cos^{-1} \left\{ \frac{1}{2} \text{tr} \left[A_{B/I}(t) A_{B/I}^T(t') \right] - \frac{1}{2} \right\} \quad (4.2-42)$$

Note that $|\bar{\rho}(t, t')|$ represents the rotation through the smallest angle connecting the initial and final attitudes, rather than the actual rotation performed in a maneuver. For a complex maneuver, it may be that $|\bar{\omega}_{\text{ave}}| \Delta t \ll |\bar{\omega}|_{\text{ave}} \Delta t > \delta$.

The computations used in ADEAS will be accurate if either a measurement or an output is processed between different arcs of a complex maneuver.

The matrix $\Omega_{\text{ave}}(t) \Delta t$, which is needed in Equation (4.2-36), is given, using Equation (4.2-12), by

$$\Omega_{\text{ave}}(t) \Delta t = \text{diag}[\bar{\omega}_{B/I}(t) \Delta t] \quad (4.2-43)$$

where $\bar{\omega}_{B/I}(t)$ means the average angular velocity from $t - \Delta t$ to t .

The nonzero elements of $\Omega_{\text{ave}}(t)\Delta t$ are numerically equal to three of the elements of the antisymmetric matrix $\tilde{\omega}_{B/I}(t)\Delta t$, which can be computed from $A_{B/I}(t)$ and $A_{B/I}(t - \Delta t)$ by taking half of the antisymmetric part of Equation (4.2-41) with $t' = t - \Delta t$:

$$\begin{aligned} & \frac{1}{2} [A_{B/I}(t - \Delta t)A_{B/I}^T(t) - A_{B/I}(t)A_{B/I}^T(t - \Delta t)] \\ &= \frac{\tilde{\rho}(t, t - \Delta t)}{|\tilde{\rho}(t, t - \Delta t)|} \sin |\tilde{\rho}(t, t - \Delta t)| \quad (4.2-44) \\ &\approx \tilde{\rho}(t, t - \Delta t) = \tilde{\omega}_{B/I}(t)\Delta t \end{aligned}$$

The approximation is valid if $|\tilde{\rho}(t, t - \Delta t)|$ is small enough so that $|\tilde{\rho}(t, t - \Delta t)| \approx \sin |\tilde{\rho}(t, t - \Delta t)|$, which is guaranteed by the choice of δ to be at least as good as other approximations made in the dynamic analysis.

Now the integrals for A_b and A_k in Equations (4.2-26) and (4.2-27) can be approximated by the sum of the corresponding values over each of the intervals Δt , as given by Equations (4.2-33) and (4.2-36). Thus, letting $t_i = t' + i\Delta t$:

$$\begin{aligned} A_b(t, t') &= \sum_{i=0}^{n-1} e^{-i\Delta t/\tau} A_b(t_{i+1}, t_i) \\ &\approx \frac{1}{2} \Delta t \sum_{i=0}^{n-1} e^{-i\Delta t/\tau} \left[A_{B/I}(t_{i+1}) e^{-\Delta t/\tau} + A_{B/I}(t_i) \right] \quad (4.2-45) \\ &= \Delta t \left\{ \frac{1}{2} \left[A_{B/I}(t') + A_{B/I}(t) e^{-n\Delta t/\tau} \right] \right. \\ &\quad \left. + \sum_{i=1}^{n-1} A_{B/I}(t_i) e^{-i\Delta t/\tau} \right\} \end{aligned}$$

$$A_k(t, t') = \sum_{i=0}^{n-1} A_k(t_{i+1}, t_i) \quad (4.2-46)$$

$$\approx \frac{1}{2} \sum_{i=0}^{n-1} \Omega_{ave}(t_{i+1}) \Delta t [A_{B/I}(t_{i+1}) + A_{B/I}(t_i)]$$

The transition matrices $\phi_{\theta b}(t, t')$ and $\phi_{\theta k}(t, t')$ can then be computed using Equations (4.2-24) and (4.2-25).

Since the submatrix $\phi_{\theta\theta}(t, t')$ is seen from Equation (4.2-21) to be orthogonal, the inverse of the full state transition matrix is given by

$$\phi^{-1}(t, t') = \begin{bmatrix} \phi_{\theta\theta}^T(t, t') & -\phi_{\theta\theta}^T(t, t') \phi_{\theta b}(t, t') \phi_{bb}^{-1}(t, t') & -\phi_{\theta\theta}^T(t, t') \phi_{\theta k}(t, t') & I - \phi_{\theta\theta}^T(t, t') \\ 0 & \phi_{bb}^{-1}(t, t') & 0 & 0 \\ 0 & 0 & I & 0 \\ 0 & 0 & 0 & I \end{bmatrix} \quad (4.2-47)$$

where

$$\phi_{bb}^{-1}(t, t') = I e^{(t-t')/\tau} \quad (4.2-48)$$

4.2.4 RANDOM EXCITATION COVARIANCE MATRIX COMPUTATION

Defining $\bar{\psi}$ as in Equation (2.1-6), then, based on Equations (4.2-14) and (4.2-15), the random excitation matrix is

$$\begin{aligned}
 d(t, t') &\equiv E[\bar{\psi}(t, t') \bar{\psi}^T(t, t')] \\
 &= \int_{t'}^t \phi(t, t'') Q_u \phi^T(t, t'') dt'' \\
 &= \begin{bmatrix} d_{\theta\theta}(t, t') & d_{\theta b}(t, t') & 0 & 0 \\ d_{\theta b}^T(t, t') & d_{bb}(t, t') & 0 & 0 \\ 0 & 0 & 0 & 0 \\ 0 & 0 & 0 & 0 \end{bmatrix} \quad (4.2-49)
 \end{aligned}$$

where

$$\begin{aligned}
 d_{\theta\theta}(t, t') &= \int_{t'}^t \left[\phi_{\theta\theta}(t, t'') Q_{\theta} \phi_{\theta\theta}^T(t, t'') \right. \\
 &\quad \left. + \phi_{\theta b}(t, t'') Q_b \phi_{\theta b}^T(t, t'') \right] dt'' \quad (4.2-50)
 \end{aligned}$$

$$d_{\theta b}(t, t') = \int_{t'}^t \phi_{\theta b}(t, t'') Q_b \phi_{bb}(t, t'') dt'' \quad (4.2-51)$$

$$d_{bb}(t, t') = \int_{t'}^t \phi_{bb}(t, t'') Q_b \phi_{bb}(t, t'') dt'' \quad (4.2-52)$$

with

$$E[\bar{u}_\theta(t) \bar{u}_\theta^T(t')] = Q_\theta \delta(t - t') \quad (4.2-53)$$

$$E[\bar{u}_b(t) \bar{u}_b^T(t')] = Q_b \delta(t - t') \quad (4.2-54)$$

Note that this partitioning of d is different from the partitioning of Equation (2.2-13). The two partitionings are related by row and column interchanges, depending on the selection of dynamic solve-for and consider parameters.

Substituting Equations (4.2-19), (4.2-21), and (4.2-24) into Equations (4.2-50), (4.2-51), and (4.2-52) gives

$$d_{\theta\theta}(t, t') = A_{B/I}(t) d'_{\theta\theta}(t, t') A_{B/I}^T(t) \quad (4.2-55)$$

$$d_{\theta b}(t, t') = -A_{B/I}(t) d'_{\theta b}(t, t') \quad (4.2-56)$$

$$d_{bb}(t, t') = \begin{cases} \frac{1}{2} \tau [1 - e^{-2(t-t')/\tau}] Q_b, & \text{if } 1/\tau \neq 0 \\ Q_b(t - t') & , \text{if } 1/\tau = 0 \end{cases} \quad (4.2-57)$$

where

$$d'_{\theta\theta}(t, t') \equiv \int_{t'}^t \left[A_{B/I}^T(t'') Q_\theta A_{B/I}(t'') + A_b^T(t, t'') Q_b A_b(t, t'') \right] dt'' \quad (4.2-58)$$

$$d_{\Theta b}^{\cdot}(t, t') \equiv \int_{t'}^t A_b^T(t, t'') e^{-(t-t'')/\tau} Q_b dt'' \quad (4.2-59)$$

Over a small interval Δt , with $|\bar{\omega}_{B/I}| \Delta t \ll 1$ and $\Delta t/\tau \ll 1$, we can use the first order approximations of Equations (4.2-28) and (4.2-30) in Equation (4.2-50) to obtain

$$\begin{aligned} d_{\Theta\Theta}(t, t - \Delta t) &\approx \int_{t-\Delta t}^t \left\{ Q_{\Theta} + [Q_{\Theta} \tilde{\omega}_{B/I}(t) - \tilde{\omega}_{B/I}(t) Q_{\Theta}](t - t') \right. \\ &\quad + Q_b(t - t')^2 + \frac{1}{2}[Q_b \tilde{\omega}_{B/I}(t) \\ &\quad - \tilde{\omega}_{B/I}(t) Q_b](t - t')^3 \\ &\quad \left. - \frac{1}{\tau} Q_b(t - t')^3 \right\} dt' \\ &= Q_{\Theta} \Delta t + \frac{1}{2}[Q_{\Theta} \tilde{\omega}_{B/I}(t) - \tilde{\omega}_{B/I}(t) Q_{\Theta}] \Delta t^2 \\ &\quad + \frac{1}{3} Q_b \Delta t^3 + \frac{1}{8}[Q_b \tilde{\omega}_{B/I}(t) - \tilde{\omega}_{B/I}(t) Q_b] \Delta t^4 \\ &\quad - Q_b \frac{\Delta t^4}{4\tau} \\ &\approx \frac{1}{2} \Delta t [Q_{\Theta} + \phi_{\Theta\Theta}(t, t - \Delta t) Q_{\Theta} \phi_{\Theta\Theta}^T(t, t - \Delta t) \\ &\quad + \frac{1}{6} Q_b (\Delta t)^2 + \frac{1}{2} \phi_{\Theta b}(t, t - \Delta t) Q_b \phi_{\Theta b}^T(t, t - \Delta t)] \\ &\quad (4.2-60) \end{aligned}$$

Substituting Equations (4.2-21) and (4.2-24) into this gives

$$\begin{aligned}
 d_{\theta\theta}(t, t - \Delta t) \approx & \frac{1}{2} \Delta t A_{B/I}(t) \left[A_{B/I}^T(t) Q_{\theta} A_{B/I}(t) \right. \\
 & + A_{B/I}^T(t - \Delta t) Q_{\theta} A_{B/I}(t - \Delta t) \\
 & + \frac{1}{6} A_{B/I}^T(t) Q_b A_{B/I}(t) (\Delta t)^2 \\
 & \left. + \frac{1}{2} A_b^T(t, t - \Delta t) Q_b A_b(t, t - \Delta t) \right] A_{B/I}^T(t)
 \end{aligned} \tag{4.2-61}$$

Then, from Equation (4.2-55)

$$\begin{aligned}
 d'_{\theta\theta}(t, t - \Delta t) \approx & \frac{1}{2} \Delta t \left[A_{B/I}^T(t) Q_{\theta} A_{B/I}(t) \right. \\
 & + A_{B/I}^T(t - \Delta t) Q_{\theta} A_{B/I}(t - \Delta t) \\
 & + \frac{1}{6} A_{B/I}^T(t) Q_b A_{B/I}(t) (\Delta t)^2 \\
 & \left. + \frac{1}{2} A_b^T(t, t - \Delta t) Q_b A_b(t, t - \Delta t) \right]
 \end{aligned} \tag{4.2-62}$$

Using the approximations of Equations (4.2-29) and (4.2-30) in Equation (4.2-51) gives

$$\begin{aligned}
 d_{\Theta b}(t, t - \Delta t) &\approx \int_{t-\Delta t}^t \left\{ -I(t - t') + \frac{1}{2} \left[\frac{1}{\tau} I \right. \right. \\
 &\quad \left. \left. + \tilde{\omega}_{B/I}(t) \right] (t - t')^2 \right\} \left(1 - \frac{t - t'}{\tau} \right) Q_b dt' \\
 &= \int_{t-\Delta t}^t \left\{ -I(t - t') + \frac{1}{2} \left[\frac{3}{\tau} I \right. \right. \\
 &\quad \left. \left. + \tilde{\omega}_{B/I}(t) \right] (t - t')^2 \right\} Q_b dt' \quad (4.2-63) \\
 &= \left\{ -\frac{1}{2} I \Delta t^2 + \frac{1}{6} \left[\frac{3}{\tau} I + \tilde{\omega}_{B/I}(t) \right] \Delta t^3 \right\} Q_b \\
 &\approx -\frac{1}{3} \Delta t \left[\frac{1}{2} I \Delta t - \phi_{\Theta b}(t, t - \Delta t) e^{-\Delta t/\tau} \right] Q_b
 \end{aligned}$$

Substituting Equation (4.2-24) into this gives

$$\begin{aligned}
 d_{\Theta b}(t, t - \Delta t) &\approx -\frac{1}{3} \Delta t A_{B/I}(t) \left[\frac{1}{2} A_{B/I}^T(t) \Delta t \right. \\
 &\quad \left. + A_b^T(t, t - \Delta t) e^{-\Delta t/\tau} \right] Q_b \quad (4.2-64)
 \end{aligned}$$

Then, from Equation (4.2-56),

$$\begin{aligned}
 d'_{\Theta b}(t, t - \Delta t) &\approx \frac{1}{3} \Delta t \left[\frac{1}{2} A_{B/I}^T(t) \Delta t \right. \\
 &\quad \left. + A_b^T(t, t - \Delta t) e^{-\Delta t/\tau} \right] Q_b \quad (4.2-65)
 \end{aligned}$$

We divide the time interval from t' to t into n subintervals of length $\Delta t = (t - t')/n$ as before. Then, from Equations (2.1-8) and (2.2-13), with $t_i = t' + i\Delta t$

$$d(t_{i+1}, t') = \phi(t_{i+1}, t_i) d(t_i, t') \phi^T(t_{i+1}, t_i) + d(t_{i+1}, t_i) \quad (4.2-66)$$

or, using the partitioning of Equations (4.2-15) and (4.2-49)

$$\begin{aligned} d_{\theta\theta}(t_{i+1}, t') &= \phi_{\theta\theta}(t_{i+1}, t_i) d_{\theta\theta}(t_i, t') \phi_{\theta\theta}^T(t_{i+1}, t_i) \\ &\quad + \phi_{\theta\theta}(t_{i+1}, t_i) d_{\theta b}(t_i, t') \phi_{\theta b}^T(t_{i+1}, t_i) \\ &\quad + \phi_{\theta b}(t_{i+1}, t_i) d_{\theta b}^T(t_i, t') \phi_{\theta\theta}^T(t_{i+1}, t_i) \\ &\quad + \phi_{\theta b}(t_{i+1}, t_i) d_{bb}(t_i, t') \phi_{\theta b}^T(t_{i+1}, t_i) \\ &\quad + d_{\theta\theta}(t_{i+1}, t_i) \end{aligned} \quad (4.2-67)$$

$$\begin{aligned} d_{\theta b}(t_{i+1}, t') &= \phi_{\theta\theta}(t_{i+1}, t_i) d_{\theta b}(t_i, t') \phi_{bb}(t_{i+1}, t_i) \\ &\quad + \phi_{\theta b}(t_{i+1}, t_i) d_{bb}(t_i, t') \phi_{bb}(t_{i+1}, t_i) \\ &\quad + d_{\theta b}(t_{i+1}, t_i) \end{aligned} \quad (4.2-68)$$

Substituting Equations (4.2-19), (4.2-21), (4.2-24), (4.2-55), and (4.2-56) into these gives

$$\begin{aligned} d'_{\theta\theta}(t_{i+1}, t') &= d'_{\theta\theta}(t_i, t') + d'_{\theta b}(t_i, t') A_b(t_{i+1}, t_i) \\ &\quad + A_b^T(t_{i+1}, t_i) d'_{\theta b}(t_i, t') \\ &\quad + A_b^T(t_{i+1}, t_i) d'_{bb}(t_i, t') A_b(t_{i+1}, t_i) \\ &\quad + d'_{\theta\theta}(t_{i+1}, t_i) \end{aligned} \quad (4.2-69)$$

$$\begin{aligned} d'_{\theta b}(t_{i+1}, t') &= d'_{\theta b}(t_i, t') + A_b^T(t_{i+1}, t_i) d'_{bb}(t_i, t') e^{-\Delta t/\tau} \\ &\quad + d'_{\theta b}(t_{i+1}, t_i) \end{aligned} \quad (4.2-70)$$

The matrices $d'_{\theta\theta}(t, t')$ and $d'_{\theta b}(t, t')$ can be computed by recursively applying Equations (4.2-69) and (4.2-70), starting from zero and using Equations (4.2-33), (4.2-57), (4.2-62), and (4.2-65) at each step. The matrices $d_{\theta\theta}(t, t')$ and $d_{\theta b}(t, t')$ can then be computed using Equations (4.2-55) and (4.2-56).

4.3 SENSOR MODELS

The three-axis sensor modeled by ADEAS are

- Gyroscopes
- IR horizon sensor
- Three-axis magnetometer
- Fixed-head star tracker
- Gimbaled star tracker
- Digital Sun sensor
- Analog Sun sensor
- Gimbaled Sun sensor

For the three-axis stabilized spacecraft, ADEAS models the measurement function $h(\bar{x}, \bar{p}')$ of Equation (2.1-13) in the following way:

$$h(\bar{x}, \bar{p}') = h(\hat{R}^S \bar{p}') \quad (4.3-1)$$

where \hat{R}^S = unit vector, expressed in sensor coordinates, representing the known direction of an externally sensed object

h = sensor-specific function of the unit vector \hat{R}^S

The functional dependence of the measurement on the spacecraft attitude and sensor alignment is through the unit reference vector \hat{R}^S . Let $\Delta\bar{\theta}$ be the vector of small rotation angles representing the spacecraft attitude errors, and let $\bar{\phi}$ be the vector of small rotation angles representing the sensor alignment errors. The following equations assume that $\Delta\bar{\theta}$ and $\bar{\phi}$ are expressed in radians. $\Delta\bar{\theta}$ is always a subset of the solved-for vector, whereas the analyst may designate any component(s) of $\bar{\phi}$ to be either solved for, considered, or ignored. The partial derivatives of the measurements with respect to $\Delta\bar{\theta}$ and $\bar{\phi}$ are given as

$$\frac{\partial y^*}{\partial \Delta\bar{\theta}} = \frac{\partial h}{\partial \hat{R}^S} \frac{\partial \hat{R}^S}{\partial \Delta\bar{\theta}} \quad (4.3-2)$$

$$\frac{\partial y^*}{\partial \bar{\phi}} = \frac{\partial h}{\partial \hat{R}^S} \frac{\partial \hat{R}^S}{\partial \bar{\phi}} \quad (4.3-3)$$

$\partial h / \partial \hat{R}^S$ is sensor and model dependent and is described for each of the three-axis sensors in the subsequent sections; $\partial \hat{R}^S / \partial \Delta\bar{\theta}$ and $\partial \hat{R}^S / \partial \bar{\phi}$ are derived below.

The unit reference vector in sensor coordinates can be expressed as

$$\hat{R}^S = [A_{S/B}][A_{B/I}] \hat{R}^I = [A_{S/B}] \hat{R}^B \quad (4.3-4)$$

where \hat{R}^S = the unit reference vector expressed in sensor coordinates

$[A_{S/B}]$ = the body-to-sensor rotation matrix

$[A_{B/I}]$ = the inertial-to-body rotation matrix

\hat{R}^I = the unit reference vector expressed in GCI coordinates

\hat{R}^B = the unit reference vector expressed in body frame coordinates

The sensor alignment errors $\bar{\phi}$ are errors in $[A_{S/B}]$, and the spacecraft attitude errors $\Delta\bar{\theta}$ are errors in $[A_{B/I}]$. Thus,

considering only small errors in the attitude and sensor alignments, the error in \hat{R}^S can be expressed as

$$\begin{aligned}
 \Delta \hat{R}^S &= \begin{bmatrix} 0 & \phi_z & -\phi_y \\ -\phi_z & 0 & \phi_x \\ \phi_y & -\phi_x & 0 \end{bmatrix} [A_{S/B}] [A_{B/I}] \hat{R}^I \\
 &+ [A_{S/B}] \begin{bmatrix} 0 & \Delta\theta_z & -\Delta\theta_y \\ -\Delta\theta_z & 0 & \Delta\theta_x \\ \Delta\theta_y & -\Delta\theta_x & 0 \end{bmatrix} [A_{B/I}] \hat{R}^I \\
 &= \begin{bmatrix} 0 & \phi_z & -\phi_y \\ -\phi_z & 0 & \phi_x \\ \phi_y & -\phi_x & 0 \end{bmatrix} \hat{R}^S + [A_{S/B}] \begin{bmatrix} 0 & \Delta\theta_z & -\Delta\theta_y \\ -\Delta\theta_z & 0 & \Delta\theta_x \\ \Delta\theta_y & -\Delta\theta_x & 0 \end{bmatrix} \hat{R}^B \\
 &= \begin{bmatrix} 0 & -R_z^S & R_y^S \\ R_z^S & 0 & -R_x^S \\ -R_y^S & R_x^S & 0 \end{bmatrix} \begin{bmatrix} \phi_x \\ \phi_y \\ \phi_z \end{bmatrix} + [A_{S/B}] \begin{bmatrix} 0 & -R_z^B & R_y^B \\ R_z^B & 0 & -R_x^B \\ -R_y^B & R_x^B & 0 \end{bmatrix} \begin{bmatrix} \Delta\theta_x \\ \Delta\theta_y \\ \Delta\theta_z \end{bmatrix}
 \end{aligned} \tag{4.3-5}$$

The necessary partials are then

$$\begin{aligned}
 \frac{\partial \hat{R}^S}{\partial \Delta\theta} &= [A_{S/B}] \begin{bmatrix} 0 & -R_z^B & R_y^B \\ R_z^B & 0 & -R_x^B \\ -R_y^B & R_x^B & 0 \end{bmatrix} & \frac{\partial \hat{R}^S}{\partial \phi} &= \begin{bmatrix} 0 & -R_z^S & R_y^S \\ R_z^S & 0 & -R_x^S \\ -R_y^S & R_x^S & 0 \end{bmatrix} \\
 & & & \tag{4.3-6}
 \end{aligned}$$

The partial derivatives $\partial h / \partial \hat{R}^S$ in Equations (4.3-2) and (4.3-3) are evaluated assuming that the components of \hat{R}^S can be independently varied. This is not strictly true because of the unit vector constraint $|\hat{R}^S| = 1$; this constraint also allows us alternate ways of expressing functions of \hat{R}^S , for instance

$$1 - \left(R_z^S\right)^2 = \left(R_x^S\right)^2 + \left(R_y^S\right)^2$$

Any resulting ambiguity in the partial derivatives $\partial h / \partial \hat{R}^S$ is eliminated upon multiplication by $\partial \hat{R}^S / \partial \Delta \bar{\theta}$ or $\partial \hat{R}^S / \partial \bar{\phi}$, so the partial derivatives $\partial y / \partial \Delta \bar{\theta}$ and $\partial y / \partial \bar{\phi}$ are unambiguous. The evaluation of $\partial \hat{R}^S / \partial \Delta \bar{\theta}$ is always performed because the attitude error vector is always a subset of the solved-for vector, whereas $\partial \hat{R}^S / \partial \bar{\phi}$ is computed only when one or more of the sensor alignment angles have been designated as solved for or considered. The formulation of h and its partial derivatives with respect to \hat{R}^S is thus a key to the sensor-related error analysis computations. The expressions for $h(\hat{R}^S, \bar{p})$ and a complete list of all partial derivatives for each sensor are given below.

For all sensors the sensor boresight is along the Z-axis of the sensor coordinate frame.

4.3.1 GYROSCOPES

Gyroscopes are modeled very differently from other sensors in ADEAS since gyroscope errors are regarded as part of the dynamic error model, as discussed in Section 4.2, rather than as measurement errors. Another major difference is that gyroscope data are assumed to be continuously available for attitude propagation, rather than being scheduled like other measurements. These differences can be summarized by saying that gyroscope data are used in a "model replacement"

mode since they replace a full dynamic model of the spacecraft motion incorporating environmental and control torques.

Thus, in distinction to other sensor models, no measurement function $h(\bar{x}, \bar{p}')$ will be derived for gyros. Rather, this section will provide a derivation of Equations (4.2-11) through (4.2-14).

The raw gyro measurement $\bar{\omega}_S$ is assumed to be related to the spacecraft angular velocity $\bar{\omega}_{B/I}$ by

$$\bar{\omega}_S = M(\bar{\omega}_{B/I} - \bar{b} - \bar{u}_\theta) \quad (4.3-7)$$

where M is a matrix incorporating gyroscope alignments and scale factors, \bar{b} is a vector of gyro biases, and $\bar{u}_\theta(t)$ is a white noise process. These quantities are not perfectly known, so the attitude determination is based on these measurements using a model

$$\bar{\omega}_S = M^*(\bar{\omega}_{B/I}^* - \bar{b}^*) \quad (4.3-8)$$

where M^* and \bar{b}^* contain estimates of the alignments, scale factors, and biases. Thus, the estimate of the spacecraft angular velocity is

$$\bar{\omega}_{B/I}^* = M^{*-1} M[\bar{\omega}_{B/I} - \bar{b} - \bar{u}_\theta] + \bar{b}^* \quad (4.3-9)$$

The matrix $M^{*-1} M$ can be written as the sum of a symmetric and an antisymmetric matrix.

$$M^{*-1} M = K + \Delta \tilde{\epsilon} \quad (4.3-10)$$

where K is symmetric and $\Delta\tilde{\epsilon}$ is skew-symmetric. It is assumed that M^* is a good estimate of M ; so K is close to the identity matrix, and $\Delta\tilde{\epsilon}$ is small. If $K = I$, the matrix $I + \Delta\tilde{\epsilon}$ represents a small rotation given by a rotation vector $\Delta\bar{\epsilon}$, the vector of gyro alignment errors. In the general case, we assume that $\Delta\tilde{\epsilon}$ has this interpretation and that

$$K = I + \text{diag}[\Delta\bar{k}] = I + \text{diag}[\Delta k_x, \Delta k_y, \Delta k_z] \quad (4.3-11)$$

where $\Delta\bar{k}$ is a vector of gyro scale factor errors. Nonzero off-diagonal elements of K would represent either higher-order effects in $\Delta\bar{\epsilon}$, which are negligible, or shear-type misalignments of the gyro input axes (as opposed to the rigid misalignment of all input axes represented by $\Delta\bar{\epsilon}$), which we assume not to be present.

Inserting Equations (4.3-10) and (4.3-11) into Equation (4.3.9), and neglecting terms of order $\Delta\bar{k}\bar{b}^T$, $\Delta\bar{k}\bar{u}_\theta^T$, $\Delta\tilde{\epsilon}\bar{b}$, and $\Delta\tilde{\epsilon}\bar{u}_\theta$ gives

$$\bar{\omega}_{B/I}^* = \{I + \text{diag}[\Delta\bar{k}] + \Delta\tilde{\epsilon}\} \bar{\omega}_{B/I} + \bar{b}^* - \bar{b} - \bar{u}_\theta \quad (4.3-12)$$

With Equation (4.2-9) written as

$$\Delta\bar{\omega}_{B/I} \equiv \bar{\omega}_{B/I}^* - \bar{\omega}_{B/I} \quad (4.3-13)$$

and with

$$\Delta\bar{b} \equiv \bar{b}^* - \bar{b} \quad (4.3-14)$$

and

$$\Omega \equiv \text{diag}[\bar{\omega}_{B/I}] \quad (4.3-15)$$

this can be written

$$\Delta \bar{\omega}_{B/I} = \Delta \bar{b} + \Omega \Delta \bar{k} - \bar{\omega}_{B/I} \Delta \bar{\epsilon} - \bar{u}_{\theta} \quad (4.3-16)$$

which is identical to Equation (4.2-11).

The remaining task is to specify the time dependence of the gyro biases, scale factors, and misalignments. The scale factor vector $\Delta \bar{k}$ and the misalignment vector $\Delta \bar{\epsilon}$ are assumed to be constant, as reflected in Equation (4.2-14). The bias, however, is assumed to obey the differential equation

$$\dot{\bar{b}} = -\bar{b}/\tau - \bar{u}_b \quad (4.3-17)$$

where τ is a correlation time and $\bar{u}_b(t)$ is another white noise process. The processes $\bar{u}_{\theta}(t)$ and $\bar{u}_b(t)$ are assumed to be independent so that

$$E[\bar{u}_{\theta}(t) \bar{u}_{\theta}^T(t')] = Q_{\theta} \delta(t - t') \quad (4.3-18)$$

$$E[\bar{u}_b(t) \bar{u}_b^T(t')] = Q_b \delta(t - t') \quad (4.3-19)$$

$$E[\bar{u}_{\theta}(t) \bar{u}_b^T(t')] = 0 \quad (4.3-20)$$

Equations (4.3-18) and (4.3-19) are identical to Equations (4.2-53) and (4.2-54). The bias estimate obeys

$$\dot{\bar{b}}^* = -\bar{b}^*/\tau \quad (4.3-21)$$

with the same correlation time as \bar{b} . Thus, $\Delta\bar{b}$ obeys the equation

$$\dot{\Delta\bar{b}} = -\Delta\bar{b}/\tau + \bar{u}_b \quad (4.3-22)$$

which is used in Equation (4.2-14).

4.3.2 IR HORIZON SENSOR MEASUREMENT MODEL AND PARTIAL DERIVATIVES

The measurement model for the IR horizon sensor is shown in Figures 4-2 and 4-3, where the reference unit vector \hat{E}^S is the Earth vector expressed in sensor coordinates. The outputs of the IR horizon sensor are the Earth-in azimuth, Earth-out azimuth, Earth width, and Earth azimuth. Each azimuth is measured with respect to a user-defined, fixed-reference azimuth expressed in degrees from the X-axis of the sensor frame. The Earth vector in sensor coordinates is given by

$$\hat{E}^S = \begin{bmatrix} E_x^S \\ E_y^S \\ E_z^S \end{bmatrix} = \begin{bmatrix} \sin \eta \cos (\Phi_E + \Phi_0) \\ \sin \eta \sin (\Phi_E + \Phi_0) \\ \cos \eta \end{bmatrix} \quad (4.3-23)$$

where $\cos \eta = \hat{E}^S \cdot \hat{Z}^S = E_z^S$ and

$$\sin \eta = \sqrt{1 - \cos^2 \eta} \geq 0 \text{ since } 0 \leq \eta \leq 180^\circ.$$

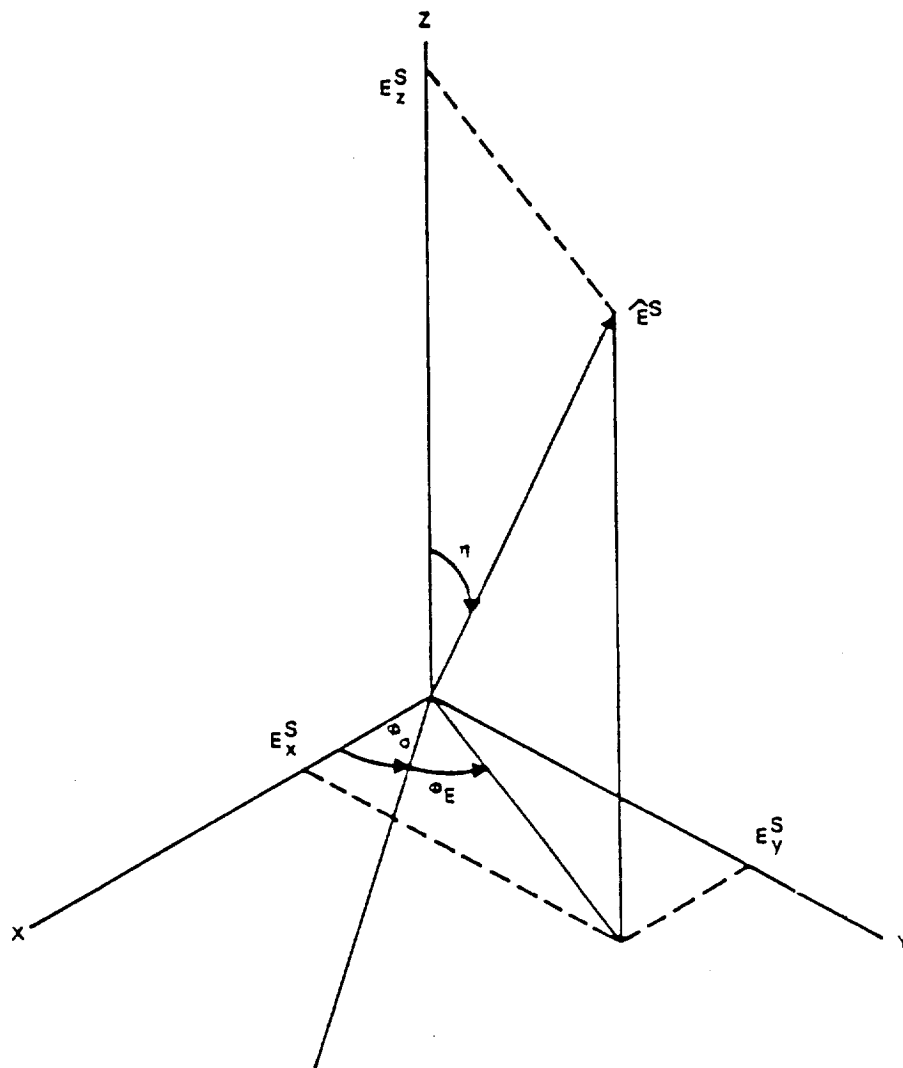


Figure 4-2. Coordinate Geometry for Earth IR Horizon Sensor

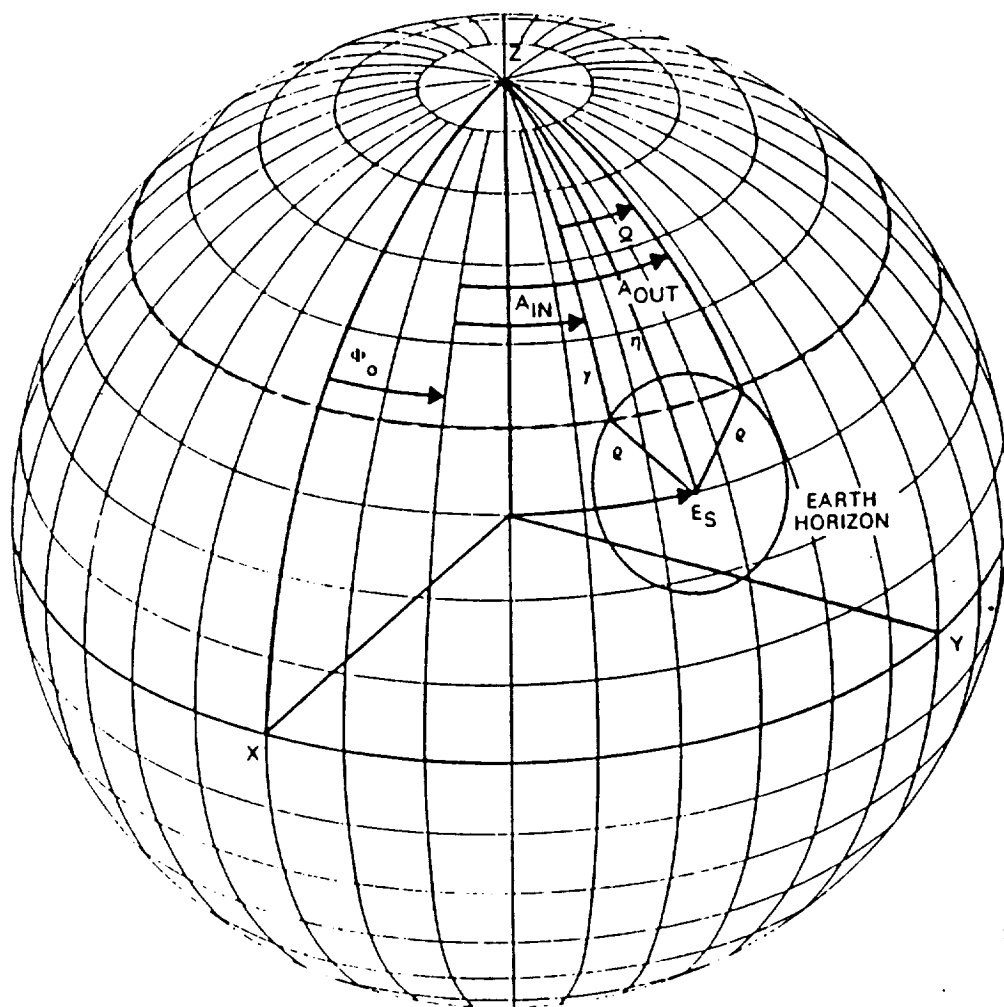


Figure 4-3. Spherical Geometry for Earth IR Horizon Sensor

Thus the measurements are calculated as

$$y^* = \text{Earth width} = h(\hat{E}^S) \quad (4.3-24)$$

$$\equiv \Omega = 2 \cos^{-1} \left\{ \frac{\cos \rho - \cos \eta \cos \gamma}{\sin \eta \sin \gamma} \right\}$$

$$y^* = \text{Earth azimuth} = h(\hat{E}^S) \equiv \Phi_E$$

$$= \tan^{-1} \left(\frac{E_Y^S}{E_X^S} \right) - \Phi_0 \quad (4.3-25)$$

$$y^* = \text{Earth-in} = h(\hat{E}^S) \equiv A_{IN} = \Phi_E - \frac{1}{2} \Omega \quad (4.3-26)$$

$$y^* = \text{Earth-out} = h(\hat{E}^S) \equiv A_{OUT} = \Phi_E + \frac{1}{2} \Omega \quad (4.3-27)$$

where E_x , E_y , E_z = x, y, and z components of Earth vector expressed in the sensor frame, the superscript S being understood

Φ_0 = reference azimuth from X-axis of sensor frame (deg)

ρ = Earth angular radius
 $= \sin^{-1} [(r + h_t)/R]$

r = Earth radius (km)

h_t = IR tangent height (km)

R = magnitude of the spacecraft position vector (km)

γ = sensor scan cone angle (deg)

η = angle between sensor boresight and Earth vector (deg)

The measurement model, in Equations (4.3-24) through (4.3-27), describes a conventional wheel-mounted horizon sensor. A very similar model describes the panoramic attitude sensor (PAS) in the planar mode. Its unit reference

vector is also the Earth vector expressed in sensor coordinates. The differences are as follows:

1. The sensor scan cone angle is 90 degrees.
2. Only the Earth-in and Earth-out signals are sensed.
3. The Earth-in and Earth-out azimuths are measured with respect to the X-axis of the sensor frame, i.e., the reference azimuth is 0 degrees.
4. The sensor does not rotate continuously in one direction as does the sensor indexed scanner, but instead scans back and forth across a user-defined arc at a user-defined rate..

The direction of the scan is important for the computation of the measurements and their partial derivatives. When the sensor is scanning in the clockwise direction, the measurements are computed as

$$y^* = \text{Earth-in} = h(\hat{E}^S) \equiv A_{IN} = \Phi_E + \frac{1}{2} \Omega \quad (4.3-28)$$

$$y^* = \text{Earth-out} = h(\hat{E}^S) \equiv A_{OUT} = \Phi_E - \frac{1}{2} \Omega \quad (4.3-29)$$

When the scanner is scanning counterclockwise, Equations (4.3-25) and (4.3-26) are used for the Earth-in and Earth-out measurements, respectively.

The measurement parameters that the user may select as either solved for or considered for the IR horizon sensor are

1. The x sensor misalignment angle (deg)
2. The y sensor misalignment angle (deg)
3. The z sensor misalignment angle (deg)
4. The Earth-in bias (deg)
5. The Earth-in scale factor

6. The amplitude of the Earth-in periodic measurement error (deg)
7. The Earth-out bias (deg)
8. The Earth-out scale factor
9. The amplitude of the Earth-out periodic measurement error (deg)
10. The Earth width bias (deg)
11. The Earth width scale factor
12. The amplitude of the Earth width periodic measurement error (deg)
13. The Earth azimuth bias (deg)
14. The Earth azimuth scale factor
15. The amplitude of the Earth azimuth periodic measurement error (deg)
16. The sensor scan cone angle (deg)
17. The fixed reference azimuth (deg)
18. The IR tangent height (km)
19. The distance from the spacecraft to Earth center (km)
20. The Earth angular radius (deg)

Note that even though the scan cone angle is always nominally 90 degrees and the reference azimuth is always nominally 0 degrees for the PAS in the planar mode, both can have a specified uncertainty about their nominal values and hence can be designated as error parameters.

In addition to specifying a name and uncertainty for each of the measurement parameters designated as either solved for or considered, the analyst must also provide the following:

1. The Euler rotation sequence and Euler angles defining the orientation of the sensor frame relative to the spacecraft body frame
2. The frequency and phase angle of the Earth-in periodic measurement error
3. The frequency and phase angle of the Earth-out periodic measurement error
4. The frequency and phase angle of the Earth width periodic measurement error
5. The frequency and phase angle of the Earth azimuth periodic measurement error
6. The reference azimuth measured from the x-axis of the sensor frame (deg)
7. The sensor scan cone angle (deg)
8. The IR tangent height (km)
9. The initial scan arc angle (deg)
10. The time rate of change of the scan arc angle (deg/sec)
11. The minimum scan arc angle (deg)
12. The maximum scan arc angle (deg)

Note that some of these parameters are not used for the PAS, and some are only used for the PAS.

When scheduling the IR horizon sensor, the user may use one or two of the sensor outputs for the error analysis computations. Since all outputs have units of degrees, the user-supplied value of the sensor white noise standard deviation for each measurement has units of degrees.

The errors in the Earth-in and Earth-out measurements are assumed to have equal standard deviations σ_A and to be uncorrelated with one another. Then, it follows from Equations (4.3-26) through (4.3-29) that the errors in the Earth-width and Earth-azimuth measurements are uncorrelated and that their standard deviations are

$$\sigma_{\Phi_E} = \sigma_A \sqrt{2} \quad (4.3-30)$$

$$\sigma_{\Omega} = \sqrt{2} \sigma_A \quad (4.3-31)$$

The correlations between the pairs (Ω, A_{IN}) , (Ω, A_{OUT}) , (Φ_E, A_{IN}) , and (Φ_E, A_{OUT}) are ignored if any such pair is selected.

Partial of the Earth azimuth wrt the unit Earth vector E:

$$\frac{\partial \Phi_E}{\partial E_x} = \frac{-E_y}{E_x^2 + E_y^2} \quad (4.3-32)$$

$$\frac{\partial \Phi_E}{\partial E_y} = \frac{E_x}{E_x^2 + E_y^2} \quad (4.3-33)$$

$$\frac{\partial \Phi_E}{\partial E_z} = 0 \quad (4.3-34)$$

Partial of the Earth azimuth wrt the sensor scan cone angle:

$$\frac{\partial \Phi_E}{\partial \gamma} = 0 \quad (4.3-35)$$

Partial of the Earth azimuth wrt the Earth angular radius:

$$\frac{\partial \Phi_E}{\partial \rho} = 0 \quad (4.3-36)$$

Partial of the Earth azimuth wrt the IR tangent height:

$$\frac{\partial \Phi_E}{\partial h_t} = 0 \quad (4.3-37)$$

Partial of the Earth azimuth wrt the spacecraft distance from Earth:

$$\frac{\partial \Phi_E}{\partial R} = 0 \quad (4.3-38)$$

Partial of the Earth azimuth wrt the bias b:

$$\frac{\partial \Phi_E}{\partial b} = 1 \quad (4.3-39)$$

Partial of the Earth azimuth wrt the scale factor k:

$$\frac{\partial \Phi_E}{\partial k} \approx h(\hat{E}) = \tan^{-1} \left(\frac{E_y}{E_x} \right) - \Phi_0 \quad (4.3-40)$$

Partial of the Earth azimuth wrt the amplitude of the periodic error a:

$$\frac{\partial \Phi_E}{\partial a} = \sin (\omega t + \psi) \quad (4.3-41)$$

Partial of the Earth width wrt the unit Earth vector \hat{E} :

$$\frac{\partial \Omega}{\partial E_x} = 0 \quad (4.3-42)$$

$$\frac{\partial \Omega}{\partial E_y} = 0 \quad (4.3-43)$$

$$\frac{\partial \Omega}{\partial E_z} = \frac{\partial \Omega}{\partial (\cos \eta)} = 2 \left[\frac{\cos \gamma - \sin \gamma \cos \frac{\Omega}{2} \cot \eta}{\sin \gamma \sin \eta \sin \frac{\Omega}{2}} \right] \quad (4.3-44)$$

Partial of the Earth width wrt the sensor scan cone angle:

$$\frac{\partial \Omega}{\partial \gamma} = 2 \left[\frac{\cos \gamma \sin \eta \cos \frac{\Omega}{2} - \sin \gamma \cos \eta}{\sin \gamma \sin \eta \sin \frac{\Omega}{2}} \right] \quad (4.3-45)$$

Partial of the Earth width wrt the Earth angular radius:

$$\frac{\partial \Omega}{\partial \rho} = 2 \left[\frac{\sin \rho}{\sin \gamma \sin \eta \sin \frac{\Omega}{2}} \right] \quad (4.3-46)$$

Partial of the Earth width wrt the IR tangent height:

$$\frac{\partial \Omega}{\partial h_t} = \frac{\partial \Omega}{\partial \rho} \left[\frac{1}{R \cos \rho} \right] \quad (4.3-47)$$

Partial of the Earth width wrt the spacecraft distance from Earth:

$$\frac{\partial \Omega}{\partial R} = - \frac{\partial \Omega}{\partial \rho} \frac{\tan \rho}{R} \quad (4.3-48)$$

Partial of the Earth width wrt the bias b:

$$\frac{\partial \Omega}{\partial b} = 1 \quad (4.3-49)$$

Partial of the Earth width wrt the scale factor k:

$$\frac{\partial \Omega}{\partial k} \approx h(\hat{E}) = 2 \cos^{-1} \left[\frac{\cos \rho - \cos \gamma \cos \eta}{\sin \gamma \sin \eta} \right] \quad (4.3-50)$$

Partial of the Earth width wrt the amplitude of the periodic error a:

$$\frac{\partial \Omega}{\partial a} = \sin (\omega t + \psi) \quad (4.3-51)$$

In the following partial derivatives with a \pm sign, the upper sign is to be used for the conventional IR scanner and for the PAS scanning in the counterclockwise direction, while the lower sign is used for the PAS scanning in the clockwise direction in accordance with Equations (4.3-28) and (4.3-29).

Partial of the Earth-in angle wrt the unit Earth vector E:

$$\frac{\partial A_{IN}}{\partial E_x} = \frac{\partial \Phi_E}{\partial E_x} \quad (4.3-52)$$

$$\frac{\partial A_{IN}}{\partial E_y} = \frac{\partial \Phi_E}{\partial E_y} \quad (4.3-53)$$

$$\frac{\partial A_{IN}}{\partial E_z} = \pm \left(-\frac{1}{2} \frac{\partial \Omega}{\partial E_z} \right) \quad (4.3-54)$$

Partial of the Earth-in angle wrt the sensor scan cone angle:

$$\frac{\partial A_{IN}}{\partial \gamma} = \pm \left(-\frac{1}{2} \frac{\partial \Omega}{\partial \gamma} \right) \quad (4.3-55)$$

Partial of the Earth-in angle wrt the Earth angular radius:

$$\frac{\partial A_{IN}}{\partial \rho} = \pm \left(-\frac{1}{2} \frac{\partial \Omega}{\partial \rho} \right) \quad (4.3-56)$$

Partial of the Earth-in angle wrt the IR tangent height:

$$\frac{\partial A_{IN}}{\partial h_t} = \pm \left(-\frac{1}{2} \frac{\partial \Omega}{\partial h_t} \right) \quad (4.3-57)$$

Partial of the Earth-in angle wrt the spacecraft distance from Earth:

$$\frac{\partial A_{IN}}{\partial R} = \pm \left(-\frac{1}{2} \frac{\partial \Omega}{\partial R} \right) \quad (4.3-58)$$

Partial of the Earth-in angle wrt the bias b:

$$\frac{\partial A_{IN}}{\partial b} = 1 \quad (4.3-59)$$

Partial of the Earth-in angle wrt the scale factor k:

$$\frac{\partial A_{IN}}{\partial k} \approx h(\hat{E}) = \Phi_E \pm \left(\frac{1}{2} \Omega \right) \quad (4.3-60)$$

Partial of the Earth-in angle wrt the amplitude of the periodic error a:

$$\frac{\partial A_{IN}}{\partial a} = \sin (\omega t + \psi) \quad (4.3-61)$$

Partial of the Earth-out angle wrt the unit Earth vector \hat{E} :

$$\frac{\partial A_{OUT}}{\partial E_x} = \frac{\partial \Phi_E}{\partial E_x} \quad (4.3-62)$$

$$\frac{\partial A_{OUT}}{\partial E_y} = \frac{\partial \Phi_E}{\partial E_y} \quad (4.3-63)$$

$$\frac{\partial A_{OUT}}{\partial E_z} = \pm \left(\frac{1}{2} \frac{\partial \Omega}{\partial E_z} \right) \quad (4.3-64)$$

Partial of the Earth-out angle wrt the sensor scan cone angle:

$$\frac{\partial A_{OUT}}{\partial \gamma} = \pm \left(\frac{1}{2} \frac{\partial \Omega}{\partial \gamma} \right) \quad (4.3-65)$$

Partial of the Earth-out angle wrt the Earth angular radius:

$$\frac{\partial A_{OUT}}{\partial \rho} = \pm \left(\frac{1}{2} \frac{\partial \Omega}{\partial \rho} \right) \quad (4.3-66)$$

Partial of the Earth-out angle wrt the IR tangent height:

$$\frac{\partial A_{OUT}}{\partial h_t} = \pm \left(\frac{1}{2} \frac{\partial \Omega}{\partial h_t} \right) \quad (4.3-67)$$

Partial of the Earth-out angle wrt the spacecraft distance from Earth:

$$\frac{\partial A_{OUT}}{\partial R} = \pm \left(\frac{1}{2} \frac{\partial \Omega}{\partial R} \right) \quad (4.3-68)$$

Partial of the Earth-out angle wrt the bias b:

$$\frac{\partial A_{OUT}}{\partial b} = 1 \quad (4.3-69)$$

Partial of the Earth-out angle wrt the scale factor k:

$$\frac{\partial A_{OUT}}{\partial k} \approx h(\hat{E}) = \Phi_E \pm \left(\frac{1}{2} \Omega \right) \quad (4.3-70)$$

Partial of the Earth-out angle wrt the amplitude of the periodic error a:

$$\frac{\partial A_{OUT}}{\partial a} = \sin (\omega t + \psi) \quad (4.3-71)$$

4.3.3 THREE-AXIS MAGNETOMETER MEASUREMENT MODEL AND PARTIAL DERIVATIVES

The three-axis magnetometer computes the three independent components of the Earth's magnetic field at any time and position, using the geomagnetic reference field updated to epoch 1985.0. The measurement is the magnetic field vector \bar{M} , which can be written $\bar{M} = M\hat{U}$, where M is the magnitude of the magnetic field, and \hat{U} is a unit vector in the direction of the field. The external reference vector is the unit vector \hat{U} :

$$y^* = x \text{ component} = h(\hat{U}) = M_x^S = MU_x^S \quad (4.3-72)$$

$$y^* = y \text{ component} = h(\hat{U}) = M_y^S = MU_y^S \quad (4.3-73)$$

$$y^* = z \text{ component} = h(\hat{U}) = M_z^S = MU_z^S \quad (4.3-74)$$

The measurement parameters, which the user may select as either solved for or considered, for the three-axis magnetometer are

1. The x sensor misalignment angle (deg)
2. The y sensor misalignment angle (deg)
3. The z sensor misalignment angle (deg)
4. The x component bias (Teslas)
5. The x component scale factor
6. The amplitude of the x component periodic measurement error (Teslas)
7. The y component bias (Teslas)
8. The y component scale factor
9. The amplitude of the y component periodic measurement error (Teslas)
10. The z component bias (Teslas)
11. The z component scale factor
12. The amplitude of the z component periodic measurement error (Teslas)

In addition to specifying a name and uncertainty for each of the measurement parameters designated as either solved for or considered, the analyst must also provide the following:

1. The Euler rotation sequence and Euler angles defining the orientation of the sensor frame relative to the spacecraft body frame
2. The frequency and phase angle of the x-component periodic measurement error
3. The frequency and phase angle of the y-component periodic measurement error

4. The frequency and phase angle of the z-component periodic measurement error

When scheduling the three-axis magnetometer, the analyst may use any or all of the sensor outputs for the error analysis computations. Since all three outputs are components of a magnetic field vector, the sensor white noise standard deviation for each measurement has units of Teslas.

Partial of the x component wrt the unit magnetic field vector \hat{U} :

$$\frac{\partial M_x}{\partial U_x} = M \quad (4.3-75)$$

$$\frac{\partial M_x}{\partial U_y} = 0 \quad (4.3-76)$$

$$\frac{\partial M_x}{\partial U_z} = 0 \quad (4.3-77)$$

Partial of the x component wrt the bias b :

$$\frac{\partial M_x}{\partial b} = 1 \quad (4.3-78)$$

Partial of the x component wrt the scale factor k :

$$\frac{\partial M_x}{\partial k} \approx h(\hat{U}) = M_x \quad (4.3-79)$$

Partial of the x component wrt the amplitude of the periodic error a:

$$\frac{\partial M_x}{\partial a} = \sin (\omega t + \psi) \quad (4.3-80)$$

Partial of the y component wrt the unit magnetic field vector \hat{U} :

$$\frac{\partial M_y}{\partial U_x} = 0 \quad (4.3-81)$$

$$\frac{\partial M_y}{\partial U_y} = M \quad (4.3-82)$$

$$\frac{\partial M_y}{\partial U_z} = 0 \quad (4.3-83)$$

Partial of the y component wrt the bias b:

$$\frac{\partial M_y}{\partial b} = 1 \quad (4.3-84)$$

Partial of the y component wrt the scale factor k:

$$\frac{\partial M_y}{\partial k} \approx h(\hat{U}) = M_y \quad (4.3-85)$$

Partial of the y component wrt the amplitude of the periodic error a:

$$\frac{\partial M_y}{\partial a} = \sin (\omega t + \psi) \quad (4.3-86)$$

Partial of the z component wrt the unit magnetic field vector \hat{U} :

$$\frac{\partial M_z}{\partial U_x} = 0 \quad (4.3-87)$$

$$\frac{\partial M_z}{\partial U_y} = 0 \quad (4.3-88)$$

$$\frac{\partial M_z}{\partial U_z} = M \quad (4.3-89)$$

Partial of the z component wrt the bias b:

$$\frac{\partial M_z}{\partial b} = 1 \quad (4.3-90)$$

Partial of the z component wrt the scale factor k:

$$\frac{\partial M_z}{\partial k} \approx h(\hat{U}) = M_z \quad (4.3-91)$$

Partial of the z component wrt the amplitude of the periodic error a:

$$\frac{\partial M_z}{\partial a} = \sin(\omega t + \psi) \quad (4.3-92)$$

4.3.4 FIXED-HEAD STAR TRACKER MEASUREMENT MODEL AND PARTIAL DERIVATIVES

The fixed-head star tracker projects the x and y coordinates of the reference unit star vector \hat{S} onto the U-V plane, as

shown in Figure 4-4. The measurements are computed as follows:

$$y^* = U = h(\hat{S}^S) = - \left(s_x^S / s_z^S \right) \quad (4.3-93)$$

$$y^* = V = h(\hat{S}^S) = - \left(s_y^S / s_z^S \right) \quad (4.3-94)$$

ADEAS allows the fixed-head star tracker to have either a conical or pyramidal field of view. The star is visible to the conical sensor only if the angle between the boresight and \hat{S}^S is less than the user-specified conical half angle. Similarly, the star is visible to the pyramidal star tracker only if

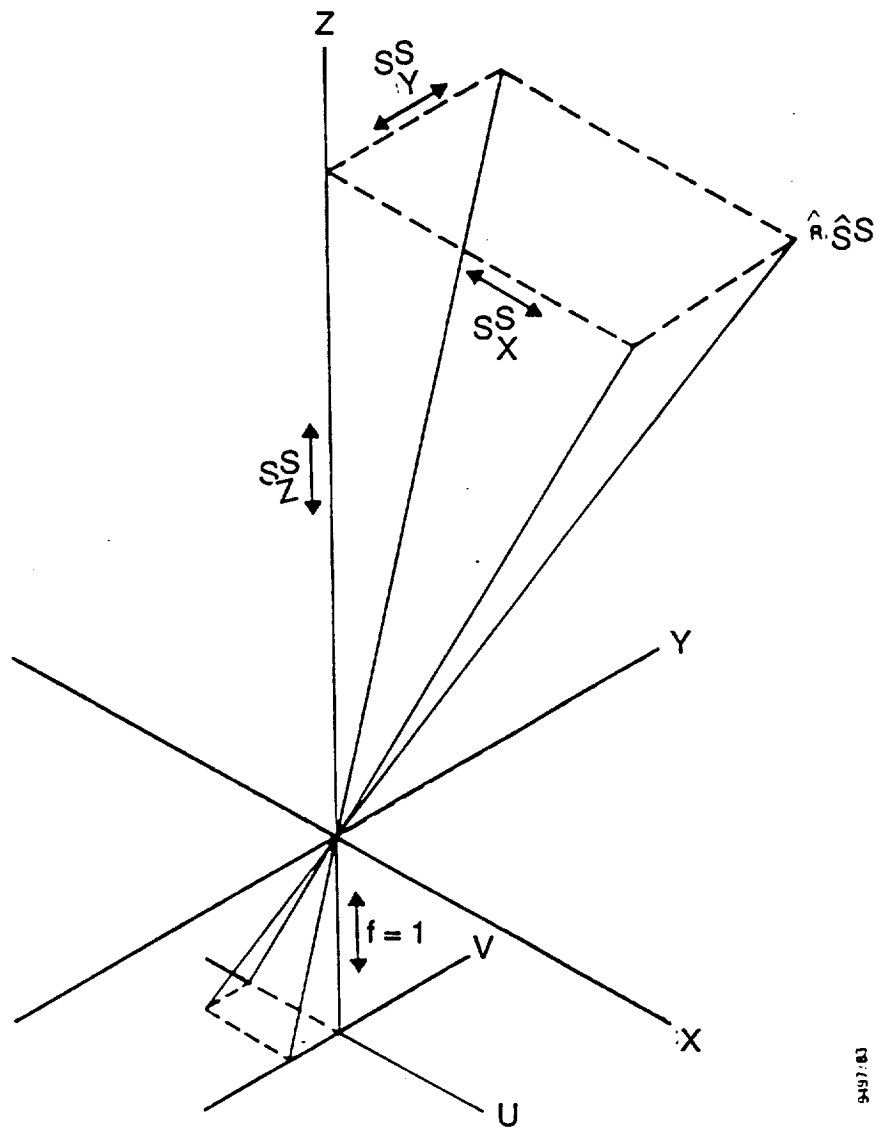
$$\text{Pyramidal } x \text{ half angle} > \left| \tan^{-1} \left(s_x^S / s_z^S \right) \right|$$

and

$$\text{Pyramidal } y \text{ half angle} > \left| \tan^{-1} \left(s_y^S / s_z^S \right) \right|$$

The measurement parameters, which the user may select as either solved for or considered, for the fixed-head star tracker are

1. The x sensor misalignment angle (deg)
2. The y sensor misalignment angle (deg)
3. The z sensor misalignment angle (deg)
4. The U bias
5. The U scale factor
6. The amplitude of the U periodic measurement error



9497.83

Figure 4-4. Fixed-Head Star Tracker Geometry

7. The V bias
8. The V scale factor
9. The amplitude of the V periodic measurement error

In addition to specifying a name and uncertainty for each of the measurement parameters designated as either solved for or considered, the analyst must also provide the following:

1. The Euler rotation sequence and Euler angles defining the orientation of the sensor frame relative to the spacecraft body frame
2. The frequency and phase angle of the U periodic measurement error
3. The frequency and phase angle of the V periodic measurement error
4. The designation of the sensor field of view as either conical or pyramidal
5. The conical half angle or the pyramidal x and y half angles

When scheduling the fixed-head star tracker, the analyst may use either or both of the sensor outputs for the error analysis computations. Since both outputs are dimensionless projections of a unit vector, the sensor white noise standard deviation has units of radians.

Partial of the U component wrt the unit star vector \hat{S} :

$$\frac{\partial U}{\partial S_x} = - \frac{1}{S_z} \quad (4.3-95)$$

$$\frac{\partial U}{\partial S_y} = 0 \quad (4.3-96)$$

$$\frac{\partial U}{\partial S_z} = \frac{S_x}{S_z^2} \quad (4.3-97)$$

Partial of the U component wrt the bias b:

$$\frac{\partial U}{\partial b} = 1 \quad (4.3-98)$$

Partial of the U component wrt the scale factor k:

$$\frac{\partial U}{\partial k} \approx h(\hat{S}) = \frac{-S_x}{S_z} \quad (4.3-99)$$

Partial of the U component wrt the amplitude of the periodic error a:

$$\frac{\partial U}{\partial a} = \sin(\omega t + \psi) \quad (4.3-100)$$

Partial of the V component wrt the unit star vector \hat{S} :

$$\frac{\partial V}{\partial S_x} = 0 \quad (4.3-101)$$

$$\frac{\partial V}{\partial S_y} = -\frac{1}{S_z} \quad (4.3-102)$$

$$\frac{\partial V}{\partial S_z} = \frac{S_y}{S_z^2} \quad (4.3-103)$$

Partial of the V component wrt the bias b:

$$\frac{\partial V}{\partial b} = 1 \quad (4.3-104)$$

Partial of the V component wrt the scale factor k:

$$\frac{\partial V}{\partial k} \approx h(\hat{S}) = \frac{-S_y}{S_z} \quad (4.3-105)$$

Partial of the V component wrt the amplitude of the periodic error a:

$$\frac{\partial V}{\partial a} = \sin (\omega t + \psi) \quad (4.3-106)$$

4.3.5 GIMBALED STAR TRACKER MEASUREMENT MODEL AND PARTIAL DERIVATIVES

The gimbaled star tracker uses azimuth (ϕ) and elevation (θ) gimbals to point a focal plane at a star. Thus, if the star unit vector is \hat{S}^S in the sensor frame, it is \hat{S}^{FP} in the focal plane frame, where (see Figure 4-5)

$$\begin{aligned} \hat{S}^{FP} &= \begin{bmatrix} \sin \theta & 0 & -\cos \theta \\ 0 & 1 & 0 \\ \cos \theta & 0 & \sin \theta \end{bmatrix} \begin{bmatrix} \cos \phi & \sin \phi & 0 \\ -\sin \phi & \cos \phi & 0 \\ 0 & 0 & 1 \end{bmatrix} \hat{S}^S \\ &= \begin{bmatrix} \sin \theta (\cos \phi S_x + \sin \phi S_y) - \cos \theta S_z \\ \cos \phi S_y - \sin \phi S_x \\ \cos \theta (\cos \phi S_x + \sin \phi S_y) + \sin \theta S_z \end{bmatrix} \end{aligned} \quad (4.3-107)$$

The superscript S has been omitted on the right side for convenience. A superscript S should be assumed where no superscript appears.

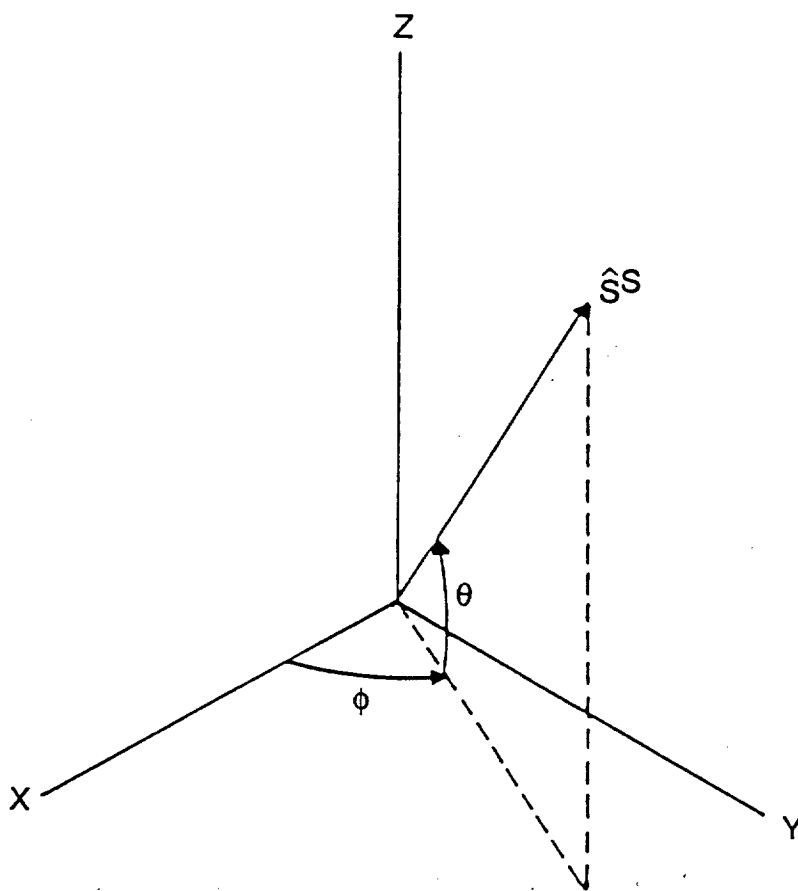


Figure 4-5. Gimbaled Star Tracker Geometry

The gimbals are nominally controlled to center the star in the focal plane, i.e., to make $\hat{S}^{FP} = [0 \ 0 \ 1]^T$, and the gimbal angles are the measurements. Thus, the measurements are computed as

$$y^* = \text{azimuth} \equiv \phi = h(\hat{S}) = \tan^{-1} \left(S_Y^S / S_X^S \right) \quad (4.3-108)$$

$$y^* = \text{elevation} \equiv \theta = h(\hat{S}) = \sin^{-1} \left(S_Z^S \right) \quad (4.3-109)$$

The azimuth equation is to be interpreted as

$$\cos \phi = S_X / \sqrt{S_X^2 + S_Y^2} \quad (4.3-110)$$

$$\sin \phi = S_Y / \sqrt{S_X^2 + S_Y^2} \quad (4.3-111)$$

The field of view of the gimballed star tracker is specified by a minimum and maximum elevation and a range of azimuths. The azimuth range is specified by its midpoint and full width; if a width of more than 360 degrees is specified, the field of view includes all azimuth values.

The sensor noise modeling must allow for imperfect centering of the star image in the sensor focal plane. Thus, if we let

$$\phi = \tan^{-1} (S_Y / S_X) + \Delta\phi \quad (4.3-112)$$

$$\theta = \sin^{-1} (S_Z) + \Delta\theta \quad (4.3-113)$$

$$\hat{S}^{FP} = \begin{bmatrix} \epsilon_x \\ \epsilon_y \\ \sqrt{1 - \epsilon_x^2 - \epsilon_y^2} \end{bmatrix} \quad (4.3-114)$$

we find, to first order in the small quantities $\Delta\phi$, $\Delta\theta$, ϵ_x , and ϵ_y

$$\Delta\phi = -\epsilon_y / \sqrt{S_x^2 + S_y^2} \quad (4.3-115)$$

$$\Delta\theta = \epsilon_x \quad (4.3-116)$$

To these gimbal errors due to focal plane centering errors, we must add intrinsic errors in the gimbal readouts. We take the mean squares of $\Delta\phi$ and $\Delta\theta$, assuming equal variances σ_{FP}^2 in the x and y focal plane errors and assuming the different errors to be uncorrelated. This gives

$$\text{variance in } \phi = \sigma_\phi^2 + \sigma_{FP}^2 / (S_x^2 + S_y^2) \quad (4.3-117)$$

$$\text{variance in } \theta = \sigma_\theta^2 + \sigma_{FP}^2 \quad (4.3-118)$$

where σ_ϕ^2 and σ_θ^2 are the variances of the gimbal readout errors and σ_ϕ , σ_θ , and σ_{FP} are all given in degrees, the units of the measurements.

The measurement parameters, which the user may select as either solved for or considered, for the gimbaledd star tracker are

1. The x sensor misalignment angle (deg)
2. The y sensor misalignment angle (deg)

3. The z sensor misalignment angle (deg)
4. The azimuth bias (deg)
5. The azimuth scale factor
6. The amplitude of the azimuth periodic measurement error (deg)
7. The elevation bias (deg)
8. The elevation scale factor
9. The amplitude of the elevation periodic measurement error (deg)

In addition to specifying a name and uncertainty for each of the measurement parameters designated as either solved for or considered, the analyst must also provide the following:

1. The Euler rotation sequence and Euler angles defining the orientation of the sensor frame relative to the spacecraft body frame
2. The frequency and phase angle of the azimuth periodic measurement error
3. The frequency and phase angle of the elevation periodic measurement error
4. The minimum and maximum azimuth and elevation defining the field of view

When scheduling the gimbaled star tracker, the analyst may use either or both of the sensor outputs for the error analysis computations.

Partial of the star azimuth ϕ wrt the unit star vector \hat{S} :

$$\frac{\partial \phi}{\partial S_x} = - \frac{S_y}{S_x^2 + S_y^2} \quad (4.3-119)$$

$$\frac{\partial \phi}{\partial S_y} = \frac{S_x}{S_x^2 + S_y^2} \quad (4.3-120)$$

$$\frac{\partial \phi}{\partial S_z} = 0 \quad (4.3-121)$$

Partial of the star azimuth wrt the bias b:

$$\frac{\partial \phi}{\partial b} = 1 \quad (4.3-122)$$

Partial of the star azimuth wrt the scale factor k:

$$\frac{\partial \phi}{\partial k} \approx h(\hat{S}) = \tan^{-1} \left(\frac{S_x}{S_z} \right) \quad (4.3-123)$$

Partial of the star azimuth wrt the amplitude of the periodic error a:

$$\frac{\partial \phi}{\partial a} = \sin (\omega t + \psi) \quad (4.3-124)$$

Partial of the star elevation Θ wrt the unit star vector \hat{S} :

$$\frac{\partial \Theta}{\partial S_x} = 0 \quad (4.3-125)$$

$$\frac{\partial \Theta}{\partial S_y} = 0 \quad (4.3-126)$$

$$\frac{\partial \Theta}{\partial S_z} = \frac{1}{\cos \Theta} = \frac{1}{\sqrt{S_x^2 + S_y^2}} \quad (4.3-127)$$

Partial of the star elevation wrt the bias b:

$$\frac{\partial \Theta}{\partial b} = 1 \quad (4.3-128)$$

Partial of the star elevation wrt the scale factor k:

$$\frac{\partial \Theta}{\partial k} \approx h(\hat{S}) = \sin^{-1} (S_y) \quad (4.3-129)$$

Partial of the star elevation wrt the amplitude of the periodic error a:

$$\frac{\partial \Theta}{\partial a} = \sin (\omega t + \psi) \quad (4.3-130)$$

If $S_z \approx 1$, the quantity $S_x^2 + S_y^2$ should be given a small, finite positive value to avoid division by zero.

4.3.6 DIGITAL SUN SENSOR MEASUREMENT MODEL AND PARTIAL DERIVATIVES

The digital Sun sensor provides measurements of the angle α between the sensor boresight and the projection of the unit Sun vector \hat{S} in the Y-Z plane and the angle β between the sensor boresight and the projection of the unit Sun vector in the X-Z plane, as shown in Figure 4-6. The sensor outputs N_α and N_β are related to these angles by Equations (7-38) and (7-39) of Reference 3:

$$\begin{aligned} \alpha = \tan^{-1} (S_y/S_z) = & A_9 + \tan^{-1} [A_1 + A_2 N_\alpha + A_3 \sin (A_4 N_\alpha \\ & + A_5) + A_6 \sin (A_7 N_\alpha + A_8)] \end{aligned} \quad (4.3-131)$$

$$\begin{aligned} \beta = \tan^{-1} (S_x/S_z) = & B_9 + \tan^{-1} [B_1 + B_2 N_\beta + B_3 \sin (B_4 N_\beta \\ & + B_5) B_6 \sin (B_7 N_\beta + B_8)] \end{aligned} \quad (4.3-132)$$

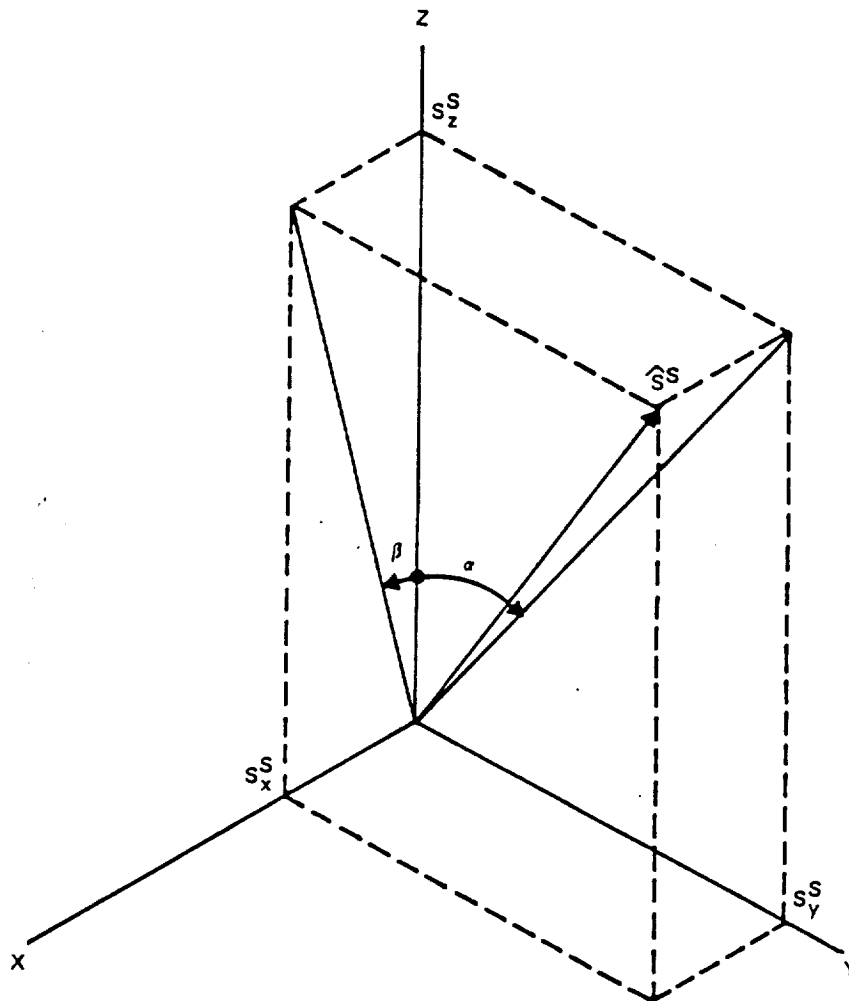


Figure 4-6. Digital Sun Sensor Geometry

where A_1, \dots, A_9 and B_1, \dots, B_9 are calibration constants provided by the manufacturer, and where the superscript S is to be understood on the components of the Sun unit vector where no superscript is shown.

The constants $A_3, A_6, B_3,$ and B_6 are very small. If A_3 and A_6 are neglected, Equation (4.3-131) gives

$$\begin{aligned} A_2 N_\alpha &\approx n_\alpha \equiv \tan(\alpha - A_9) - A_1 \\ &= \frac{S_y - S_z \tan A_9}{S_y \tan A_9 + S_z} - A_1 \end{aligned} \quad (4.3-133)$$

This expression for N_α can be substituted into the sinusoidal terms on the right side of Equation (4.3-131), and a similar procedure can be used in Equation (4.3-132) to obtain measurement equations valid to first order in $A_3, A_6, B_3,$ and B_6 . Thus, the measurements are computed as

$$\begin{aligned} y^* = N_\alpha &= h(\hat{S}^S, A_1, \dots, A_9) \\ &= [n_\alpha - A_3 \sin(A_5 + A_4 n_\alpha/A_2) - A_6 \sin(A_8 + A_7 n_\alpha/A_2)]/A_2 \end{aligned} \quad (4.3-134)$$

$$\begin{aligned} y^* = N_\beta &= h(\hat{S}^S, B_1, \dots, B_9) \\ &= [n_\beta - B_3 \sin(B_5 + B_4 n_\beta/B_2) - B_6 \sin(B_8 + B_7 n_\beta/B_2)]/B_2 \end{aligned} \quad (4.3-135)$$

where n_α is given by Equation (4.3-133) and

$$\begin{aligned} n_\beta &\equiv \tan(\beta - B_9) - B_1 \\ &= \frac{S_x - S_z \tan B_9}{S_x \tan B_9 + S_z} - B_1 \end{aligned} \quad (4.3-136)$$

In ADEAS, it is assumed that the Sun sensor outputs are in units of degrees.

ADEAS allows the Sun sensor to have either a conical or a pyramidal field of view. The Sun is visible to the conical sensor only if the angle between the boresight and \hat{S}^S is less than the user-specified conical half angle. Similarly, the Sun is visible to the pyramidal Sun sensor only if

$$\text{Pyramidal x half angle} > \left| \tan^{-1} \left(s_x^S / s_z^S \right) \right|$$

and

$$\text{Pyramidal y half angle} > \left| \tan^{-1} \left(s_y^S / s_z^S \right) \right|$$

For either configuration, ADEAS also determines whether the sensor is occulted by the Earth.

The measurement parameters, which the user may select as either solved for or considered, for the two-axis digital Sun sensor are

1. The x sensor misalignment angle (deg)
2. The y sensor misalignment angle (deg)
3. The z sensor misalignment angle (deg)
4. The N_α calibration constants A_1 , A_3 , A_4 , A_6 , and A_7 (dimensionless)
5. The N_α calibration constant A_2 (deg^{-1}), nominal value $\pi/180$.
6. The N_α calibration constants A_5 , A_8 , and A_9 (deg)
7. The N_α bias (deg)

8. The N_α scale factor
9. The N_α amplitude of the periodic measurement error (deg)
10. The N_β calibration constants B_1 , B_3 , B_4 , B_6 , and B_7 (dimensionless)
11. The N_β calibration constant B_2 (deg^{-1}), nominal value $\pi/180$.
12. The N_β calibration constants B_5 , B_8 , and B_9 (deg)
13. The N_β bias (deg)
14. The N_β scale factor
15. The N_β amplitude of the periodic measurement error (deg)

In addition to specifying a name and uncertainty for each of the measurement parameters designated as either solved for or considered, the analyst must also provide the following:

1. The Euler rotation sequence and Euler angles defining the orientation of the sensor frame relative to the spacecraft body frame
2. The frequency and phase angle of the α periodic measurement error
3. The frequency and phase angle of the β periodic measurement error
4. The designation of the sensor field of view as either conical or pyramidal
5. The conical half angle or pyramidal x and y half angles

When scheduling the two-axis Sun sensor, the user may use either or both of the sensor outputs for the error analysis computations. Since the outputs have units of degrees, the

value of the sensor white noise standard deviation for each measurement has units of degrees.

Partials of N_α wrt the unit Sun vector \hat{S} :

$$\partial N_\alpha / \partial S_x = 0 \quad (4.3-137)$$

$$\partial N_\alpha / \partial S_y = (\partial N_\alpha / \partial n_\alpha) S_z (1 + \tan^2 A_9) / (S_z + S_y \tan A_9)^2 \quad (4.3-138)$$

$$\partial N_\alpha / \partial S_z = (\partial N_\alpha / \partial n_\alpha) S_y (1 + \tan^2 A_9) / (S_z + S_y \tan A_9)^2 \quad (4.3-139)$$

where

$$\begin{aligned} \partial N_\alpha / \partial n_\alpha = & [A_2 - A_3 A_4 \cos (A_5 + A_4 n_\alpha / A_2) \\ & - A_6 A_7 \cos (A_8 + A_7 n_\alpha / A_2)] / A_2^2 \end{aligned} \quad (4.3-140)$$

Partials of N_α wrt the calibration constants:

$$\partial N_\alpha / \partial A_1 = -\partial N_\alpha / \partial n_\alpha \quad (4.3-141)$$

$$\partial N_\alpha / \partial A_2 = -N_\alpha / A_2 + (n_\alpha / A_2^2) (1 - A_2 \partial N_\alpha / \partial n_\alpha) \quad (4.3-142)$$

$$\partial N_\alpha / \partial A_3 = -A_2^{-1} \sin (A_5 + A_4 n_\alpha / A_2) \quad (4.3-143)$$

$$\partial N_\alpha / \partial A_4 = -(A_3 n_\alpha / A_2^2) \cos (A_5 + A_4 n_\alpha / A_2) \quad (4.3-144)$$

$$\partial N_\alpha / \partial A_5 = -(A_3 / A_2) \cos (A_5 + A_4 n_\alpha / A_2) \quad (4.3-145)$$

$$\partial N_{\alpha} / \partial A_6 = -A_2^{-1} \sin (A_8 + A_7 n_{\alpha} / A_2) \quad (4.3-146)$$

$$\partial N_{\alpha} / \partial A_7 = -\left(A_6 n_{\alpha} / A_2^2\right) \cos (A_8 + A_7 n_{\alpha} / A_2) \quad (4.3-147)$$

$$\partial N_{\alpha} / \partial A_8 = -(A_6 / A_2) \cos (A_8 + A_7 n_{\alpha} / A_2) \quad (4.3-148)$$

$$\partial N_{\alpha} / \partial A_9 = -(\partial N_{\alpha} / \partial n_{\alpha}) \left(S_Y^2 + S_Z^2 \right) \left(1 + \tan^2 A_9 \right) / \left(S_Z + S_Y \tan A_9 \right)^2 \quad (4.3-149)$$

Partial of N_{α} wrt the bias b_{α} :

$$\partial N_{\alpha} / \partial b_{\alpha} = 1 \quad (4.3-150)$$

Partial of N_{α} wrt the scale factor k_{α} :

$$\partial N_{\alpha} / \partial k_{\alpha} \approx h\left(\hat{S}^S, A_1, \dots, A_9\right) = N_{\alpha} \quad (4.3-151)$$

Partial of N_{α} wrt the amplitude of the periodic error:

$$\partial N_{\alpha} / \partial a_{\alpha} = \sin (\omega t + \psi) \quad (4.3-152)$$

Partials of N_{β} wrt the unit Sun vector \hat{S} :

$$\partial N_{\beta} / \partial S_x = (\partial N_{\beta} / \partial n_{\beta}) S_z \left(1 + \tan^2 B_9 \right) / \left(S_z + S_x \tan B_9 \right)^2 \quad (4.3-153)$$

$$\partial N_{\beta} / \partial S_y = 0 \quad (4.3-154)$$

$$\partial N_{\beta} / \partial S_z = -(\partial N_{\beta} / \partial n_{\beta}) S_x (1 + \tan^2 B_9) / (S_z + S_x \tan B_9)^2 \quad (4.3-155)$$

where

$$\begin{aligned} \partial N_{\beta} / \partial n_{\beta} = [B_2 - B_3 B_4 \cos (B_5 + B_4 n_{\beta} / B_2) \\ - B_6 B_7 \cos (B_8 + B_7 n_{\beta} / B_2)] / B_2^2 \end{aligned} \quad (4.3-156)$$

Partials of N_{β} wrt the calibration constants:

$$\partial N_{\beta} / \partial B_1 = -\partial N_{\beta} / \partial n_{\beta} \quad (4.3-157)$$

$$\partial N_{\beta} / \partial B_2 = -N_{\beta} / B_2 + (n_{\beta} / B_2^2) (1 - B_2 \partial N_{\beta} / \partial n_{\beta}) \quad (4.3-158)$$

$$\partial N_{\beta} / \partial B_3 = -B_2^{-1} \sin (B_5 + B_4 n_{\beta} / B_2) \quad (4.3-159)$$

$$\partial N_{\beta} / \partial B_4 = -(B_3 n_{\beta} / B_2^2) \cos (B_5 + B_4 n_{\beta} / B_2) \quad (4.3-160)$$

$$\partial N_{\beta} / \partial B_5 = -(B_3 / B_2) \cos (B_5 + B_4 n_{\beta} / B_2) \quad (4.3-161)$$

$$\partial N_{\beta} / \partial B_6 = -B_2^{-1} \sin (B_8 + B_7 n_{\beta} / B_2) \quad (4.3-162)$$

$$\partial N_{\beta} / \partial B_7 = -(B_6 n_{\beta} / B_2^2) \cos (B_8 + B_7 n_{\beta} / B_2) \quad (4.3-163)$$

$$\partial N_{\beta} / \partial B_8 = -(B_6 / B_2) \cos (B_8 + B_7 n_{\beta} / B_2) \quad (4.3-164)$$

$$\partial N_{\beta} / \partial B_9 = -(\partial N_{\beta} / \partial n_{\beta}) (S_x^2 + S_z^2) (1 + \tan^2 B_9) / (S_z + S_x \tan B_9)^2 \quad (4.3-165)$$

Partial of N_β wrt the bias b_β :

$$\partial N_\beta / \partial b_\beta = 1 \quad (4.3-166)$$

Partial of N_β wrt the scale factor k_β :

$$\partial N_\beta / \partial k_\beta \approx h(\hat{S}^S, B_1, \dots, B_9) = N_\beta \quad (4.3-167)$$

Partial of N_β wrt the amplitude of the periodic error

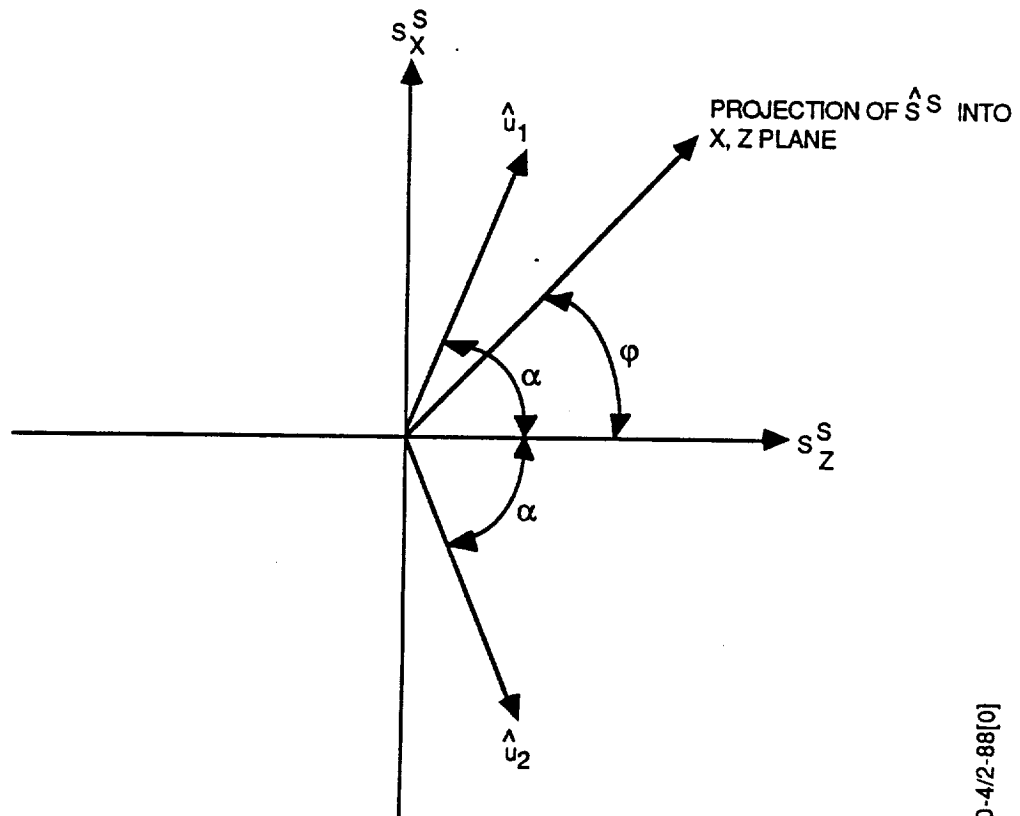
$$\partial N_\beta / \partial a_\beta = \sin(\omega t + \psi) \quad (4.3-168)$$

4.3.7 ANALOG SUN SENSOR MEASUREMENT MODEL AND PARTIAL DERIVATIVES

The geometry of the one-axis analog Sun sensor is shown in Figure 4-7. The z-axis is chosen to be the boresight of the sensor. The unit vector \hat{S}^S is the direction to the Sun in sensor coordinates. The one-axis CSS has two simple photo-cell "eyes" whose outputs, f_1 and f_2 , are proportional to the cosine of the angle between the spacecraft to Sun vector and the normal to the eye surface. The sensor output f_{CSS} is zero unless both eyes are illuminated, in which case the output is the difference of the two eye outputs. Thus the measurement is computed as:

$$y^* = h(\hat{S}^S) = f_{CSS}(\hat{S}_x^S, \hat{S}_z^S) \quad (4.3-169)$$

$$= \begin{cases} f_1 - f_2 & \text{if } \hat{S}^S \cdot \hat{U}_1 \geq C_1 \text{ and } \hat{S}^S \cdot \hat{U}_2 \geq C_2 \\ 0 & \text{if } \hat{S}^S \cdot \hat{U}_1 < C_1 \text{ or } \hat{S}^S \cdot \hat{U}_2 < C_2 \end{cases}$$



0450-4/2-88[0]

Figure 4-7. Analog Sun Sensor Geometry

where

$$f_1 = \frac{1 + b_1}{2s} \hat{S}^S \cdot \hat{U}_1 = \frac{1 + b_1}{2s} (S_z^S \cos \alpha + S_x^S \sin \alpha) \quad (4.3-170)$$

$$f_2 = \frac{1 + b_2}{2s} \hat{S}^S \cdot \hat{U}_2 = \frac{1 + b_2}{2s} (S_z^S \cos \alpha - S_x^S \sin \alpha) \quad (4.3-171)$$

The parameters b_1 and b_2 are scale factor errors; C_1 and C_2 are the cosines of user-supplied fields of view of the two eyes, and \hat{U}_1 and \hat{U}_2 are unit vectors specifying the normals of the eye surfaces:

$$\hat{U}_1 = \begin{bmatrix} \sin \alpha \\ 0 \\ \cos \alpha \end{bmatrix} \quad (4.3-172a)$$

$$\hat{U}_2 = \begin{bmatrix} -\sin \alpha \\ 0 \\ \cos \alpha \end{bmatrix} \quad (4.3-172b)$$

The calibration factor s is nominally equal to $\sin \alpha$. Thus, with the Sun vector in sensor coordinates written as

$$\hat{S}^S = \begin{bmatrix} \cos \theta \sin \phi \\ \sin \theta \\ \cos \theta \cos \phi \end{bmatrix} \quad (4.3-173)$$

and with $b_1 = b_2 = 0$, $\hat{S}^S \cdot \hat{U}_1 \geq C_1$, and $\hat{S}^S \cdot \hat{U}_2 \geq C_2$, the sensor output is

$$f_{CSS} = \cos \theta \sin \phi \quad (4.3-174)$$

This output is nominally equal to ϕ in radians if both ϕ and θ are small angles, which is if the Sun is close to the sensor boresight. Note that errors in s do not have to be considered independently, since they are equivalent to errors in the scale factor k .

The measurement parameters, which the user may select as either solved for or considered, for the analog Sun sensor are

1. The measurement bias (radians)
2. The measurement scale factor
3. The amplitude of the measurement periodic error (radians)
4. The half-angle between the eye normals, α (deg)
5. The individual eye scale factor errors, b_1 and b_2

In addition to specifying a name and uncertainty for each of the measurement parameters designated as either solved for or considered, the analyst must also provide the following:

1. The frequency and phase factor of the periodic measurement error
2. The half-angle between the eye normals, α (deg)
3. The individual eye scale factor errors, b_1 and b_2 (nominally zero)
4. The cosines of the eye fields of view, C_1 and C_2

When scheduling the analog Sun sensor, the analyst does not have a choice of measurements to use because there is only one.

In computing the partial derivatives, s is set equal to $\sin \alpha$ after carrying out the differentiations. The values given by Equations (4.3-175) through (4.3-183) are for the

case that both eyes are illuminated. If either $\hat{S}^S \cdot \hat{U}_1 < C_1$ or $\hat{S}^S \cdot \hat{U}_2 < C_2$, the partial derivatives are all identically zero.

Partial wrt the Sun vector \hat{S} (superscript S to be understood):

$$\frac{\partial f_{CSS}}{\partial S_x} = \frac{2 + b_1 + b_2}{2} \quad (4.3-175)$$

$$\frac{\partial f_{CSS}}{\partial S_y} = 0 \quad (4.3-176)$$

$$\frac{\partial f_{CSS}}{\partial S_z} = \frac{b_1 - b_2}{2} \cot \alpha \quad (4.3-177)$$

Partial wrt the half angle α :

$$\frac{\partial f_{CSS}}{\partial \alpha} = \frac{2 + b_1 + b_2}{2} S_x \cot \alpha - \frac{b_1 - b_2}{2} S_z \quad (4.3-178)$$

Partials wrt the scale factors b_1 and b_2

$$\frac{\partial f_{CSS}}{\partial b_1} = \frac{1}{2} (S_z \cot \alpha + S_x) \quad (4.3-179)$$

$$\frac{\partial f_{CSS}}{\partial b_2} = -\frac{1}{2} (S_z \cot \alpha - S_x) \quad (4.3-180)$$

Partial wrt the bias b :

$$\frac{\partial f_{CSS}}{\partial b} = 1 \quad (4.3-181)$$

Partial wrt the scale factor k:

$$\frac{\partial f_{\text{CSS}}}{\partial k} = f_{\text{CSS}} \quad (4.3-182)$$

Partial wrt the amplitude of the periodic error

$$\frac{\partial f_{\text{CSS}}}{\partial a} = \sin (\omega t + \phi) \quad (4.3-183)$$

4.3.8 GIMBALED SUN SENSOR MEASUREMENT MODEL AND PARTIAL DERIVATIVES

The gimbaled Sun sensor measurement model and partial derivatives are identical to those for the gimbaled star tracker, described in Section 4.3.5, except that the Sun unit vector is used in place of the star unit vector. The numerical values of parameters in the models may differ, of course.

SECTION 5 - REFERENCE SYSTEMS AND VECTORS

5.1 COORDINATE SYSTEMS

5.1.1 GEOCENTRIC INERTIAL (GCI) COORDINATE SYSTEM

The GCI coordinate system, illustrated in Figure 5-1, defines a fixed set of axes in inertial space. The \hat{Z}_I axis is parallel to the Earth's spin vector or north pole. The \hat{X}_I axis is along the vernal equinox, the Earth to Sun direction when the Sun crosses the equatorial plane. The \hat{Y}_I axis is given by the vector cross product $\hat{Z}_I \times \hat{X}_I$. In summary,

$$\begin{aligned}\hat{X}_I &= \text{vernal equinox} \\ \hat{Y}_I &= \hat{Z}_I \times \hat{X}_I / |\hat{Z}_I \times \hat{X}_I| \\ \hat{Z}_I &= \text{Earth spin vector}\end{aligned}\tag{5.1-1}$$

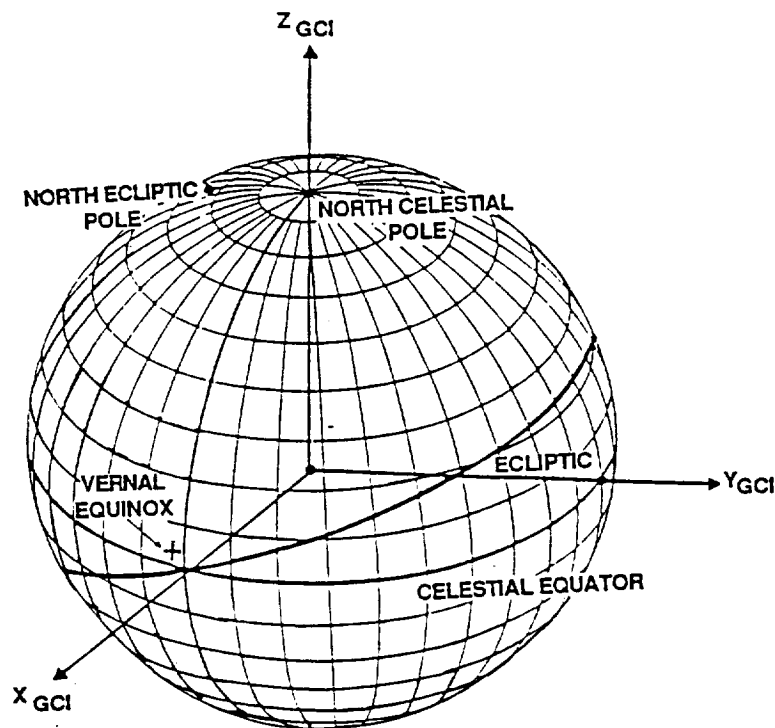


Figure 5-1. Definition of the GCI Coordinate System

The GCI coordinate system can be true-of-date, mean-of-date, or mean-of-epoch for some fixed epoch. Only mean-of-epoch coordinate systems are truly inertial, but the effects of the motion of true-of-date and mean-of-date coordinate systems are negligible for attitude error analysis computations. For high accuracy applications, all reference vectors (stars, Sun, Moon, spacecraft) should be expressed in the same inertial coordinate system.

5.1.2 EARTH-CENTER POINTING COORDINATE SYSTEM

The Earth-center pointing coordinate system $(\hat{x}_E, \hat{y}_E, \hat{z}_E)$ is defined by the spacecraft orbital position and velocity.

These give two orthogonal axes: $\hat{E} = \vec{E}/|\vec{E}|$, where \vec{E} is the spacecraft-to-Earth vector; $\hat{E} \times \hat{N}$, where \hat{N} is the orbit normal vector. The vector $\pm\hat{E}$ can be chosen as one coordinate axis of the Earth-center pointing system, and $\pm\hat{E} \times \hat{N}$ as a second axis. Then the third axis is defined to give a right-hand orthogonal triad $\hat{x}_E, \hat{y}_E, \hat{z}_E$.

The transformation matrix from GCI coordinates to Earth-center pointing coordinates is

$$A_{R/I} = \begin{bmatrix} \left(\hat{x}_E^I \right)^T \\ - - - - \\ \left(\hat{y}_E^I \right)^T \\ - - - - \\ \left(\hat{z}_E^I \right)^T \end{bmatrix} \quad (5.1-2)$$

where \hat{x}_E^I , \hat{y}_E^I , and \hat{z}_E^I are 3×1 column vectors containing the components along the GCI axes of the vectors \hat{x}_E , \hat{y}_E , and \hat{z}_E , respectively.

5.1.3 LOCAL VERTICAL POINTING COORDINATE SYSTEM

The local vertical pointing coordinate system ($\hat{x}_L, \hat{y}_L, \hat{z}_L$) is defined in terms of the local vertical pointing (\hat{p}_{LV}) and orbit normal (\hat{N}) unit vectors. The local vertical pointing unit vector components in GCI coordinates are given by

$$\hat{p}_{LV}^I = \begin{bmatrix} -\cos \phi \cos \tau \\ -\cos \phi \sin \tau \\ -\sin \phi \end{bmatrix} \quad (5.1-3)$$

where τ = geodetic longitude

$$= \arctan [R_Y/R_X] \quad (5.1-4)$$

ϕ = geodetic latitude

$$= \arctan \left\{ R_Z (1 - e^2) \sqrt{R_X^2 + R_Y^2}^{-1} \right\} \quad (5.1-5)$$

where e = Earth eccentricity and $\bar{R} = -\bar{E}^I$ is the Earth-to-spacecraft vector resolved in GCI coordinates.

The user specifies which unit vector ($-\hat{x}_L, +\hat{x}_L, -\hat{y}_L, +\hat{y}_L, -\hat{z}_L, +\hat{z}_L$) is defined as the pointing axis (\hat{p}_{LV}) and which unit vector is defined as the axis $\hat{p}_{LV} \times \hat{N}$. The third axis is defined to give a right-hand orthogonal triad $\hat{x}_L, \hat{y}_L, \hat{z}_L$.

The transformation matrix from GCI coordinates to local vertical pointing coordinates is

$$A_{R/I} = \begin{bmatrix} (\hat{x}_L^I)^T \\ (\hat{y}_L^I)^T \\ (\hat{z}_L^I)^T \end{bmatrix} \quad (5.1-6)$$

where \hat{X}_L^I , \hat{Y}_L^I , and \hat{Z}_L^I are 3 x 1 column vectors continuing the components along the GCI axes of the vectors \hat{X}_L , \hat{Y}_L , and \hat{Z}_L , respectively.

5.1.4 SUN-POINTING COORDINATE SYSTEM

The Sun-pointing coordinate system (\hat{X}_S , \hat{Y}_S , \hat{Z}_S) is defined in terms of the following unit vectors:

$$\begin{aligned}\hat{S} &\equiv \text{Spacecraft-to-Sun Unit Vector} \\ &= \frac{\vec{R}_{ES} - \vec{R}_I}{|\vec{R}_{ES} - \vec{R}_I|}\end{aligned}\quad (5.1-7)$$

$$\hat{U} \equiv \hat{S} \times \hat{N}_E \quad (5.1-8)$$

where \vec{R}_{ES} = Earth-to-Sun vector

\vec{R}_I = Earth-to-spacecraft vector (= $-\vec{E}$)

\hat{N}_E \equiv GCI z-axis (North Pole)

The vector $\pm\hat{S}$ is chosen as one coordinate axis of the Sun-pointing system, and $\pm\hat{U}$ as a second axis. Then the third axis is defined to give a right-hand orthogonal triad \hat{X}_S , \hat{Y}_S , \hat{Z}_S .

The transformation matrix from GCI coordinates to Sun-pointing coordinates is

$$A_{R/I} = \begin{bmatrix} \frac{(\hat{X}_S^I)^T}{} \\ \frac{(\hat{Y}_S^I)^T}{} \\ \frac{(\hat{Z}_S^I)^T}{} \end{bmatrix} \quad (5.1-9)$$

where \hat{x}_S^I , \hat{y}_S^I , and \hat{z}_S^I are 3 x 1 column vectors containing the components along the GCI axes of the vectors \hat{x}_S , \hat{y}_S , \hat{z}_S , respectively.

5.2 SPACECRAFT EPHEMERIS GENERATION

ADEAS has two options for spacecraft ephemeris generation: internal ephemeris generation by numerical integration and reading of an externally-generated ephemeris file.

5.2.1 NUMERICAL INTEGRATION

The Cartesian position \bar{r} and velocity \bar{v} of the spacecraft in an inertial coordinate system, obey the coupled ordinary differential equations

$$d\bar{r}/dt = \bar{v} \quad (5.2-1)$$

$$d\bar{v}/dt = \bar{a} \quad (5.2-2)$$

where \bar{a} is the acceleration of the spacecraft. The next three sections specify the algorithms for computing \bar{a} . Then, the last two sections present the numerical integration and interpolation algorithms.

5.2.1.1 Earth Potential Including J_2 Term

The force per unit mass on the spacecraft due to the Earth's gravity is

$$a_x = -\mu x/r^3 \{1 - (3/2) J_2 (R/r)^2 [5(z/r)^2 - 1]\} \quad (5.2-3)$$

$$a_y = -\mu y/r^3 \{1 - (3/2) J_2 (R/r)^2 [5(z/r)^2 - 1]\} \quad (5.2-4)$$

$$a_z = -\mu z/r^3 \{1 - (3/2) J_2 (R/r)^2 [5(z/r)^2 - 3]\} \quad (5.2-5)$$

where

$$\mu = 3.986005 \times 10^5 \text{ km}^3/\text{s}^2 \quad (5.2-6)$$

is the default gravitational constant of the Earth

$$J_2 = 1.08263 \times 10^{-3} \quad (5.2-7)$$

is the default geopotential coefficient for the Earth's oblateness,

$$R = 6378.140 \text{ km} \quad (5.2-8)$$

is the default equatorial radius of the Earth, and x , y , and z are the GCI components of the spacecraft position vector.

Higher order effects of the nonsphericity of the Earth are not modeled in ADEAS. If these terms are important for an application, an externally-generated spacecraft ephemeris must be used.

On user option, the J_2 terms can be omitted. The central body term of the Earth, $-\mu\bar{r}/r^3$, is always included.

5.2.1.2 Atmospheric Drag Effects

Atmospheric drag acceleration is modeled as a drag force in the direction of the relative wind vector acting on a satellite of constant surface area. The velocity of the satellite relative to the atmosphere is computed in the inertial coordinate system by subtracting the motion of the atmosphere, assumed to rotate with the Earth, from that of the satellite:

$$\bar{V}_{\text{rel}} = \dot{\bar{r}} - \bar{\omega} \times \bar{r} \quad (5.2-9)$$

The Earth's rotation vector, $\bar{\omega}$, is directed along the Earth's instantaneous spin axis with a magnitude equal to the rotation rate of the Earth and components $(\omega_1, \omega_2, \omega_3)$.

Ignoring the effects of precession and nutation, the Z-axis is aligned with the north polar spin axis such that ω_1 and ω_2 are equal to zero, and $\omega_3 = 7.29211585494 \times 10^{-5}$ rad/sec is constant. Therefore, in this approximation, Equation (4-12) reduces to

$$\bar{v}_{rel} = \begin{bmatrix} \dot{x} + \omega_3 y \\ \dot{y} - \omega_3 x \\ \dot{z} \end{bmatrix} \quad (5.2-10)$$

For the case of a spherical satellite, the atmospheric drag acceleration is computed as

$$\bar{a}_D = -\frac{1}{2} \frac{C_D A}{m} \rho_0(h) \bar{v}_{rel} |\bar{v}_{rel}| \quad (5.2-11)$$

where C_D = aerodynamic force coefficient, which is an adjustable parameter
 A = cross-sectional area of the satellite
 m = mass of the satellite
 $\rho_0(h)$ = altitude density function computed from the atmospheric drag model

Nominally, for a spherical satellite, the aerodynamic force coefficient, C_D , is equal to 2.0. In ADEAS, the altitude density function, $\rho_0(h)$, is modeled using a Harris-Priester atmospheric model. Harris and Priester determined the physical properties of the upper atmosphere theoretically by solving the heat conduction equation under quasi-hydrostatic conditions. Approximations for fluxes from the extreme ultraviolet and corpuscular heat sources were included, but the model averages the semiannual and seasonal-latitudinal

variations and does not attempt to account for the extreme ultraviolet 27-day effect.

The atmospheric model presented here is a modification of the Harris-Priester concept. The modification attempts to account for the diurnal bulge by including a cosine variation between a maximum density profile at the apex of the diurnal bulge (which is located approximately 30 degrees east of the subsolar point) and a minimum density profile at the antapex of the diurnal bulge. Discrete values of the maximum- and minimum-density altitude profiles, corresponding to mean solar activity, are stored in tabular form as $\rho_{\max}(h_i)$ and $\rho_{\min}(h_i)$, respectively. Different maximum and minimum profiles are available for different levels of solar activity. Exponential interpolation is used between entries; i.e., the minimum and maximum densities, ρ_{\min} and ρ_{\max} , are given by

$$\begin{aligned}\rho_{\min}(h) &= \rho_{\min}(h_i) \exp\left(\frac{h_i - h}{H_{\min}}\right) \\ \rho_{\max}(h) &= \rho_{\max}(h_i) \exp\left(\frac{h_i - h}{H_{\max}}\right)\end{aligned}\tag{5.2-12}$$

where $(h_i \leq h \leq h_{i+1})$ and the respective scale heights, H_{\min} and H_{\max} , are given by

$$H_{\min} = \frac{h_i - h_{i+1}}{\ln[\rho_{\min}(h_{i+1})/\rho_{\min}(h_i)]}\tag{5.2-13}$$

$$H_{\max} = \frac{h_i - h_{i+1}}{\ln[\rho_{\max}(h_{i+1})/\rho_{\max}(h_i)]}\tag{5.2-14}$$

A good approximation (neglecting polar motion) for the satellite height, h , is given by

$$h = r - R_E \quad (5.2-15)$$

where R_E is the mean radius of the Earth, given as

$$R_E = \frac{R_e(1 - f_E)}{\sqrt{1 - (2f_E - f_E^2) \cos^2 \delta}} \quad (5.2-16)$$

and r = magnitude of the satellite position vector

R_e = equatorial radius of the Earth

f_E = Earth's flattening coefficient
 $= 1 - (\text{polar radius}) / (\text{equatorial radius})$

δ = declination of the satellite (it is assumed that δ equals the geocentric latitude of the subsatellite point)

If the density is assumed to be maximum at the apex of the bulge, the cosine variation between the maximum and minimum density profiles is

$$\rho_0(h) = \rho_{\min}(h) + [\rho_{\max}(h) - \rho_{\min}(h)] \cos^n \left(\frac{\gamma}{2} \right) \quad (5.2-17)$$

where γ is the angle between the satellite position vector and the apex of the diurnal bulge.

The cosine function in Equation (5.2-17) can be determined directly as

$$\cos^n \frac{\gamma}{2} = \left[\frac{1 + \cos \gamma}{2} \right]^{n/2} = \left[\frac{1}{2} + \frac{\bar{r} \cdot \bar{U}_B}{2|\bar{r}|} \right]^{n/2} \quad (5.2-18)$$

where \bar{r} = satellite position vector

\bar{U}_B = unit vector directed toward the apex of the diurnal bulge

For ADEAS, n has been assigned the value of 6.

The vector \bar{U}_B has the following components:

$$U_{B_X} = \cos \delta_S \cos(\alpha_S + \bar{\lambda}) \quad (5.2-19)$$

$$U_{B_Y} = \cos \delta_S \sin(\alpha_S + \bar{\lambda}) \quad (5.2-20)$$

$$U_{B_Z} = \sin \delta_S \quad (5.2-21)$$

where δ_S = declination of the Sun

α_S = right ascension of the Sun

$\bar{\lambda}$ = lag angle between the Sun line and the apex of the diurnal bulge = 30 degrees

5.2.1.3 Sun and Moon Perturbations

The perturbations on the spacecraft's orbit due to its attraction by a point mass Sun and/or Moon are optionally included in ADEAS. The acceleration experienced by a satellite due to the Sun and Moon, expressed in an inertial coordinate system, is

$$\ddot{\bar{r}}_g = - \sum_{k=1}^2 \frac{\mu_k}{r_{kp}^3} \bar{r}_{kp} \quad (5.2-22)$$

where \bar{r} = vector from the center of an inertial coordinate system to the satellite

μ_k = product of the universal gravitational constant and the mass of the kth point mass

\bar{r}_{kp} = vector from the kth point mass to the satellite

r_{kp} = magnitude of the vector r_{kp}
 $k = 1$ for the Sun
 $k = 2$ for the Moon

In ADEAS, the motion of the spacecraft is referenced to the Earth's position. The desired form for the acceleration is obtained by subtracting the acceleration acting on the reference body,

$$\ddot{\bar{r}}_e = \sum_{k=1}^2 \frac{\mu_k}{r_k^3} \bar{r}_k \quad (5.2-23)$$

where \bar{r}_k = vector from the k th point mass to the reference body (the Earth)

r_k = magnitude of the vector \bar{r}_k

from each side of Equation (4-25) to obtain

$$\bar{a} \equiv \ddot{\bar{r}}_g - \ddot{\bar{r}}_e = - \sum_{k=1}^2 \left(\frac{\mu_k}{r_{kp}^3} \bar{r}_{kp} - \frac{\mu_k}{r_k^3} \bar{r}_k \right) \quad (5.2-24)$$

For the case in which the reference central body, i.e., the center of the coordinate system, is the Earth, and the perturbing point masses are the Sun and the Moon, Equation (4-27) becomes

$$\bar{a}_e = \bar{a}_S + \bar{a}_M \quad (5.2-25)$$

where

$$\bar{a}_S = \mu_S \left(\frac{\bar{r}_S - \bar{r}}{|\bar{r}_S - \bar{r}|^3} - \frac{\bar{r}_S}{|\bar{r}_S|^3} \right) \quad (5.2-26)$$

$$\bar{a}_M = \mu_M \left(\frac{\bar{r}_M - \bar{r}}{|\bar{r}_M - \bar{r}|^3} - \frac{\bar{r}_M}{|\bar{r}_M|^3} \right) \quad (5.2-27)$$

The quantities μ_S and μ_M are the gravitational constants of the Sun and the Moon, respectively, and \bar{r}_S and \bar{r}_M are the position vectors of the Sun and the Moon, referenced to the Earth.

5.2.1.4 Runge-Kutta Integration

The orbital equations of motion can be written compactly in terms of the 6-component vector

$$\bar{X} \equiv \begin{bmatrix} \bar{r} \\ \bar{v} \end{bmatrix} \quad (5.2-28)$$

as

$$d\bar{X}/dt = f(\bar{X}, t) \quad (5.2-29)$$

The fourth-order Runge-Kutta numerical integration gives values \bar{X}_n of the vector at a sequence of times t_n , for $n = 1, 2, \dots$, given the initial value

$$\bar{X}_0 \equiv \bar{X}(t_0) \quad (5.2-30)$$

The solution is advanced from time t_n to

$$t_{n+1} = t_n + h \quad (5.2-31)$$

by

$$\bar{X}_{n+1} = \bar{X}_n + (h/6)(\bar{f}_1 + 4\bar{f}_3 + \bar{f}_4) \quad (5.2-32)$$

where

$$\bar{f}_1 \equiv f(\bar{X}_n, t_n) \quad (5.2-33)$$

$$\bar{f}_2 \equiv f(\bar{X}_n + h\bar{f}_1/4, t_n + h/4) \quad (5.2-34)$$

$$\bar{f}_3 \equiv f(\bar{X}_n + h\bar{f}_2/2, t_n + h/2) \quad (5.2-35)$$

$$\bar{f}_4 = f(\bar{X}_n + h(\bar{f}_1 - 2\bar{f}_2 + 2\bar{f}_3), t_n + h) \quad (5.2-36)$$

The integration stepsize h is determined by accuracy considerations. For ADEAS the stepsize is a user input.

5.2.1.5 Hermite Interpolation

The spacecraft position and velocity are typically required at points other than the points $\bar{X}_0, \bar{X}_1, \bar{X}_2, \dots$ given by the Runge-Kutta integration. For output at intermediate times, a Hermite interpolation scheme is used.

Assume we have the spacecraft position and velocity \bar{r}_i, \bar{v}_i at the n equally-spaced times $t_{k+1}, t_{k+2}, \dots, t_{k+n}$ with spacing $h \equiv t_{i+1} - t_i$. Then, the n -point Hermite interpolation for the time

$$t = t_{k+1} + sh \quad (5.2-37)$$

is

$$\bar{r}(t) = \sum_{i=1}^n [g_{rr}(i, s) \bar{r}_{k+i} + g_{rv}(i, s) \bar{v}_{k+i}] \quad (5.2-38)$$

$$\bar{v}(t) = \sum_{i=1}^n [g_{vr}(i, s) \bar{r}_{k+i} + g_{vv}(i, s) \bar{v}_{k+i}] \quad (5.2-39)$$

where

$$g_{rr}(i, s) = [1 - 2C_i(s) B_i] D_i(s)^2 \quad (5.2-40)$$

$$g_{rv}(i, s) = C_i(s) D_i(s)^2 h \quad (5.2-41)$$

$$g_{vr}(i, s) = (2/h)[A_i(s) - 2A_i(s) B_i C_i(s) - B_i D_i(s)] D_i(s) \quad (5.2-42)$$

$$g_{vv}(i, s) = [D_i(s) + 2 A_i(s) C_i(s)] D_i(s) \quad (5.2-43)$$

with

$$A_i(s) \equiv \sum_{\substack{j=1 \\ j \neq i}}^n \left[(i - j)^{-1} \prod_{\substack{k=1 \\ k \neq i, j}}^n (s - k + 1)/(i - k) \right] \quad (5.2-44)$$

$$B_i \equiv \sum_{\substack{j=1 \\ j \neq i}}^n (i - j)^{-1} \quad (5.2-45)$$

$$C_i(s) \equiv s - i + 1 \quad (5.2-46)$$

$$D_i(s) \equiv \prod_{\substack{j=1 \\ j \neq i}}^n [(s - j + 1)/(i - j)] \quad (5.2-47)$$

For the Runge-Kutta integration a four-point interpolator ($n = 4$) is used. A six-point interpolator ($n = 6$) is used for interpolating data from the ephemeris file, as described in Section 5.2.2.

5.2.2 EPHEMERIS FILE

The position and velocity for a spacecraft at a specified time may be evaluated by accessing a standard GTDS EPHEM file (Reference 4).

5.3 GEOMAGNETIC FIELD VECTOR COMPUTATION

Whenever the analyst specifies a spacecraft using a magnetometer, the desired magnetic field order must be specified between 2 and 10. The computation of the direction of the Earth's magnetic field at any time and position is based on the spherical harmonic model of Appendix H (Reference 3). Specifically, the field is computed using Equations (H-12) to (H-15) of that reference.

5.4 SUN AND MOON EPHEMERIS GENERATION

The following sections specify the computation of the Sun and Moon vectors in an Earth-centered coordinate system. The spacecraft-to-Sun and spacecraft-to-Moon vectors are computed by subtracting the Earth-to-spacecraft vector from the Earth-to-Sun and Earth-to-Moon vectors, respectively.

5.4.1 SLP FILE

SLP ephemeris data files are regularly created using a JPL planetary ephemeris tape as a data source.

The solar and lunar positions are calculated from

$$\bar{X}(t) = \sum_{i=1}^N \bar{K}_i \left(\frac{t - t_m}{86400} \right)^{i-1} \quad (5.4-1)$$

where $\bar{X}(t)$ = desired position vector

\bar{K}_i = ephemeris polynomial coefficients from SLP data file

t = time in seconds from beginning of ephemeris year

t_m = time in seconds from beginning of ephemeris year to the midpoint of the curve-fit interval, from SLP data file

N = degree of polynomial plus one
for Moon, $N = 9$
for Sun, $N = 5$

5.4.2 ANALYTIC SUN EPHEMERIS COMPUTATION

The position of the Sun (X_S , Y_S , Z_S) in mean-of-date GCI coordinates is determined by evaluating a series expansion in the longitude of the Sun. The components of the Sun's position are related to the solar orbital elements by

$$X_S = r_S (\cos \tau_S) \quad (5.4-2)$$

$$Y_S = r_S (\cos \bar{\epsilon} \sin \tau_S) \quad (5.4-3)$$

$$Z_S = r_S (\sin \bar{\epsilon} \sin \tau_S) \quad (5.4-4)$$

where $\bar{\epsilon}$ = mean obliquity of the ecliptic

τ_S = solar longitude

r_S = Earth-to-Sun distance

The mean obliquity of the ecliptic ($\bar{\epsilon}$) is defined as

$$\bar{\epsilon} = 23^{\circ}.4522940 - 0^{\circ}.0130125 T_c \quad (5.4-5)$$

where T_c represents the full Julian date of the current time as the number of Julian centuries since 1900.00:

$$T_c = \frac{(\text{Julian date of current time}) - 2415020.0}{36525.0} \quad (5.4-6)$$

The solar longitude (τ_s) in degrees is defined as

$$\tau_s = G_s + \ell_s + (360^{\circ}/\pi) e_s \sin (\ell_s) \quad (5.4-7)$$

where G_s = longitude of perigee of the solar orbit

$$= 281^{\circ}.220844 + 0^{\circ}.0000470684 \Delta D$$

ℓ_s = solar mean anomaly

$$= 358^{\circ}.475833 + 0^{\circ}.985600267 \Delta D$$

e_s = eccentricity of the Earth's orbit about the Sun

$$= 0.01675104 - 0.11444 \times 10^{-8} \Delta D$$

and ΔD represents the full Julian date of the current time as the number of days since 1900.00:

$$\Delta D = 36525.0 T_c \quad (5.4-8)$$

The Earth-to-Sun distance (r_s) is defined as

$$\frac{d_s}{r_s} = 1 + e_s \cos (\ell_s) \quad (5.4-9)$$

where d_s = mean solar geocentric distance
 = 149597871.0 kilometers

5.4.3 ANALYTIC MOON EPHEMERIS COMPUTATION

The position of the Moon (X_m , Y_m , Z_m) in mean-of-date GCI coordinates is determined by evaluating series expansions in the latitude and longitude of the Moon. The components of the Moon's position are related to the lunar orbital elements by

$$X_m = r_m (\cos \Theta_m \cos \tau_m) \quad (5.4-10)$$

$$Y_m = r_m (\cos \Theta_m \sin \tau_m \cos \bar{\epsilon} - \sin \Theta_m \sin \bar{\epsilon}) \quad (5.4-11)$$

$$Z_m = r_m (\cos \Theta_m \sin \tau_m \sin \bar{\epsilon} + \sin \Theta_m \cos \bar{\epsilon}) \quad (5.4-12)$$

where $\bar{\epsilon}$ = mean obliquity of the ecliptic

τ_m = lunar ecliptic longitude

Θ_m = lunar ecliptic latitude

r_m = Earth-to-Moon distance

The mean obliquity of the ecliptic ($\bar{\epsilon}$) is defined by Equations (5.4-5) and (5.4-6).

The lunar ecliptic longitude (τ_m) is defined as

$$\tau_m = L_m + \text{series}_1 (D_m, F_m, \ell_m, \ell_s) \quad (5.4-13)$$

where

L_m = the mean longitude of the Moon, measured in the ecliptic plane from the mean equinox of date to the mean ascending node of the lunar orbit, and then along the orbit

$$= 270^{\circ}26'02''.99 + (480960^{\circ}.0 + 307^{\circ}52'59''.31)T_C - 4''.08 T_C^2$$

series₁ (D_m , F_m , ℓ_m , ℓ_s) = a series expansion in the angles D_m , F_m , ℓ_m , and ℓ_s presented in Table 5-1

The terms within the series expansion are defined as

$$\begin{aligned} D_m &= \text{mean elongation of the Moon from the Sun} \\ &= 350^{\circ}44'14''.95 + (444960^{\circ}.0 + 307^{\circ}06'51''.18)T_C \quad (5.4-14) \\ &\quad - 5''.17 T_C^2 \end{aligned}$$

$$\begin{aligned} F_m &= \text{argument of latitude of the Moon} \\ &= 11^{\circ}15'03''.20 + (483120^{\circ}.0 + 82^{\circ}01'30''.54)T_C \quad (5.4-15) \\ &\quad - 11''.56 T_C^2 \end{aligned}$$

$$\begin{aligned} \ell_m &= \text{lunar mean anomaly} \\ &= 296^{\circ}06'16''.59 + (477000^{\circ}.0 + 198^{\circ}50'56''.79)T_C \quad (5.4-16) \\ &\quad + 33''.09 T_C^2 \end{aligned}$$

$$\begin{aligned} \ell_s &= \text{solar mean anomaly} \\ &= 358^{\circ}28'33''.00 + (35640^{\circ}.0 + 359^{\circ}02'59''.10)T_C \quad (5.4-17) \end{aligned}$$

The lunar ecliptic latitude is (Θ_m) is defined as

$$\Theta_m = \text{series}_2 (D_m, F_m, \ell_m, \ell_s) \quad (5.4-18)$$

Table 5-1. Series for λ_M

Coefficient (radians)		Argument Multiple of			
		ℓ_M	F_M	D_M	ℓ_S
-0.000607	sin	0	0	1	0
0.011490	sin	0	0	2	0
-0.000267	sin	0	2	-2	0
-0.001996	sin	0	2	0	0
-0.000801	sin	0	0	-2	1
-0.003238	sin	0	0	0	1
-0.000118	sin	0	0	2	1
0.000138	sin	1	0	-2	-1
0.000716	sin	1	0	0	-1
0.000192	sin	1	-2	0	0
-0.000186	sin	1	0	-4	0
-0.022236	sin	1	0	-2	0
0.10976	sin	1	0	0	0
0.000931	sin	1	0	2	0
-0.000219	sin	1	2	0	0
-0.000999	sin	1	0	-2	1
-0.000532	sin	1	0	0	1
-0.000149	sin	2	0	-4	0
-0.001026	sin	2	0	-2	0
0.003728	sin	2	0	0	0
0.000175	sin	3	0	0	0

where series₂ (D_m , F_m , ℓ_m , ℓ_s) = a series expansion in the angles D_m , F_m , ℓ_m , and ℓ_s presented in Table 5-2

The Earth-to-Moon distance (r_m) is defined as

$$\frac{d_m}{r_m} = 1 + \text{series}_3 (D_m, F_m, \ell_m, \ell_s) \quad (5.4-19)$$

where

d_m = mean lunar geocentric distance

= 384399.06 kilometers

series₃ (D_m , F_m , ℓ_m , ℓ_s) = a series expansion in the angles D_m , F_m , ℓ_m , and ℓ_s presented in Table 5-3

As noted previously, the series are summarized in Tables 5-1 through 5-3. These tables give the coefficients of each trigonometric term and the angles that appear in that term. The trigonometric terms contain only integer multiples of the four angles. The first term in Θ_M is

$$\Theta_M = 0.089503 \sin (F_M) \text{ radians}$$

The formulas for the lunar position include the leading terms of Brown's lunar theory. All perturbation terms with amplitudes greater than 50 kilometers are included (21 terms in the ecliptic longitude, 11 terms in the ecliptic latitude, and 11 terms in the distance); this achieves an overall positional accuracy of 1 arc-minute (0.005 radian or 200 kilometers).

Table 5-2. Series for Θ_M

Coefficient (radians)		Argument Multiple of			
		l_M	F_M	D_M	l_S
0.089503	sin	0	1	0	0
0.000569	sin	0	1	2	0
-0.003023	sin	0	1	-2	0
-0.000144	sin	0	1	-2	1
0.004897	sin	1	1	0	0
-0.000807	sin	1	1	-2	0
0.004847	sin	1	-1	0	0
-0.000967	sin	1	-1	-2	0
0.000301	sin	2	1	0	0
0.000154	sin	2	-1	0	0
0.000161	sin	1	-1	2	0

Table 5-3. Series for κ_M

Coefficient (radians)		Argument Multiple of			
		l_M	F_M	D_M	l_S
0.0082488	cos	0	0	2	0
0.0005604	cos	0	0	-2	1
0.0003369	cos	1	0	0	-1
-0.0002086	cos	1	-2	0	0
0.0100247	cos	1	0	-2	0
0.0545008	cos	1	0	0	0
0.0009017	cos	1	0	2	0
0.0004219	cos	1	0	-2	1
-0.0002773	cos	1	0	0	1
0.0029700	cos	2	0	0	0
0.0001817	cos	3	0	0	0

5.5 STAR CATALOG GENERATION

ADEAS will enable the user to provide a star catalog through user input, by specifying a SKYMAP Run Star Catalog file, or by specifying the internal generation of a uniform star distribution.

5.5.1 SKYMAP FILE

ADEAS will have the capability to access a user-specified SKYMAP Run Star Catalog data set (Reference 5) to retrieve star magnitudes and positions (x, y, and z components) directly from the data set. The information will be contained within the data set in a format as specified for the GRO Run Star Catalog defined as

Word 1	INTEGER*4	SKYMAP ID number
Word 2	REAL*4	x-component of GCI vector, epoch 2000.0, proper motion to 1990.0
Word 3	REAL*4	y-component of GCI vector, epoch 2000.0, proper motion to 1990.0
Word 4	REAL*4	z-component of GCI vector, epoch 2000.0, proper motion to 1990.0
Word 5	REAL*4	Visual magnitude
Word 6	REAL*4	Not required
Word 7	REAL*4	Not required
Word 8	REAL*4	Not required

5.5.2 UNIFORM STAR DISTRIBUTION

ADEAS will have the capability to distribute n stars uniformly over the celestial sphere, where n is a user input. The following method is used to distribute the stars.

The unit sphere has an area of 4π , so if a square patch were allocated to each star, it would have a side of

$$d = \sqrt{4\pi/n} \text{ radians} \quad (5.5-1)$$

It is impossible to cover a sphere with nonoverlapping square patches, but this equation should be a good approximation to the star spacing for large n .

The uniform distribution algorithm puts the first star at the north pole, the second star at the south pole, and any remaining stars on m rings of constant latitude,

where

$$m = \text{TRUNC} \sqrt{\frac{\pi}{4} (n - 1)} \quad (5.5-2)$$

TRUNC denotes truncation, i.e., TRUNC(X) is the largest integer less than or equal to X . This function is chosen to give a good distribution for small n and to tend to spacing d for large n . The rings are at latitude,

$$\lambda_k = (\pi/2)[1 - (k + 1)/(m + 1)] \quad \text{for } k = 1, 3, 5, \dots \quad (5.5-3)$$

$$\lambda_k = -\lambda_{k-1} \quad \text{for } k = 2, 4, 6, \dots \quad (5.5-4)$$

where k runs up to m . This indexing is chosen so that the rings move toward the equator for increasing k .

The algorithm is initialized for $n > 2$ by

$$n_{\text{remaining}} = n - 2 \quad (5.5-5)$$

$$\alpha_{\text{remaining}} = \sum_{k=1}^m \cos \lambda_k \quad (5.5-6)$$

The quantity $\alpha_{\text{remaining}}$ is the total length around the rings divided by 2π . Then, the following computations are performed for $k = 1$ to m :

$$\text{Set } n_k = \text{ROUND} \left(n_{\text{remaining}} \frac{\cos \lambda_k}{\alpha_{\text{remaining}}} \right) \quad (5.5-7)$$

where $\text{ROUND}(X)$ is the closest integer to X .

Put n_k stars on the ring at latitude λ_k and longitude $2\pi j/n_k$ for $j = 0, 1, \dots, n_k - 1$. Set

$$n_{\text{remaining}} = n_{\text{remaining}} - n_k$$

and

$$\alpha_{\text{remaining}} = \alpha_{\text{remaining}} - \cos \lambda_k$$

5.6 LINE-OF-SIGHT SENSOR VISIBILITY

Occultation and interference of all line-of-sight sensors will be evaluated as requested by the user. Both computations may be independently enabled or disabled for each sensor. When the occultation and interference computations have been enabled for a sensor, the interference computation will be evaluated first.

5.6.1 OCCULTATION

The occultation of a sensor will be defined as the intersection of the line-of-sight vector from the spacecraft to the observed object and the disk of the occulting object as defined by that object's angular radius. Line-of-sight sensors may be occulted by the Earth or Moon.

Given the position vector of the occulting object (\bar{o}_B) in body coordinates and the radius of this object (r), the angular radius of this object (θ) is computed as:

$$\theta = \sin^{-1} \left[\frac{r}{|\bar{o}_B|} \right] \quad (5.6-1)$$

The sensor is occulted by this object when

$$\theta \geq \cos^{-1} \left[\frac{\hat{L}_B \cdot \bar{o}_B}{|\bar{o}_B|} \right] \quad (5.6-2)$$

where \hat{L}_B = line-of-sight unit vector from the spacecraft to the observed object in body coordinates

5.6.2 INTERFERENCE

The interference of a sensor, excluding the V-slit and gimbaled sensors, will be defined as the intersection of the sensor boresight and the disk of the interfering object as defined by the sum of that object's angular radius and an interference angle associated with that object as defined by the user. The V-slit and gimbaled sensor interference computations replace the sensor boresight with the line-of-sight vector from the spacecraft to the observed star. Line-of-sight sensors may be interfered with by the Earth, Sun, or Moon.

Given the position vector of the interfering object (\bar{o}_B) in body coordinates and the radius of this object (r), the angular radius of this object (θ) is computed as defined in Equation (5.6-1). The sensor, excluding the V-slit and gimbaled sensors, is interfered with by this object when

$$(\theta + \tau) \geq \cos^{-1} \left[\frac{\hat{L}_B \cdot \bar{o}_B}{|\bar{o}_B|} \right] \quad (5.6-3)$$

where \hat{B} = unit boresight vector in body coordinates

τ = user defined interference angle for the interfering
object being evaluated

The V-slit and gimbaled sensors, similarly, are interfered
with by this object when

$$(\theta + \tau) \geq \cos^{-1} \left[\frac{\hat{L}_B \cdot \bar{o}_B}{|\bar{o}_B|} \right] \quad (5.6-4)$$

where \hat{L}_B = line-of-sight unit vector from the spacecraft to
the observed object in body coordinates

REFERENCES

1. Systems Technology Laboratory, STL-87-005, Attitude Determination Error Analysis System (ADEAS) Release 4 Requirements Document, F. Markley, E. Seidewitz, and D. Weidow, October 1987
2. Computer Sciences Corporation, CSC/TM-83/6175, Attitude Determination Error Analysis (ADEAS) Program Requirements and Mathematical Specifications (Preliminary) B. Fang and W. Davis, December 1983
3. J. R. Wertz, ed., Spacecraft Attitude Determination and Control. Dordrecht, Holland: D. Reidel, 1978
4. Computer Sciences Corporation, CSC/SD-83/6051, Data Set Layouts for the Goddard Trajectory Determination System (GTDS) (Revision 1), December 1985, pp. FRN 24-1 to FRN 24-17
5. --, CSC/SD-80/6035, SKYMAP System User's Guide, August 1980

C

C

C